CONTROLLED SEQUENTIAL DELIVERY OF PDGF-BB AND BMP-2 FOR VASCULARIZED BONE REGENERATION

by

Emily Anne Bayer

B.S. in Civil Engineering and Biomedical Engineering, Carnegie Mellon University, 2011

Submitted to the Graduate Faculty of
The Swanson School of Engineering in partial fulfillment
of the requirements for the degree of
Doctor of Philosophy

University of Pittsburgh

2016

UNIVERSITY OF PITTSBURGH

SWANSON SCHOOL OF ENGINEERING

This dissertation was presented

by

Emily Anne Bayer

It was defended on

October 11, 2016

and approved by

Prashant N. Kumta, Ph.D., Edward R. Weidlein Chair Professor, Departments of Bioengineering, Chemical and Petroleum Engineering, Mechanical Engineering and Materials Science, and Oral Biology, Center for Craniofacial Regeneration

Kacey Marra Ph.D., Associate Professor, Departments of Plastic Surgery and Bioengineering

Alan Wells, Ph.D., Thomas Gill Professor, Departments of Pathology and Bioengineering

Dissertation Director: Steven R. Little, Ph.D., William Kepler Whiteford Professor, Departments of Chemical and Petroleum Engineering, Bioengineering, and Immunology

CONTROLLED SEQUENTIAL DELIVERY OF PDGF-BB AND BMP-2 FOR VASCULARIZED BONE REGENERATION

Emily Anne Bayer, Ph.D.

University of Pittsburgh, 2016

Bone regeneration consists of a series of complex biological events, that *in vivo*, requires the highly coordinated presentation of biochemical cues to regulate these stages of healing. Taking inspiration from the natural healing process, a wide variety of growth factors are currently being released from tissue engineered scaffolds to aid in healing non-union fractures and bone defects. Currently, several scaffolding design techniques exist for releasing multiple growth factors with unique release profiles, which include polymer encapsulation, layer-by-layer fabrication, and core-shell construction, as well as growth factor delivery through other biological agents, such as plasmids and platelet-rich plasma. Several studies have suggested that the efficacy of multiple growth factor presentation may be influenced by several factors, including the sequence of presentation, and the dosage at various stages. Accordingly, building evidence suggests that *in vivo* growth factor presentation consists of highly coordinated temporal appearance, intricate crosstalk, and multi-pathway signaling. Therefore, determining effective growth factor release schedules for incorporation in bone scaffolding requires an assay platform that, in some ways, begins to account for these complexities. For the purposes of our studies, we have developed a three-dimensional assay system, capable of supporting multiple cell types, that providing control over growth factor delivery presentation schedules.

To begin to understand the effects of multiple growth factor presentation on the stages of bone repair, we have used this assay system to assess cellular responses to a variety of growth factor delivery schedules with variations in sequence, length of delivery, and overlap in delivery. By varying these parameters, we have identified a schedule of PDGF and BMP-2 presentation capable of promoting angiogenic tubule formation in co-cultures of hMSCs and HUVECs. Based on this information, we have engineered a biomaterial-based system to controllably release this sequential schedule of PDGF and BMP-2 autonomously. This preprogrammed controlled release system was then incorporated with a three-dimensional, porous calcium phosphate scaffold, and resulting material properties and cellular responses were characterized. The following experiments and results aim to take inspiration from the *in vivo* bone healing milieu, and to use specific cellular responses to guide the fabrication of a truly biomimetic scaffolding system.

TABLE OF CONTENTS

LIST OF TABLES

LIST OF FIGURES

PREFACE

This thesis represents not only years of research in the Little Lab, but also mentorship and collaboration from many different areas. First, I would like to recognize and thank Dr. Steven Little, my primary advisor for his support through the years. Dr. Little has unquestionably shaped and strengthened my technical writing abilities, presentation skills, and experimental approaches. He has challenged me on a daily basis and taught me how to produce good results in the face of adversity. I would also like to thank Dr. Prashant Kumta, Dr. Kacey Marra, and Dr. Alan Wells, for serving on my committee and providing advice. I have benefited from their feedback and advice at many steps along the way. In particular, thanks to Dr. Kumta and Dr. Roy for their collaboration and support for several components of this project. During my time at the University of Pittsburgh, I have also been fortunate enough to be part of the Cellular Approaches to Tissue Engineering and Regeneration (CATER) Fellowship Program. Through this fellowship program, I have been supported not only financially, but by a great network of peers and mentors. Thank you to the CATER director, Dr. Paul Monga for his mentorship and guidance. With his support, my doctoral program has included many opportunities for personal and professional growth and development. Thank you also to Dr. Gary Gruen, who gave me a firsthand clinical experience in orthopedic trauma and surgery. I am very appreciative of the opportunity I had to be integrated with his team and gain a clinical perspective for bone tissue engineering. I would also like to thank Dr. Morgan Fedorchak for her leadership and mentorship. She has been an integral component of my growth

and development as an engineer, and inspires me to push beyond expectations and standards to find greater success.

On a personal note, I would like to thank my family for their support. Thanks to my parents, Joe and Sue, for challenging me to hold myself to high expectations. Thanks to my sister, Halley, for her advice, proofreading expertise, and friendship. And thank you to my husband, Zack, who has offered me support in every way possible. Thank you for standing by my side through late nights and working weekends. I look forward to our future as we conquer major milestones together. Additionally, I would like to recognize my colleagues in the lab, many of whom have gone beyond their duties as coworkers, and become life-long friends.

1.0 INTRODUCTION

Bone tissue, like liver tissue, is one of the few tissues in the human body capable of some capacity of self-renewal, or regeneration [2-4]. As humans develop and grow, bone tissue is constantly undergoing phases of resorption (via osteoclasts) and reformation (via osteoblasts) [5]. These remodeling mechanisms are particularly useful when injury occurs to the skeletal system; in mild cases of injury, fractures may naturally remodel and therefore, require little medical intervention to heal [1]. However, when high impact, severe injuries cause complex fractures, successful healing may require titanium screws and plates, or in some cases, the addition of grafting material in the fracture space [6, 7].

While these practices are the gold-standard method of treatment [8, 9], there are still several issues that may arise during the course of treatment, such as misalignment of the bone or failure of the fracture to heal (non-union) [10]. In addition to these complications, the secondary surgeries and increased morbidities associated with autologous grafts have motivated efforts in the field of tissue engineering to create synthetic materials to encourage bone healing and overcome the hurdles of non-unions [11, 12]. A traditional tissue engineering approach is considered to consist of a mixture of cells, bioactive factors, and scaffolding [13, 14]. To effectively utilize these guidelines to create a successful biomaterial for fracture healing, it is advantageous to have an understanding of the cellular and physiological processes that constitute fracture healing.

Additionally, we may gain insight from current clinical methods of stimulating bone healing and their physiological relevance.

1.1 CLINICAL DESCRIPTION OF FRACTURES

In the US, 15.3 million fractures occur annually [2]; Fractures may occur as a result of stress, high impact, or other trauma and their likelihood of occurring may be increased by physiological conditions, such as osteoporosis [3]. Severity of fractures range from simple stable fractures, which may not even require casting or stabilization and take several weeks to heal, to complex, comminuted fractures, which may require multiple surgeries and external or internal fixation. The likelihood for successful healing also depends on several physiological factors; for example, the bone regeneration process has been shown to be hampered in individuals with compromised immunological systems due to diabetes, tobacco use, and aging [4].

1.1.1 Timeline of Normal Healing Events

In successful fracture healing, a stage-wise series of events orchestrate new bone formation. Following injury, a hematoma forms at the site of fracture, which will be swollen and undergo inflammation for approximately one week [15, 16]. For fracture sites that can be reduced so that they are separated by less than 200μm, the fracture may be sufficiently stabilized to prevent micromotion, allowing the fracture to heal via primary healing [7, 17], that is, without the

formation of a fracture callus. For fracture with larger gaps that are subject to micromotion, healing occurs via secondary healing [7], a multi-stage process illustrated in Figure 1. Following inflammation in secondary healing, a soft callus, comprised of spongy, cartilaginous granulation tissue forms in the fracture space over the next 4-8 weeks [15]. During this phase, angiogenic infiltration of the soft callus occurs, bringing circulating cells into the fracture space [16, 18]. Subsequently, a hard callus, or the formation and mineralization of new bone will begin to bridge the gap, and typically fill the fracture space within 8-12 weeks after injury [18]. Finally, bone remodeling will occur, a stage that may last several years and involves the replacement of woven bone with more highly organized lamellar bone through the activity of osteoblasts (bone forming cells) and osteoclasts (bone resorbing cells)[15].

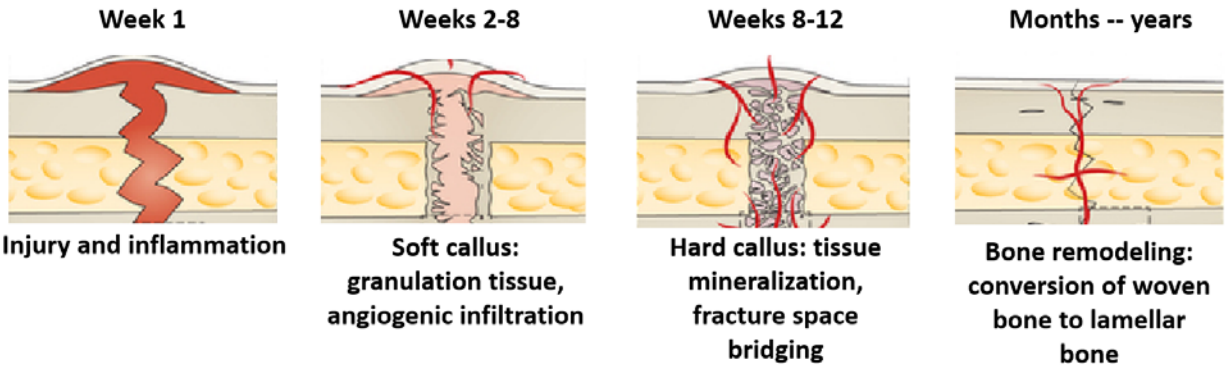

Figure 1. Timeline of fracture healing events during secondary healing. Adapted from Einhorn et. al., 2015 [19].

Depending on fracture type, location and severity, methods of treatment may involve casting, surgery, and the placement of stainless steel or titanium hardware to mechanically stabilize bone fragments as they heal [20, 21]. However, several problems may arise during fracture healing, such as infection, malunion (a fracture that heals out of alignment) and nonunion (fractures that do

not heal within a normal timeframe) [22-24]. These cases often necessitate additional measures (beyond casting and the use of plates and screws) to facilitate healing [6].

1.2 CLINICAL NEED FOR ASSISTED BONE HEALING

Of the 15.3 million fractures occurring in the US, 5-10% result in non-unions, clinically meaning that are no observable signs of healing over time and that biological progress has ceased without fracture union occurring [7, 8]. Non-unions are classified in two categories: hypertrophic and atrophic. Hypertrophic non-unions show signs of callus formation and biological activity in the fracture space and occur due to failure to adequately stabilize the fracture. Because hypertrophic non-unions show biological activity, they can be remediated by reducing the motion at the fracture site through improved fixation. Atrophic fractures, however, occur due to a lack of biological activity [5]. Particularly in the case of atrophic non-unions, bone healing fails due to a lack of adequate vascularization and biological activity of bone-forming cells [9].

1.2.1 Current Techniques to Stimulate Bone Healing

Current methods of addressing atrophic non-unions include the application of autologous, allogeneic, or synthetic bone grafting material, nail exchange surgical revisions, as well as less invasive techniques, such as electrostimulation. The use of these methods depends on the type of fracture, its anatomical location, and previous techniques applied.

1.2.1.1 Nail Exchange Surgical Revisions

Nail exchange surgical revisions are applicable to fractures that have been previously addressed with the insertion of an intramedullary nail, typically in the femoral and tibial diaphysis [10-12]. The nail exchange method involves removing the current intramedullary nail, reaming and enlargement of the medullary canal, and the insertion of a larger nail, which may have an increase of 1-4mm in diameter over the original nail [10-12]. This method is effective for addressing both hypertrophic and atrophic non-unions, as it addresses the underlying causes of both non-union types [10]. In the case of hypertrophic non-union, the insertion of a larger nail mechanically stabilizes the fracture, whereas in the case of atrophic non-union, the reaming of the intramedullary canal increases blood flow, bringing circulating cells to the wound space and stimulating biological healing [10]. Additionally, nail exchange revisions are theorized to promote healing due to increased load or compression across the fracture site, or dynamization [25]. Although nail exchange surgical revisions have been shown to be very effective in achieving union in the femoral and tibial shafts, this method is limited to those anatomical locations, and is not recommended in the case of comminuted fractures.

1.2.1.2 Electrostimulation

Electrostimulation, a method for stimulating bone healing that gained popularity in the 1950s, can be categorized into three main techniques: direct electric current, capacitive coupling, and inductive coupling [13, 14]. Stimulation via direct electric current is the most invasive of the techniques, delivering an electric field via cathode implantation at the site of the fracture [4, 15].

In contrast, capacitive coupling and inductive coupling are both non-invasive methods that deliver electric fields to the fracture through cathodes or coils placed on the skin surface [13, 15]. While the cellular mechanisms underlying the efficacy of these methods is not completely understood, the primary model supporting electrostimulation is that bone tissue is formed under electronegative potentials (and resorbed under electropositive potentials) [13]. Relating this concept to mechanical forces on bones, compression generates electronegative potentials, causing bone formation (while tension generates electropositive forces) [13]. Because fractured bones should generally not be subject to mechanical forces, particularly during early healing stages, electrostimulation may be a way to bypass mechanical stresses while still delivering bone-forming electric potentials. Studies of non-invasive capacitive and inductive coupling techniques have shown the upregulation of intracellular calcium production, extracellular matrix proteins, as well as increased production of bone morphogenetic protein (BMP) mRNA [4, 13]. However, electrostimulation currently delivers mixed clinical results [14], which may be, in part, due to a lack of standard dosage (electrical field strength) and configuration of the field over the fracture space [13, 14].

1.2.1.3 Autografts and Allografts

Autografts are bone tissues taken from the patient's own body at a separate location from the fracture, typically harvested from the iliac crest [16]. Autografts are the gold-standard grafting material, as they are osteogenic (contain osteoblasts or osteoblast precursors) osteoconductive (meaning that it provides a viable matrix to facilitate new bone growth) and even osteoinductive (meaning that it will recruit and differentiate mesenchymal stem cells into new bone tissue) [17, 18]. Autografts may consist of either cortical or cancellous bone [16], which each have benefits and drawbacks; cancellous autografts will be easily revascularized, but provide minor structural

support, while cortical autografts initially provide structural strength, but are slower to become revascularized and resorbed [19]. However, autografts still have several drawbacks: because they are harvested from a separate site from the fracture, obtaining autograft material requires a secondary surgical site, which increases operating time and the chances of infection. Additionally, the quantity and quality of autografts may be less than sufficient, depending on patient physiology [19].

Allografts, harvested from donor sources, are typically frozen, freeze-dried, or demineralized before use as a graft [16]. Therefore, the harvesting, processing and storage methods weigh heavily on the efficacy of allograft material. Under ideal conditions, however, allograft material may still be moderately osteoinductive [16]. Because allografting material may be harvested from a single donor, or aggregated from multiple donors, the biological capacity is also variable and influenced by the source [16, 19]. While allografts overcome some of the issues associated with autografting, such as secondary surgical sites and limited graft quantity, they present problems of their own. For example, because allografts are not derived from the recipient, there is a chance that the graft will be immunologically incompatible, and subsequently, prevent revascularization and bone formation, or even be rejected [16]. Additionally, allografts are associated with a higher incidence of delayed union or nonunion in comparison to autografts [16].

1.2.1.4 Synthetic Scaffolding and BMP-2 Therapy

As an alternative to autografts and allografts, synthetic grafting materials offer several benefits, such as eliminating the need for a secondary surgical site to harvest bone material (in the case of autografting) and reduction of the likelihood for an immunogenic response or rejection (in the case

of allografting). Currently available for clinical surgical repair are a class of calcium phosphate ceramics, which are available in several forms, including granules, non-porous blocks, and porous blocks [19]. Calcium phosphates are a promising biomaterial for bone repair, as these materials do not elicit a foreign body response, and can be either resorbed or converted into hydroxyapatite in the body [19]. Also available for clinical use is a combination graft, comprised of calcium phosphate, hydroxyapatite, collagen, and autologous bone marrow. These grafts are advantageous for bone repair because they serve not only as an osteoconductive material, but also include osteoprogenitor cells and osteoinductive growth factors from the incorporated bone marrow [19]. As an alternative to using autologous bone marrow in combination with synthetic scaffolds to provide a source of growth factors (which requires a second surgical site), bone grafting substitutes have been developed that include recombinant human BMP-2 (rhBMP-2) [20], which is produced ex vivo in a laboratory setting. Typically administered via collagen sponge to enhance bone repair, the administration supplemental BMP-2 *in vitro* and *in vivo* has been shown to aid in the proliferation and differentiation of pre-osteoblastic cells [21]. rhBMP-2 therapies initially gained FDA-approval in 2002 for lumbar spinal repair, and have since expanded to be FDA-approved for use in tibial fracture healing [22-24] and to include several applications for rhBMP-7.

While the inclusion of recombinant BMPs in synthetic scaffolding have been shown to be clinically viable options for fracture repair, several drawbacks are associated with this treatment. One of the dominant issues with *in vivo* BMP delivery is the overproduction of bone tissue, sometimes in nearby, dissimilar tissues (ectopic bone formation) which in spinal repair, may cause the undesirable complete fusion of vertebrae [26, 27]. BMPs are also currently delivered in dosages nearly a million times greater than physiological concentrations [20], making treatments costly and increasing the likelihood for ectopic bone formation. For these reasons, several methods of

more effectively delivering BMPs, have been explored, such as its encapsulation in natural and synthetic polymers [28].

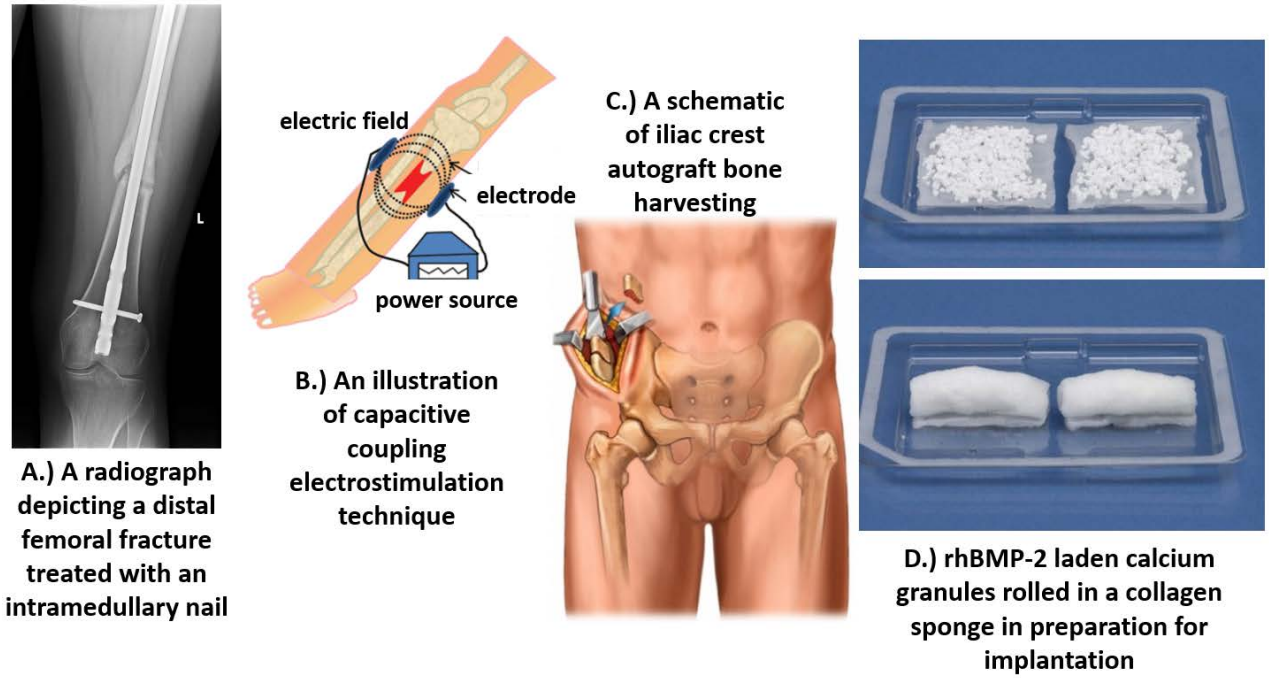

Figure 2. Examples and illustrations of current fracture healing techniques, including: A) intramedullary nail insertion [1], B) electrostimulation [29], C) autograft harvesting for implantation [1], and D) preparation of synthetic scaffolding with rhBMP-2 for implantation [30].

1.3 CURRENT CHALLENGES IN BONE HEALING

To address the occurrence of non-unions in fracture healing, there exist several diverse, clinically-approved option, including nail exchange surgical revisions, non-invasive electrostimulation, the placement of auto- or allografts, and synthetic scaffolding materials, that may or may not include supplemental rhBMP-2. For treating atrophic non-unions, it is important to select a treatment

option that will stimulate biological healing, as atrophic non-unions are characterized by a lack of observable biological activity, due to an absence of adequate vascularization and activity of bone-forming cells [9].

To overcome this lack of biological healing and enhance bone repair, supplemental rhBMP-2 may be administered to aid in the proliferation and differentiation of pre-osteoblastic cells [31]. However, in addition to osteoblast-driven bone matrix formation and mineralization, bone fracture healing and repair is widely recognized as a complex, multi-stage process of restorative steps [17, 25, 26]. During successful bone healing, revascularization of the wound space first occurs (angiogenesis), followed by either cartilaginous callus formation or primary bone healing (osteogenesis) [5, 17]. While osteogenesis is enhanced by the addition of BMP-2, angiogenesis is also a critical stage of bone healing, may not be adequately enhanced with BMP-2 treatment alone [27]. Importantly, angiogenesis plays a significant role in bone repair, as newly formed vessels provide critical supply of nutrients, waste removal, and promotion of cell migration into the bone regenerating niche [28]. Without substantial angiogenesis, bone grafts necrose and ultimately fail [32, 33]. Additionally, it has been shown that particular anatomical locations, such as the distal tibia, femoral head, and talus have an extremely poor chance of healing due to the likelihood of the disruption of angiogenic supply from surrounding tissue [29-31].

While the administration of rhBMP-2 has been shown effective in upregulating bone repair via osteoblast proliferation and differentiation [31], the clinical efficacy of growth factor administration as a fracture repair therapy may be advanced if rhBMP-2 is delivered with growth factors that also upregulate the critical stage of angiogenesis. Additionally, if these growth factors could be delivered with greater control, dosages closer to physiological concentration could be used in these therapies, lowering their cost and preventing unwanted overproduction of targeted

tissues. To achieve this, however, requires the identification of (at minimum) an angiogenic and osteogenic growth factor, an understanding of how these growth factors function in situ in the bone regeneration niche, as well as their potential interactions with cells and each other.

2.0 GROWTH FACTORS IN BONE HEALING

Growth factors exert influence over more than one biological process during regeneration. For example, beyond the most commonly recognized roles of BMP-2 (discussed below), this signal also appears to play a role in regulating angiogenesis [34-36]. In fact, earlier studies indicate that multiple forms of BMP (in part) promote angiogenesis by inducing the secretion of VEGF-A from preosteoblastic cells [36]. Yet, notably, a more recent investigation of BMP effects on angiogenesis suggests that depending on the form of BMP and its physiological setting, either a pro- or anti-angiogenic effect may be observed [34]. Furthermore, it has been shown that certain BMPs may have either a pro- or anti-angiogenic effect depending on the type of endothelial cell targeted [35].

BMP is not the only growth factor that exhibits multiple functions within the regenerating niche. Other common growth factors used for bone regeneration, including VEGF, PDGF, and FGF, have all been demonstrated to provide different instructions to different cell types (Fig. 3). For instance, studies suggest that FGF not only plays a role in upregulating bone formation by promoting osteoblast proliferation (and possible differentiation) via multiple signaling pathways [37], but it also has a well-recognized influence on endothelial cells, promoting angiogenesis [38, 39]. Similarly, although VEGF is typically associated with the upregulation of angiogenesis, it also plays a part in ossification and can affect bone formation by attracting mesenchymal stem cells (MSCs) and promoting their differentiation towards an osteoblastic phenotype [40]. PDGF,

another growth factor typically known for its role in regulating angiogenesis through the stimulation of VEGF production [41] and the recruitment of stabilizing mural cells [42, 43], also acts as a chemoattractant and mitogen for MSCs [44] (Fig. 3). Overall, it can be concluded that growth factors generally are not limited to a single function, but rather, are each activating multiple signaling pathways that may drive (or inhibit) regeneration [45].

2.1 BMP-2 FOR BONE FORMATION

BMP-2 has been frequently incorporated in scaffolds for bone regeneration because of its well-recognized ability to promote bone formation [46, 47]. At the cellular level, BMP-2 is a potent inducer of osteoblast proliferation as well as a differentiator of mesenchymal stem cells towards an osteoblastic phenotype [48] (Fig 3). Accordingly, BMP-2 increases bone formation at the defect site for applications ranging from spinal fusion [49] to dental and craniofacial regeneration [50]. While these studies are evidence of the usefulness of BMP-2 for inducing mineralized tissue, there are large variations in the success of human response to BMP-2 treatment. For example, in one clinical investigation, stimulation of bone regeneration stimulation following administration of BMP-2-soaked collagen sheets ranged from excellent bone formation, to no bone formation with fibrous tissue in patients receiving the same delivery construct [51]. This may be explained by the rapid delivery of BMP-2 from collagen-soaked scaffolds, mediated primarily by protein desorption, with no barriers to diffusion to create sustained release rates [52]. As noted in other studies, when BMP-2 (or other growth factors) are delivered via bolus administration, they rapidly diffuse from the site of administration with a lack of temporal and spatial control, resulting in only

transient cellular stimulation with supra-physiological concentrations of the growth factor[53] . In an attempt to present proteins in a more physiologically relevant manner, several methods to sustain BMP-2 release have been explored, including its encapsulation within (and release from) polymers, its expression through delivery of plasmids, and its entrapment within scaffold coatings [54-56]. While basic sustained release provides a more extended signal to cells to direct bone regeneration, a major shortcoming of delivering only BMP-2 is the limited capacity for BMP-2 alone to initiate vascular network formation [57]. As previously described, vascular infiltration is a required and necessary phase of overall bone healing that precedes ossification [17, 58]. Hence, in addition to (and, in the context of vascularization, more significantly than) BMP-2, delivery of several known angiogenic growth factors have also been explored during bone regeneration to promote vessel development and growth

2.2 ANGIOGENIC GROWTH FACTORS

Angiogenic factors include (amongst others) VEGF, a potent mitogen for endothelial cells [40], and platelet endothelial growth factor (PDGF), which has been shown to act as a chemoattractant for cell types that stabilize growing vasculature [43, 59] (Fig. 3). Moreover, PDGF has also been observed to upregulate VEGF production for continued angiogenesis [44]. Beyond VEGF and PDGF, additional angiogenic factors observed in the bone regeneration niche include fibroblast growth factor (FGF), which plays a role in the sprouting of new capillaries [39], and insulin like growth factor (IGF) a growth factor known to play a role in adult neoangiogenesis [58]. Each of these angiogenic factors have also been delivered to enhance bone healing and, specifically, the

vascularization stage of regeneration. Notably, several studies suggest that delivering angiogenic factors alone for bone regeneration leads to the inability to produce organized bone regeneration [57, 60, 61]. Indeed, when releasing VEGF alone, no bone formation was observed in either ectopically or orthotopically implanted scaffolds. [57]. These results are in agreement with the building body of evidence suggesting that the delivery of a single growth factor is oversimplifying the regenerative process [59]. At the same time, when delivering multiple growth factors, we must understand their role in the regenerative niche to properly coordinate their spatiotemporal presentation [62].

2.3 GROWTH FACTOR ROLES IN THE REGENERATIVE NICHE

Growth factors exert influence over more than one biological process during regeneration. For example, beyond the most commonly recognized roles of BMP-2 (discussed above), this signal also appears to play a role in regulating angiogenesis [34-36]. In fact, earlier studies indicate that multiple forms of BMP promote angiogenesis by inducing the secretion of VEGF-A from preosteoblastic cells [36]. Yet, notably, a more recent investigation of BMP effects on angiogenesis suggests that depending on the form of BMP and its physiological setting, either a pro- or anti-angiogenic effect may be observed [34]. Furthermore, it has been shown that certain BMPs may have either a pro- or anti-angiogenic effect depending on the type of endothelial cell targeted [35].

In addition to BMP, several other growth factors, including VEGF, PDGF, and FGF have been found to stimulate stages of bone regeneration [37-39]. Interestingly, these growth factors have been shown to play several roles, acting on multiple cell types. For example, PDGF has been

shown to both promote angiogenesis, and also acts as a powerful mitogen for (pre-osteoblast) MSCs [41, 44]. In Table 1, these signaling pathways are summarized to highlight the various roles that growth factors may play across multiple phases of bone regeneration.

Table 1. Common Growth Factors and their Roles in the Bone Regeneration Niche

Growth Factor	Roles in Bone Regeneration	Cell Types Involved
BMP-2	1. Differentiates osteoprogenitors to osteoblast cell type [51] 2. Upregulates osteoblast proliferation [51] 3. May promote or antagonize angiogenesis [34]	Secreted by vascular and mesenchymal stem cells [63]; acts on osteoprogenitors and osteoblasts [51]
TGF-β	1. Recruits osteoblast precursors [64, 65]	Inactively present in bone matrix until proteolytically activated; acts on osteoblast precursors [64]
PDGF	1. Induces proliferation of mesenchymal stem cells [44] 2. Upregulates angiogenesis and VEGF production; stabilizes newly forming vessels, [44] 3. Induces chemotaxis of mesenchymal stem cells to support forming vasculature [43, 59] 4. Induces chemotaxis of mesenchymal stem cells to the bone healing space [66]	Secreted by platelets, neutrophils, and macrophages [67]; acts on mesenchymal stem cells [43, 44, 59, 66]
VEGF	1. Upregulates angiogenesis; acts as a potent mitogen for endothelial cells [40, 68] 2. Chemoattractant for mesenchymal stem cells [40]	Secreted by osteogenic cells and platelets; acts on endothelial cells [69] and mesenchymal stem cells [40]
IGF	1. Upregulates angiogenesis; induces adult neoangiogenesis [58] 2. Enhances bone matrix synthesis [65]	Bound in bone matrix and secreted by osteocytes [65]; acts on preosteoblasts [65] and endothelial cells [70]
FGF	1. Upregulates angiogenesis; induces sprouting of new capillaries [38, 39] 2. Promotes osteoblast proliferation and differentiation [37]	Secreted by osteoblasts, macrophages, and endothelial cells [65]; acts on mesenchymal stem cells, osteoblasts [37], and endothelial cells [38, 39]

2.4 GROWTH FACTORS AND CELLULAR CROSSTALK

In addition to the multiple individual roles of growth factors, there is also evidence that presentation of multiple growth factors at the same time can produce varied effects, sometimes resulting in a synergistic outcome and other times inhibitory effects that are deleterious for tissue formation [65]. As previously described, the combined delivery of VEGF and BMP-2 often results in better outcomes in terms of vascularized bone formation [57, 71, 72]. It has been suggested that VEGF and BMP-2, function synergistically, activating complex crosstalk and feedback mechanisms between growth factors and cell types. As an example, VEGF upregulates angiogenesis and, at the same time, signals the recruitment of pre-osteoblast cell types [40]. BMP-2, in turn, promotes osteoblast proliferation and pre-osteoblast differentiation while also instructing osteoblastic cells to release VEGF, creating a cycle of intercellular signaling that enhances bone formation [36].

Although exact molecular mechanisms are not fully elucidated, multiple studies have shown that synergistic effects of growth factor combinations are often dependent on dosage and timing [65]. For example, in multiple studies investigating the effects of BMP delivered in combination with FGF, a range of FGF dosages was delivered with the same amount of BMP, allowing observance of FGF dose dependency [65, 73-75]. Interestingly, in each of these studies, BMP dosage was maintained constant and the amount of FGF was varied, indicating that the synergistic effect may not be a result of individual dosages, but rather it depends on the ratio between the amounts of FGF and BMP [65, 73-75]. In all of these studies it was found that the BMP/FGF combination was synergistic for bone formation at lower ratios (1:5000-1:125, FGF:BMP), but inhibitory at higher ratios (1:50-4:1, FGF:BMP) [73-75]. These observations

indicate that delivery of multiple growth factors initiates a very complex set of instructions that are dependent on how and when each signal is presented. This needs to be accounted for when designing scaffolds for bone regeneration.

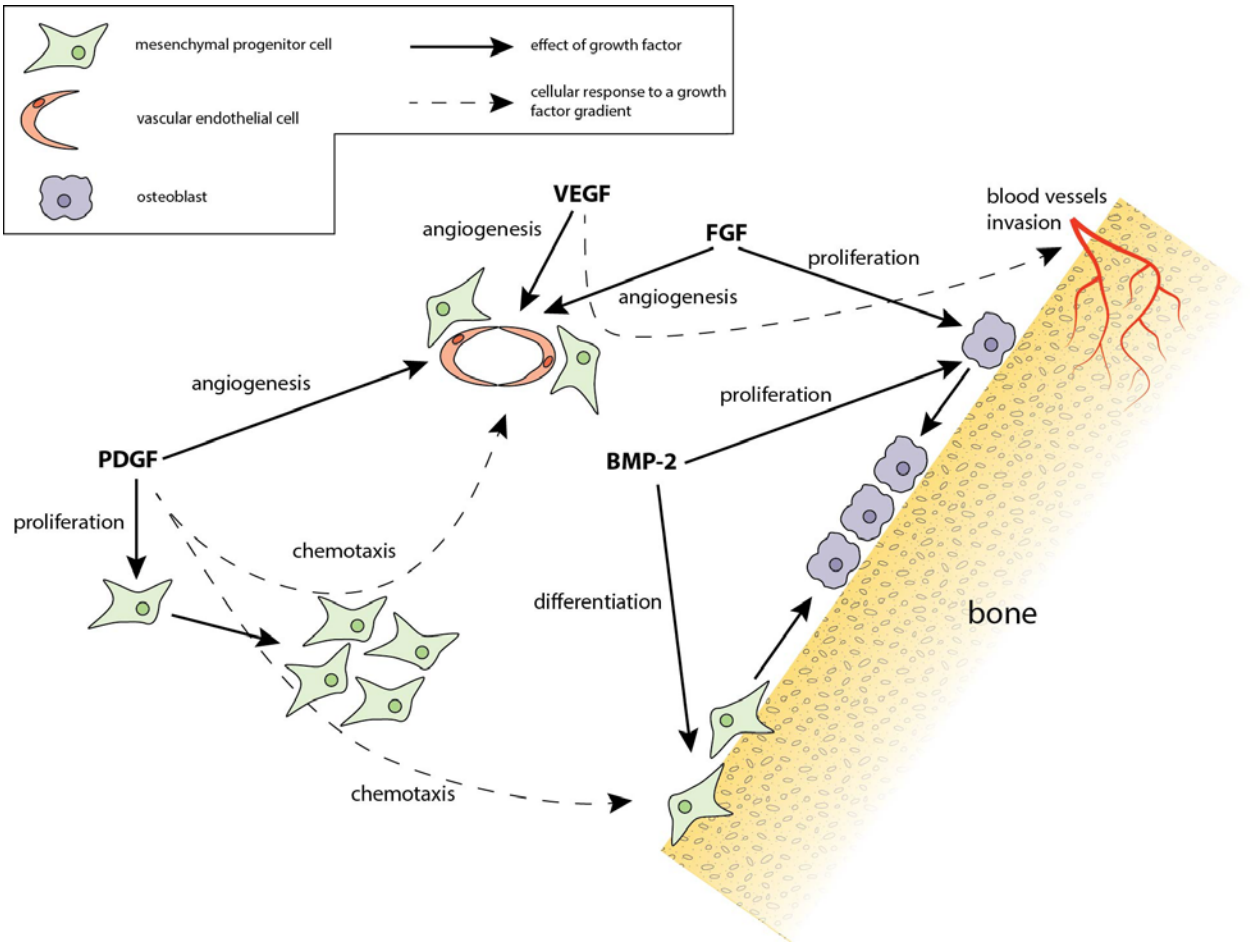

Figure 3. Growth factors signaling: Examples of the action of several prevalent growth factors related to vascularized bone regeneration.

2.5 DUAL GROWTH FACTOR DELIVERY

To create bone scaffolds with a better likelihood of vascularity, the simultaneous incorporation of both an angiogenic factor (to jumpstart vessel formation) and an osteogenic factor (typically BMP-

2, to induce bone formation) has been explored. A controlled, “dual release” of two growth factors at the same time could be argued to be closer to mimicking the natural healing process. There is indeed some evidence that the delivery of an osteogenic and angiogenic factor can enhance bone formation in some circumstances when compared to the delivery of an osteogenic factor alone [61, 71]. For example, Huang et al. have shown that the delivery of both VEGF and BMP-2 from scaffolding seeded with human bone marrow stromal cells (hBMSCs) resulted in significantly greater amounts of bone formation than when BMP-2 was delivered alone from the same subcutaneously implanted scaffold at 15 weeks using a murine severe combined immunodeficiency model [61]. More recently, Subbiah et al. promoted osteogenesis and angiogenesis by delivering BMP-2 in combination with VEGF from a subcutaneous scaffold without the addition of seeded cells[71]. In this model, scaffolds delivering both factors appeared to promote significantly higher levels of osteocalcin expression as well as significantly deeper more dense blood vessel penetration than scaffolds delivering BMP-2 alone [71]. These positive results have been observed not only in subcutaneous models, but also in bone defect models. For instance, in a study by Ratanavaraporn et al. [76], an ulnar critical size defect model was used to investigate the co-delivery of stromal derived factor 1 (SDF-1) and BMP-2 [76]. Although bone formation after four weeks was observed in scaffolds releasing BMP-2 alone as well as scaffolds releasing both BMP-2 and SDF-1, it was found that a larger area of bone with significantly higher bone density formed in scaffolds releasing both growth factors [76]. The authors hypothesized that this phenomenon may be due to the synergistic mechanisms of SDF-1 recruitment of hematopoietic cells and BMP-2 differentiation of osteoprogenitor cells [76]. In a different study by Su et al., BMP-2 was delivered in combination with FGF to rabbit mandibular defects and the combined growth factor delivery resulted in significantly higher bone formation compared to the

delivery of BMP-2 alone when evaluated at 12 weeks post-implantation [77]. Together, these results may indicate that releasing both an angiogenic and an osteogenic factor from scaffolding could have the potential to improve bone regeneration outcomes over single growth factor delivery in some circumstances.

Although these results are promising, there are other examples of scaffolds delivering multiple growth factors that, in contrast to the studies mentioned above, fail to generate significantly improved long-term results. For instance, dual delivery of VEGF and BMP-2 in a rabbit femoral defect demonstrated only a weak synergistic effect at earlier time points, whereas at later time points, dual growth factor delivery groups were indistinguishable from defects receiving BMP-2 alone [78]. A similar study of VEGF and BMP-2 delivery to a rabbit cranial defect, revealed a higher volume of bone formation and early defect bridging for dual delivery at 4 weeks, but no significant differences at 12 weeks between groups delivering dual growth factors and only BMP at 12 weeks [60]. These results suggest that, although multiple growth factor release may initially lead to increased tissue formation or vascularity, dual (or simultaneous) delivery of VEGF and BMP does not always lead to significant overall long-term improvement.

Importantly, in addition to growth factor choice, another component of experimental design that must be considered when comparing outcomes is preclinical animal model selection. In early investigational stages, it is generally more feasible and cost effective to employ small mammal models (mouse, rat, etc.) [79]. Using these models, general effects of growth factors may be observed using a subcutaneous design (ectopic implant), but more relevant data may be collected from *in situ* implantation in long bones or craniofacial defects (orthotopic implant) [79]. When delivering growth factors in combination with human stem cells or other human tissue, it may be necessary to use an immunocompromised animal model to avoid adverse immunogenic results

[80]. In this instance the greater biosimilarity achieved using human cells/tissues might be partially discounted by an incomplete biological response of the immunocompromised animal. In general, while convenient from multiple point of views, small animal models have drawbacks that may influence experimental outcomes. For example, rodent and rabbit bone composition share few similarities with human bone [79, 81]. After data collection and proof-of-concept in smaller animal models, translational studies may progress to larger animal models (canine, sheep, goats, etc.) to more closely replicate the human bone healing process [81].

2.6 MULTIPLE GROWTH FACTOR DELIVERY AND TIMING

The combined evidence of the multiple roles that each growth factor can play within the regeneration niche and the complex cross-talk between growth factors and major cell types would suggest that simple scaffolds do not currently capture the intricacy of the natural healing process. In particular, it has been observed that the large number of growth factors that are secreted in the *in vivo* bone healing microenvironment are not presented simultaneously, rather, they are presented in a cascading fashion to coordinate the stages of bone regeneration [69, 82]. In fact, the ordered presence and absence of growth factors appears to correspond with different stages of regeneration [83, 84]. These observations may provide clues as to why single factor or multiple factor delivery together may not always achieve the desired outcomes. It may also provide clues as to why the simultaneous delivery of two growth factors may or may not achieve a desired outcome. The concept of timing in growth factor delivery has been previously investigated in vascular tissue regeneration models [38, 59, 85, 86]. For example, in studies performed to observe angiogenesis *in vivo*, it was found that early release of one angiogenic factor (VEGF) in the first 24 hours, and

the subsequent release of a second angiogenic factor (SDF-1) from 24-48 hours, significantly improved vascularization compared to singular delivery of either growth factors, to their simultaneous delivery, or to their delivery in reverse order [85]. These studies suggest that the absence of a growth factor at a given stage of regeneration may be just as important as the presence of another, illustrating not only the importance of including relevant growth factors in a scaffold, but also presenting them in a biologically meaningful order.

When specifically considering the stages of angiogenesis and osteogenesis during bone regeneration, there is evidence that growth factors for each phase have temporal roles and may be most effective when delivered in sequence. For example, as described above, PDGF is responsible for the recruitment of mesenchymal stem cells and other osteoblastic precursors to the site of bone regeneration [87, 88], and it has additionally been shown to upregulate VEGF, in turn, promoting blood vessel formation and regulating angiogenesis [44, 89]. Using these observations to inform temporal presentation suggests that PDGF release may be effective when restricted to early of bone formation (the initial days, possibly up to a few weeks of the regeneration process depending on the specific conditions), partly because in fracture healing, the infiltration of vessel networks into the healing callus occurs prior to ossification [90]. Importantly, PDGF also upregulates VEGF production [88, 89], which if expressed for more than 72 hours, can inhibit maturation of vessel networks and produce leaky vessels [91, 92]. Aside from its beneficial effects in recruiting osteoblast precursors and upregulating angiogenesis, other studies have shown that for a range of PDGF dosages, BMP-induced bone formation was inhibited [65], further supporting the hypothesis that some degree of temporal separation may be beneficial for organized regeneration. Collectively, these studies suggest that early expression of angiogenic factors during the initial few days of regeneration may be advantageous for bone regeneration not only to promote vasculature

formation and recruit osteoblast precursors, but also to prevent potentially adverse effects after mature vascular networks have been established, such as leaky vasculature and interference with tissue mineralization.

And while it appears that angiogenic factors are most effective when delivered in the early days of bone regeneration, studies of BMP delivery suggest that a delayed BMP delivery is likely beneficial such that BMP is presented during later stages of bone regeneration, following the establishment of a mature vascular network. [63, 93-95]. Specifically, several of these studies show that delaying the delivery of BMP for days or weeks after scaffold implantation will generate a greater amount of bone formation, presumably by allowing osteoblast precursors the opportunity to migrate into the scaffold prior to differentiation [93, 96]. During other types of bone formation, particularly distraction osteogenesis (the induction of osteogenesis by the slow, surgical separation of bone [97]), BMP was not even expressed until 5 days after distraction in the granulation tissue and endothelial cells of the healing microenvironment [63]. Together, results from these studies indicate that delayed delivery of BMP-2 from the time of scaffold implantation is recommended in order to promote organized bone regeneration.

With all of these above studies in mind, it must be noted that attempts to truly match the intricate orchestration of instructions provided by the body would most likely be time and cost prohibitive to translation, as the scalability of fabricating vascularized scaffolds is only now starting to be addressed [98]. Furthermore, to ideally direct bone tissue healing as is done naturally, each growth factor based “instruction” would need to be administered at just the right time, in just the right amount, especially considering crosstalk potential and the stage-wise process of angiogenesis and osteogenesis. To balance the feasibility of scaffold production with the requirements of generating vascularized bone tissue, it will be important to carefully select only

the most necessary “instructions” with only the simplest possible temporal spacing. In the next chapter, we explore several design methods for incorporating controlled release growth factors into scaffolding constructs that attempt to balance these constraints.

3.0 DEVELOPMENT OF SYNTHETIC SCAFFOLDING FOR CONTROLLED GROWTH FACTOR DELIVERY

3.1 POLYMER ENCAPSULATION SCAFFOLDING

Scaffolds fabricated from synthetic polymers offer a high level of control over material properties which play an important role in protein release, such as degradation rates, porosity, and microstructure [99]. Various categories of polymers have been used to create scaffolding for growth factor delivery, including hydrogels and polyesters [100]. These polymers can be processed in a multitude of ways, including casting, crosslinking and gas foaming, to create entire scaffolds while encapsulating growth factors for controlled release [99, 100]. In addition, one way of delivering multiple growth factors with distinct profiles from a polymeric scaffold is to use a combination of polymers in scaffold fabrication. By using polymers with different degradation behaviors to separately incorporate growth factors, multiple, distinct release profiles can be achieved (Fig. 4). For example, Kanczler et al. were able to release VEGF and BMP-2 from a compartmentalized scaffold comprised of alginate and poly-lactic acid (PLA) [72]. By incorporating VEGF in the alginate phase, and BMP-2 in the more slowly degrading PLA phase of the scaffold (Fig. 4a), independent release kinetics were realized, generating fast VEGF release

and slower, more sustained BMP-2 release [72]. Another way of achieving distinct release profiles while using a single polymer scaffold is by using differing methods of growth factor incorporation. For example, Richardson et al. produced a poly(lactide-co-glycolide) (PLG) scaffold with fast-releasing VEGF and slow-releasing PDGF for vascular regeneration by using two methods of growth factor inclusion [59]: lyophilized VEGF was mixed with PLG particulate, while PDGF was encapsulated within PLG microspheres. Both PLG components were then fused to create the scaffold, which quickly released VEGF from its surface. PDGF release, on the other hand, was dependent on microsphere degradation/erosion rates. Together, these release profiles resulted in larger, more mature blood vessels [59]. Microsphere encapsulation has also been successfully used to create protein-releasing scaffolds with multiple material phases, that is, microspheres fabricated from one polymer and then embedded into a scaffold composed of a second polymer (Fig. 4b). Using this approach Basmanav et al. encapsulated BMP-7 and BMP-2 in poly(4-vinyl pyridine)/alginate hybrid microspheres, which were then incorporated into a poly(lactic-co-glycolic) acid (PLGA) foam scaffold [101]. The most striking difference in release profiles was the change in the burst release of proteins, achieved by altering the percentage of polymer in the microspheres. When modeling release with bovine serum albumin (BSA) as a proof of concept, it was found that burst release was reduced with increasing microspheres polymer concentration (ranging from 4-10%). Crosslinking temperature was also found to influence release rates; BSA release was accelerated for microspheres prepared at lower crosslinking temperatures, likely because crosslinking was retarded. In one experimental condition, BMP-2 was released from quickly degrading microspheres (4% polymer), and BMP-7 was released from more slowly degrading microspheres (10% polymer) to *in vitro* bone marrow stromal cell cultures. The highest alkaline phosphatase (ALP) activity, an indicator of calcification, was observed in scaffolds

containing both types of microspheres, when compared to scaffolds releasing either BMP-2 or BMP-7 alone [101]. In another instance of using of multiple polymer formulations, Kim et al. constructed a chitosan gel scaffold with embedded gelatin microspheres [102]. In this case, to create distinct release profiles, insulin growth factor (IGF-1) was encapsulated in the gelatin microspheres, whereas BMP-2 was directly mixed into the chitosan gel. This system released BMP-2 more quickly and IGF-1 more slowly, resulting in more *in vitro* ALP production at day 7 compared to scaffolds releasing BMP-2 alone, and scaffolds releasing both BMP-2 and IGF-1 from the gel phase of the scaffolds (no microsphere encapsulation, i.e., no sequential release) [102]. A key advantage in using polymer microspheres for protein encapsulation is that recent mathematical models have been developed to accurately predict release profiles of individual molecules [103]. Predictive modeling is particularly beneficial for the design of controlled release formulations for multiple growth factors, since microsphere compositions can be tuned *ab initio* to produce a pre-programmed "lag phase," or phase of delayed release, that allows for the engineering of sequential release profiles. In particular, PLGA microspheres can be engineered exploiting these predictive methods to preferentially sequester depots of growth factors, delaying their presentation to the body by manipulating polymer material properties including molecular weight, co-polymer ratio, and microsphere surface porosity [103].

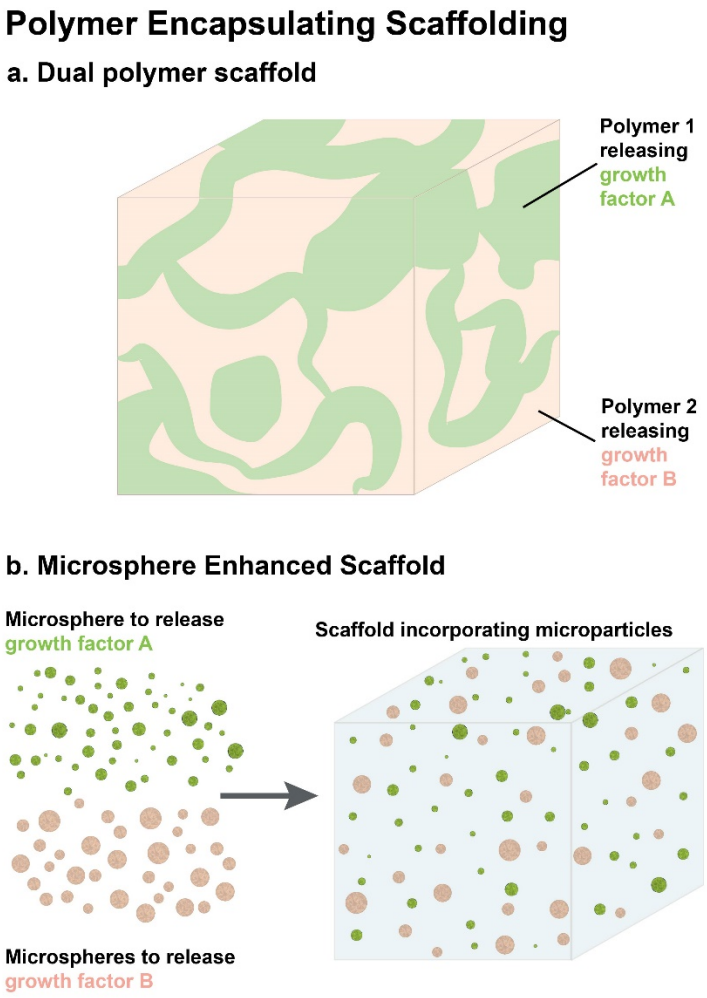

Figure 4. Polymer Encapsulating Scaffolding. Examples of polymer-based encapsulation strategies for multiple growth factors based on (a) dual polymer interpenetrating scaffolds [72] or on (b) scaffold incorporating growth factor eluting microspheres [59, 101, 102].

Although distinct release profiles were achieved using these polymer encapsulation methods, in some cases other key material properties, such as osteoconductivity and structural integrity, may be compromised when fabricating scaffolding from only synthetic polymers [72]. These additional material properties can be rescued by incorporating protein-encapsulating polymeric microspheres within another material matrix that is naturally osteoconductive, such as calcium phosphate.

Several studies have characterized material properties of composite polymer/calcium phosphate scaffolds [104-107], which together can offer the benefits of tunable growth factor delivery (endowed by the use of synthetic polymers) with material properties such as high compressive strength, osteoconductivity, and biodegradability (endowed by natural ceramics) [82]. In a study of scaffold mechanical properties, Link et al. found that calcium phosphate scaffolds with 20% weight PLGA microparticles showed increases in shear strength over an 8 week study as a result of bone formation within pockets left by degrading polymer microparticles [104]. While still mechanically insufficient for load bearing applications, the calcium phosphate scaffold provided a structural template and an osteoconductive interface. Additional studies have explored the effects of polymer microsphere chemistry on the material properties of composite scaffolding. Differences in polymer microsphere charge [108], density (hollow vs. solid) [105], and material composition [106] have been shown to influence scaffold degradation rates and subsequent bone ingrowth [105, 108]. Therefore microspheres can be optimized not only to control protein release, but also to modulate overall scaffold properties. Several studies have explored release of a single drug or protein from such a polymer/ceramic composite scaffold [109, 110]. Combining release profile information with material property characterization of the hybrid scaffolding [104-106] shows promises for these composites, which could be used as templates for temporal release of multiple growth factors while at the same time contributing desirable bone scaffold physical properties.

Overall, polymer encapsulation methods constitute a versatile platform for growth factor delivery. Polymers may be used to create full scaffolds, or fabricated as a secondary construct, such as microspheres. Although polymers alone may lack the material properties, such as mechanical strength, required for bone engineering, stronger, more osteoconductive materials, such as calcium phosphate, may be used in combination with growth factor-releasing polymers to

create composite scaffolding. However, the addition of polymer microparticles to calcium phosphate may reduce the strength of the scaffold [110]. Furthermore, when secondary materials, such as calcium phosphate, are used with controlled release polymer formulations, growth factor release is greatly reduced, most likely because released proteins are sequestered by adsorption to the material's surface [110, 111]. For these reasons, secondary materials must be carefully chosen to provide structural integrity and osteoconductivity while not overly interfering with growth factor release kinetics. An additional consideration when using polymer encapsulation methods for controlled protein delivery is the preservation of protein bioactivity. There exist several potential mechanisms of protein inactivation; for example, it has been demonstrated that proteins encapsulated in PLGA may be irreversibly inactivated due to conditions including elevated moisture levels, the acidic microenvironment created via PLGA degradation, adsorption of the protein to the polymer surface, or the aggregation of insoluble protein masses [112, 113]. To combat these potential sources of protein inactivation, it may be necessary to include additional components during the encapsulation process, such as a basic salt to reduce the acidity of the microenvironment [113], or even to pre-encapsulate proteins within dextran nanoparticles to protect against exposure to solvents and prevent protein aggregation [114].

3.2 CORE-SHELL SCAFFOLDING

Another method of fabricating temporally distinct release patterns is the physical separation of growth factors using core-shell scaffolds. Specifically, distinct temporal release profiles can be achieved through the degradation properties of the core-shell design, in part through the selection

of bulk-eroding and surface-eroding materials [115]. Generally, the core-shell scaffold arrangement allows for temporal release through its construction of a quickly degrading shell, which protects a more slowly degrading core [116]. Using a core-shell approach, Perez et al. created a microfibrous scaffold with a concentric injection nozzle, in which each fiber was comprised of one phase of pure alginate and a second phase of alginate with α-tri calcium phosphate (α-TCP) (Fig. 5a). The protein for delivery, cytochrome C, was loaded into either the "core" or "shell" phase of the fiber [117]. Depending on the protein location (core vs shell) and the composition of the phase (percentage of α-TCP, of alginate, and amount of crosslinking), differing release profiles were generated. It was found that the addition of α-TCP resulted in prolonged release profiles with minimized burst release. Furthermore, the release profiles of the core-encapsulated protein could be altered either by changing core composition or by varying shell composition, because the mechanism for release depends (at least in part) upon diffusion through both the core and shell materials [116]. While effective in creating unique release profiles, one of the possible limitations of the core-shell fiber design for multiple growth factor release is that modulation of release properties requires changing the material properties of the scaffold. In the previously described example, release profiles were altered most drastically with the addition of α-TCP, which also notably altered the storage and loss moduli of the scaffold [117].

To avoid the potential pitfall of sacrificing desired material properties to achieve release profiles (or vice versa) another approach to the core-shell design can be implemented using a secondary material phase to control release of proteins. One approach to creating this design of core-shell scaffolding is to first encapsulate growth factors in polymer microparticles that are then incorporated in a secondary scaffolding material directly loaded with the second growth factor (Fig. 5b). This approach was used by Kempen et al. to release VEGF and BMP-2 [57]. In this

study, the microparticles were meant to act as the “core” and the embedding material as the “shell.” The use of degradable polymer microparticles allows for a further level of control since they can be designed to produce different release profiles independently from the overall scaffold structure. To create a sustained BMP-2 release profile, BMP-2 was encapsulated in degradable microspheres (composed of PLGA) and then embedded into poly propylene fumarate (PPF) to create the core of the scaffold. A gelatin phase into which VEGF was directly incorporated served as the scaffold “shell”. It was found that the complete *in vitro* release of VEGF leveled off within 2 weeks, whereas BMP-2 release from the core was sustained for more than 4 weeks. A high burst release of VEGF from its hydrogel shell was observed both *in vitro* and *in vivo* [57]. Using this core-shell approach, Kempen et al. achieved distinct release profiles for BMP-2 and VEGF, which was found to enhance ectopic bone formation, as indicated by significantly higher bone volume formation in scaffolds releasing combined VEGF and BMP-2 [57].

In addition to using microspheres as the “core” phase that is then incorporated into a secondary “shell” scaffolding material, microspheres that act themselves as core-shell configurations can be produced [118-120] (Fig. 5c). The main advantage of this core-shell configuration is that microspheres can easily be packed into irregular bone defect shapes, a more difficult feat for prefabricated block scaffolding [118]. A recent example is provided by Wang et al. [119] who used a PLLA core to encapsulate BMP-2, and a PLGA shell to encapsulate FGF. These core-shell microparticles were capable of releasing both growth factors with distinct release profiles and could be used without a scaffold to improve fracture healing [119].

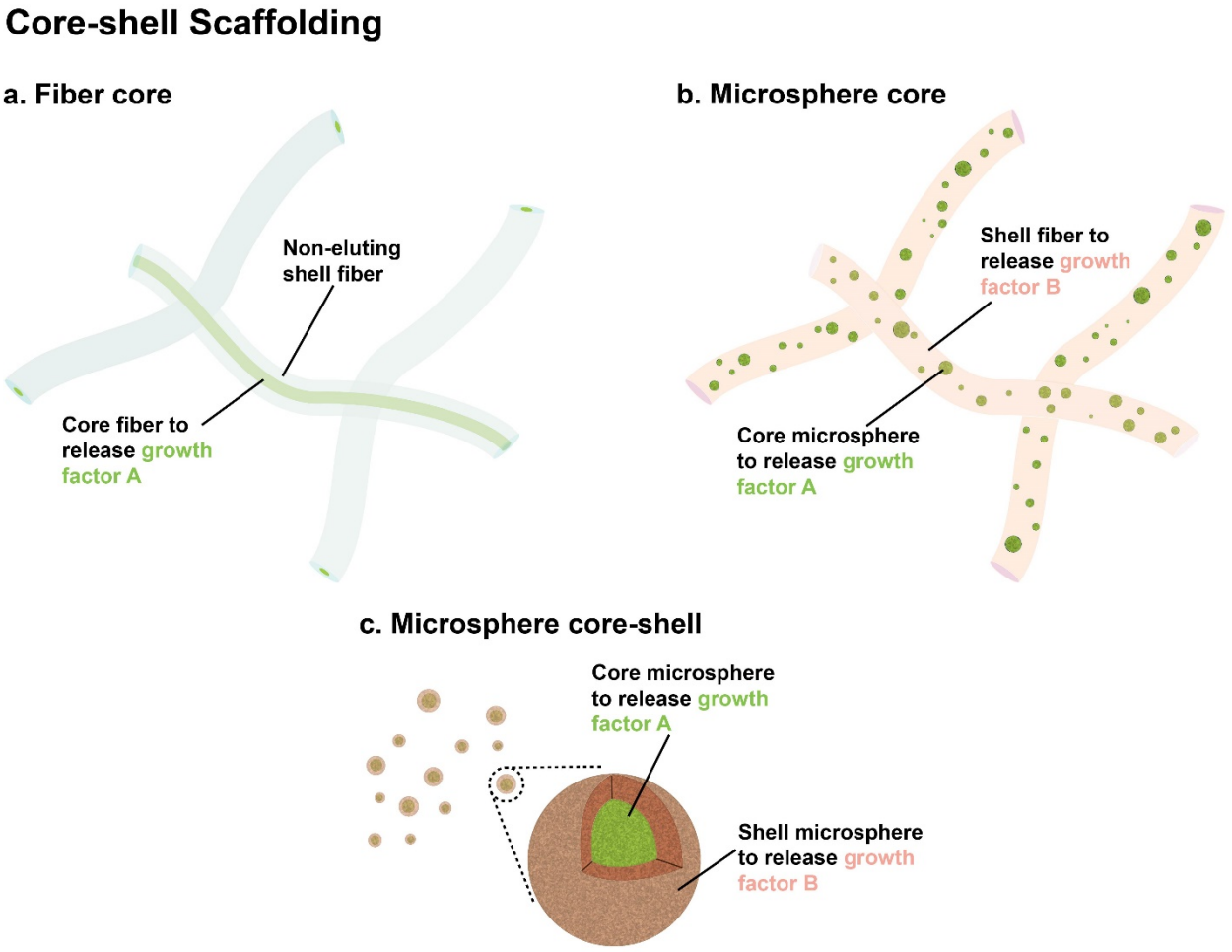

Figure 5. Core-Shell Scaffolding: Examples of different strategies to obtain a core-shell scaffold, by fabricating (a) a growth factor eluting fiber core within a polymeric fiber [116, 117], by (b) incorporating growth factor eluting microspheres in a polymer fiber incorporating a second growth factor [57], and by (c) creating microspheres with a core that incorporates a first growth factor and an outer shell that contains the second growth factor [118-120].

Overall, core-shell scaffolding offers the possibility to control the local spatial separation of growth factors release [116]. Furthermore, implementation of the core-shell system through the incorporation of microparticles may allow for more control over material properties of the scaffolding material in which they are embedded, or core-shell microparticles may even be used a stand-alone system [118-120]. However, one remaining limitation of this approach is that the shell

phase influences release of growth factors incorporated in both the core and shell phases of the scaffold. Because the shell is the outermost tier of the scaffold, whether proteins are incorporated within the core or shell phase, they must either diffuse through the shell phase or be delayed until its erosion [116]. This configuration could even prove advantageous to allow longer term release, but must be accounted for when designing core-shell release systems and selecting the core material properties.

3.3 LAYER-BY-LAYER SCAFFOLDING

Another category of scaffolding architecture for temporal delivery of multiple growth factors is layer-by-layer (LbL) scaffolding. Like core-shell scaffolding, LbL scaffolds are created by depositing a series of biomaterial sheets or molecular layers, while allowing curing or hardening of each layer (if necessary) before the next is placed. Growth factors are thus spatially separates into different physical material layers to govern their release, similarly to the separation in core-shell scaffolding. Although the categories of core-shell and LbL designs may be considered to describe somewhat similar scaffolding configurations, in this review, the term “LbL scaffolding” will refer to 1) scaffolds composed of two or more side-by-side layers (that are non-concentric), or 2) thin layers used to coat a scaffolding material that does that does not have a growth factor-filled core.

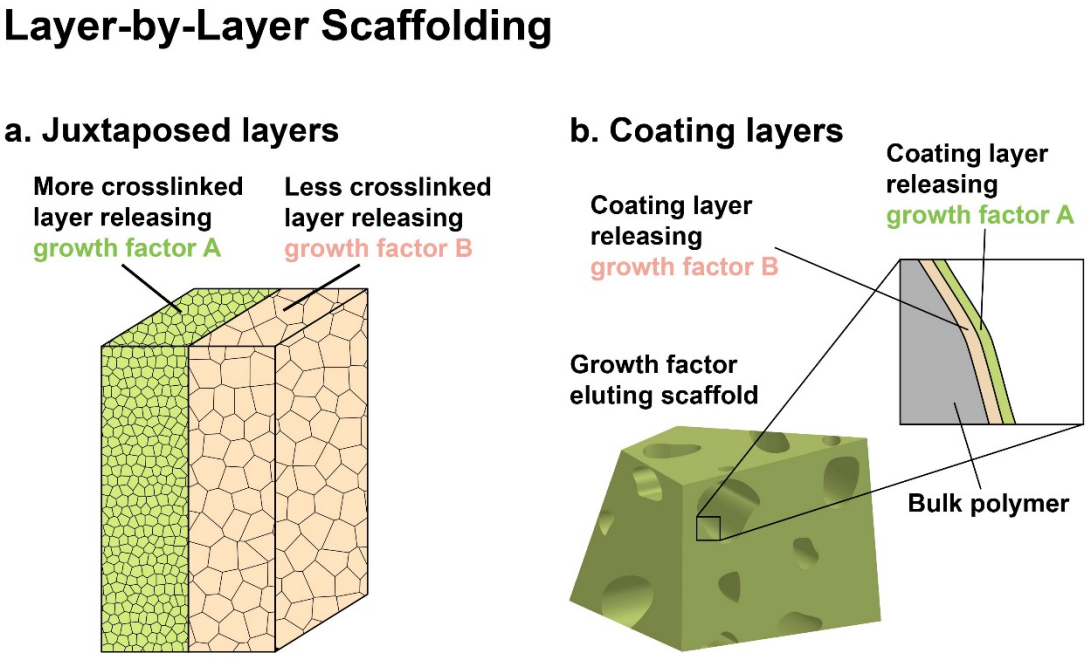

Figure 6. Layer-by-Layer Scaffolding: Examples of layer-by-layer scaffolds realized by (a) juxtaposing growth factor incorporating polymers with different degrees of crosslinking [121, 122], or by (b) coating a porous scaffold with a dual polymeric layer containing different growth factors [123, 124].

One way that LbL scaffolding takes advantage of chemical and material properties to release multiple growth factors is by modifying the curing process of each layer to modulate release profiles. For example, when using the same polymer to fabricate multiple layers, differing release profiles can be achieved by crosslinking to a different degree each layer (Fig. 6a). Raiche and Puleo [121] used this method to create a BMP-2 and IGF-1 eluting scaffold consisting of two gelatin layers: a “top” layer which was crosslinked to a lesser degree than the second highly-crosslinked “bottom” gelatin layer When added into the lesser crosslinked layer, BMP-2 release was accelerated, with peak release on day 1 and completion of release approximately after 7 days.

However, when added to the more highly crosslinked layer, peak BMP-2 release was delayed until day 6. Using a similar crosslinking method for LbL fabrication, Kim et al. [122] released IGF-1 and TGF-β from a oligo(poly(ethylene glycol)fumarate) (OPF) scaffold. While IGF-1 release profiles remained constant for all groups, TGF-β release was altered by incorporating it into different layers of the scaffolding. Burst release was suppressed through increasing polymer crosslinking in the layer impregnated with TGF-β. To even further minimize the burst release of TGF-β, the growth factor was first encapsulated into gelatin microspheres before its inclusion in the more highly crosslinked layer of the scaffold. Although the TGF-β release profile was successfully altered by its incorporation in differing layers and microspheres, increased temporal separation of these two growth factors may be required, as better subchondral bone morphology was observed in scaffolds delivering IGF-1 alone, indicating potential remaining antagonistic growth factor signaling [122].

While useful in advancing the LbL technology platform, methods of fabricating an entire scaffold in two distinct spatial layers may not be directly applicable in creating a scaffold for vascularized bone. Although capable of temporal release of multiple growth factors, if layers releasing growth factors are too spatially separated, they may prevent the necessary co-localization of vascular and mineralized tissue formation. An alternative approach to the LbL design that may offer more co-localized growth factor presentation is to create layered scaffold coatings rather than a layered scaffold (Fig. 6b). Shah, et al.[123] adopted this approach to the LbL method to create a layered coating for the release of PDGF and BMP-2. Differences in electrostatic attraction between each growth factor and polyelectrolyte membranes were exploited to create the “layers” onto a PLGA scaffold. The PLGA scaffold was first dipcoated with a layer contained BMP-2, and then dipcoated in a second layer containing PDGF, resulting in PDGF releasing more quickly than

BMP-2. This temporal release of PDGF and BMP-2 resulted in bone formation with higher compressive strength and other mechanical properties that better matched that of native bone as compared to scaffolds releasing only BMP-2 [123]. An advantage to this method is the possibility for creating a spatio-temporal gradient of growth factors release. As the coatings surface degrade, the outer PDGF-laden layer releases its growth factor concentration more quickly, followed later by a BMP-2 release. One potential drawback to using the LbL method to generate coatings rather than entire scaffolds is that the underlying scaffold material must be carefully chosen and fabricated so that cells will be encouraged to completely infiltrated and create tissue after growth factor coatings have degraded, particularly if used for filling large defects.

Similar to core-shell scaffolding, when additional control over protein release is desired, a secondary material may be used to first encapsulate the growth factor into microspheres before these are added into a layer composed of a different material [122, 125]. A unique advantage of the LbL method is that layers can be fabricated more thickly, to create an entire scaffold, or when applied more thinly, may be used as a coating. One challenge to the LbL method lies in striking the correct balance between layer thickness and spatial growth factor separation. When considering LbL applications for vascularized bone, it is important that in the creation of growth factor gradients, protein release does not become so spatially separated as to prevent vascularity throughout the scaffold. At the same time, when LbL techniques are used to generate thin coatings, properties of the underlying scaffold material, such as porosity and osteogenicity, must be selected to continue the promotion of tissue formation in the absence of degraded growth factor-laden LbL coatings. Additionally, at this time, LbL coatings are capable of generating independent release of multiple growth factors but, although release profiles are not identical, they are still simultaneous [126]. While the LBL delivery design has been effective for generating more trabecular bone

formation over the same scaffolds delivering BMP-2 alone [124], if entirely sequential release profiles were to be desired, significant design modification may be required to block interlayer diffusion, such as the inclusion of a “barrier” layer to separate growth factor-eluting layers [127, 128].

3.4 OTHER GROWTH FACTOR DELIVERY TECHNIQUES

In addition to the above described synthetic techniques for controlled delivery of soluble growth factors, temporal delivery of multiple growth factors is also being addressed using biological approaches. Comparison of these methods to those described throughout section 4 are described in Table 2. One example of an alternative biological delivery method is the use of platelet rich plasma (PRP), which can be derived autologously or allogeneically. Notable growth factors present in PRP include IGF, FGF, PDGF, TGF-β, and VEGF [129, 130]. However there appears to be great variability in concentrations of these growth factors from donor to donor which represents an issue for both clinical application and scientific research [131]. To use PRP as a source of delivery for these growth factors in bone regeneration, it is often incorporated into other scaffolding material, as (by itself) it lacks the mechanical properties required for load bearing, even after activation to form a fibrin matrix to fill local lesions [132-134]. Furthermore, PRP can be processed to form a thin membrane [135], which could be used to wrap other scaffold or grafting material. While PRP supplies an abundance of growth factors useful for bone regeneration, the main hurdle to implementation is the control over the release of each of these growth factors. One option pursued by Lu et al. is the incorporation of PRP into different types of alginate carriers, which entailed a sustained release of growth factors, and, depending on the carrier fabrication

method (internal vs. external gelation), growth factor release, could be delayed for up to 7 days [136]. Interestingly, the two growth factors assayed in this study exhibited different release profiles when PRP was incorporated into externally gelated carriers, with PDGF release beginning on day 1, while TGF-β did not release until day 7 [136]. PRP has also been incorporated into various other scaffolding materials and designs for delivery to the bone niche, such as nanofibers, sponges, and demineralized bone matrix, for more sustained release, but challenges still remain in standardizing the amount of active growth factors in each PRP sample [137]. Additionally, it may be difficult to finely tune the release of growth factors individually since they are incorporated together, as part of the PRP complex into scaffold designs.

A second, biological alternative for the presentation of growth factor "instructions" is gene delivery. Plasmids (non-viral vectors), as well as adenoviruses, have been used to encode several growth factor genes and are incorporated in scaffolding for placement in the bone regeneration niche. Some early examples of plasmid use for bone regeneration include the delivery of a BMP-4 plasmid [138] and parathyroid hormone [139], both of which caused the local and sustained expression of growth factors locally (up to 6 weeks). More recently, a plasmid for the expression of VEGF was able to sustain transgene expression for 105 days [140]. To achieve sequential or, at minimum, temporally separated growth factor expression, adenoviruses have been used in combination with other growth factor delivery methods. For example, Luo et al. [141] loaded polymer scaffolds with VEGF protein and adenoviruses expressing BMP-2. This delivery method resulted in a burst release of VEGF during the first few days of the *in vitro* release study, and sustained BMP-2 expression through day 21. When implanted *in vivo*, these scaffolds exhibited significantly enhanced bone volume formation as well as higher torque values required to remove the scaffolds [141]. Although effective in generating greater bone volume [142], growth factor

presentation still overlapped to some degree. If greater temporal separation were desired using gene therapy, another possible and more sophisticated approach is the inclusion an inducible promoter for more control over gene expression [142]. While gene delivery does show promise as potential systems for sequential growth factor delivery, there still remain a number of safety concerns that could severely limit its clinical implementation [143].

Another biological alternative to growth factor delivery (and to growth factor expression through gene delivery) is the presentation of small molecules. Unlike proteins, small molecules are typically too small (< 1000 Daltons) to induce immunogenic responses, do not require higher-order structural integrity to maintain bioactivity, and are highly thermally stable [144, 145]. A multitude of small molecules that have the potential to stimulate osteogenesis have been identified through high-throughput screening methods, several of which have been studied preclinically for their efficacy in promoting bone formation in non-unions and long bone fractures [144]. For example, simvastatin, a statin traditionally used to combat cholesterol synthesis, was encapsulated in PLGA/hydroxyapatite microspheres by Tai et al. [146] to induce bone formation in a mouse tibial gap fracture model. In this study, significantly greater callus formation and a significantly greater amount of new blood vessel were observed at two and four weeks post-treatment in groups receiving simvastatin delivery over control groups. In another study, Monjo et al. [147] delivered rosuvastatin from a collagen sponge to rabbit tibial defect and observed significantly higher bone density and volume in rosuvastatin treatment groups versus control groups. Both simvastatin and rosuvastatin are hypothesized to result in greater bone formation by upregulating osteogenesis via the BMP/Smad pathway [144]. Although effective in generating bone formation [146, 147], a major challenge in the use of these (and other) small molecules is preventing unwanted effects in other cell and tissue types due to nonspecific targeting [144, 145]. To overcome this hurdle,

controlled release scaffolding must be designed to deliver small molecules with spatial and temporal control to ensure only localized effects to the specific target tissue [144].

Table 2. Delivery Method Comparison. Advantages and disadvantages of each delivery method

Delivery Method	Advantages	Disadvantages
Polymer Encapsulation	1. Can be used to make a wide variety of scaffolding or scaffolding components (ex. fibers, microspheres, full constructs). 2. Degradation rates and resulting release profiles are easily manipulated, some of which can be predicted by mathematical models.	1. Lack mechanical strength. 2. Lack osteoconductive/ osteoinductive properties. 3. Potential for protein inactivation.
Core-shell Scaffolding	1. Spatially separates growth factors.	1. Core depot release is influenced by the degradation and/or diffusional properties of the shell.
Layer-by-layer Scaffolding	1. Spatially separates growth factors. 2. When applied in thin layers (nano-micron scale), can be used as a coating for other scaffolding material.	1. Growth factors may be too spatially separated for adequate bone/vessel co-localization when thicker layers are constructed. 2. Interlayer diffusion may occur, the prevention of which requires "barrier" layers.
Platelet-rich Plasma	1. Includes many relevant growth factor in one medium.	1. Great variability in growth factor concentrations, depending on harvesting and processing techniques. 2. Difficult to controllably release individual growth factors.
Gene Delivery	1. Provides long term local protein expression. 2. Inclusion of inducible promoters provides a high level of control over expression.	1. Limited clinical translatability.
Small molecules	1. Does not induce unwanted immune responses. 2. Highly thermally stable. 3. Bioactivity does not require higher-order structural integrity.	1. Risk of nonspecific effects on untargeted tissues

4.0 DELIVERY OF PDGF AND BMP-2 FOR TUBULE FORMATION AND ORGANIZATION

4.1 INTRODUCTION

As described in Chapters 1 and 2, a critical challenge to successfully regenerating bone tissue is the adequate vascularization of grafts or scaffolding used in repair efforts [148]. As previous studies have illustrated, angiogenesis plays a significant role in bone repair, as newly formed vessels provide critical supply of nutrients, waste removal, and promotion of cell migration into the bone regenerating niche [149].

While the importance of angiogenesis in bone repair is apparent, the only current FDA-approved growth factor for addressing poor bone healing is bone morphogeneic protein-2 (BMP-2), an osteogenic growth factor [46, 150-152]. Though there is some evidence supporting the involvement of BMP-2 during angiogenesis [36], it was also demonstrated that BMP-2 delivery alone has limited capacity to upregulate vascular formation at the fracture site [57]. Further, BMPs have even been shown to inhibit angiogenesis in some situations [34], and antagonisms are known to exist between angiogenic growth factors, such as platelet derived growth factor (PDGF), and members of transforming growth factor-β (TGF-β) superfamily (including BMP-2) [153]. This lack of understanding of the interplay between BMP-2 and angiogenic growth factors may explain

the inconsistent results of those studying combined delivery of angiogenic growth factors (such as VEGF, PDGF, IGF, etc.) with BMP-2 [82, 154].

Taking clues from studies reporting that bone fracture healing is a complex, multi-stage process of restorative steps [17, 90, 155], we hypothesize that the ordered presentation angiogenic and osteogenic growth factors will influence angiogenic network formation. Notably, the role, if any, of additional parameters of growth factor presentation, including length of delivery and degree of overlap, has yet to be fully explored for angiogenesis during bone tissue regeneration.

The resulting effects of order and spacing of multiple growth factor timing and overlap may help guide the development of biomimetic therapeutics, including controlled release systems for temporal or spatiotemporal separation of growth factors [102, 119, 121]. To gain further information regarding the effects of variation in growth factor presentation for upregulating angiogenesis in bone repair, we developed a new *in vitro* Matrigel plug model assay to assess tubule formation in response to various growth factor delivery schemes. While Matrigel is known to intrinsically contain low levels of present growth factors [156], it was chosen for use as a three-dimensional substrate in this application as it is a preferable matrix for assaying the activity of endothelial cells and allowing *in vitro* tubule formation [157, 158]. Because of the background levels of growth factors innately present in Matrigel, control groups of cells receiving no additional delivered growth factor were included in experimental set-ups to evaluate base levels of tubule formation in Matrigel matrices alone. A co-culture of human umbilical vascular endothelial cells (HUVECs) and human mesenchymal stem cells (hMSCs) allows for the exploration of both angiogenic (organization of HUVECs) and osteogenic (differentiation of hMSCs towards an osteogenic phenotype) responses to growth factor treatment groups. HUVECs were chosen for this study as they are traditionally one of the most commonly used cell type for *in vitro* angiogenesis

assays [159, 160]. However, we also acknowledge that while HUVECs can be used to model angiogenic responses, these cells are derived from a different lineage and may exhibit differing properties in comparison to the microvascular endothelial cells that would more commonly be found in the bone regeneration niche [161-163]. In addition to tubule formation by HUVECs, hMSCs have the potential to differentiate into mural cells that support the maturation of newly formed tubules [164]. Using the HUVEC/hMSC co-culture in this Matrigel plug assay, we are able to assess cellular responses to length, sequence, and degree of overlap in growth factor delivery. We have used this model to investigate our hypothesis that the sequence and degree of overlap in PDGF and BMP-2 delivery will impact tubule formation in the context of bone repair, as previous studies have shown the importance of growth factor sequence regarding angiogenesis alone [38, 85].

4.2 MATERIALS AND METHODS

A three-dimensional *in vitro* Matrigel plug was used as a model to explore delivery patterns of platelet derived growth factor (PDGF) and bone morphogenetic protein (BMP-2) to a co-culture of human mesenchymal and endothelial cells. In the following experiments, we observed how various presentation schedules of PDGF and BMP-2 influenced microtubule formation by human mesenchymal stem cells and human umbilical vascular endothelial cells. We assayed for tubule formation in response to sequence of growth factor deliver, growth factor delivery timing, dosage, and overlap.

4.2.1 Tubule Development Assay

Well inserts of a 24-well transwell plate (Sigma Aldrich) were filled with 250 μL of growth factor reduced, phenol-free Matrigel (LDEV free, Fisher Scientific). Human umbilical vascular endothelial cells (HUVECs, Lonza) and human bone marrow-derived mesenchymal stem cells (hMSCs, Life Technologies) were seeded at a density of 1.5×10^5 cells per well, in a 1:1 (hMSC : HUVEC) ratio. The lower reservoirs of MSC-HUVEC co-cultures we filled with 500 μL of a 1:1 ratio of endothelial basal media and minimum essential media (Life Technologies) supplemented with 1% penicillin-streptomycin and 1% antibiotic-antimycotic to provide hydration to Matrigel plugs.

4.2.2 Growth Factor Delivery to Cell Cultures

Growth factor enriched media was prepared by combining endothelial basal media and minimum essential media in a 1:1 ratio, and supplementing it 1% penicillin-streptomycin and 1% antibiotic-antimycotic. For PDGF treatment groups, soluble PDGF-BB (Fisher Scientific) was added to the media for a final concentration of 10 ng/mL PDGF. For BMP treatment groups, soluble BMP-2 (Fisher Scientific) was added to the media for a final concentration of 100 ng/mL BMP, and for PDGF + BMP treatment groups, PDGF and BMP were added to the media for a final concentration of 10 ng/mL and 100 ng/mL, respectively. Growth factor concentrations were chosen based on dose-dependency studies found in literature references [165, 166]. Based on these studies, the lowest dose for which a cellular response was observed was chosen for use in this study. Prepared

media was delivered to corresponding groups by injecting 20 μL aliquots per well per day for the duration of the experiment. PDGF and BMP were each delivered for a minimum of one day, to a maximum of 10 days, with between 0-10 days of overlap, depending on the conditions studied.

4.2.3 Immunofluorescence

At the conclusion of the experimental timeframe (10 days) Matrigel plugs were removed from transwell inserts, embedded in TissueTek (Fisher Scientific) and snap frozen in liquid nitrogen. Frozen sections (10 μm) were incubated with primary antibody mouse anti-human CD31/PECAM-1 (R&D Systems) and secondary antibody donkey anti-mouse IgG (R&D Systems) to identify endothelial cell activity and vessel formation. Images of CD31-stained sections were taken at 20X and 10X using a Nikon inverted light microscope, then analyzed using WimTube software (Wimasis Image Analysis, GmbH). 10X images were used for analysis to gain a larger representative sample area. WIMASIS software was used for analysis of four parameters for every image: total area covered by vessels, total length of vessels, number of branching points, and number of closed loops. These parameters were measured for each representative area imaged at 10X magnification, and are illustrated in more detail in Supplementary Figure 7.

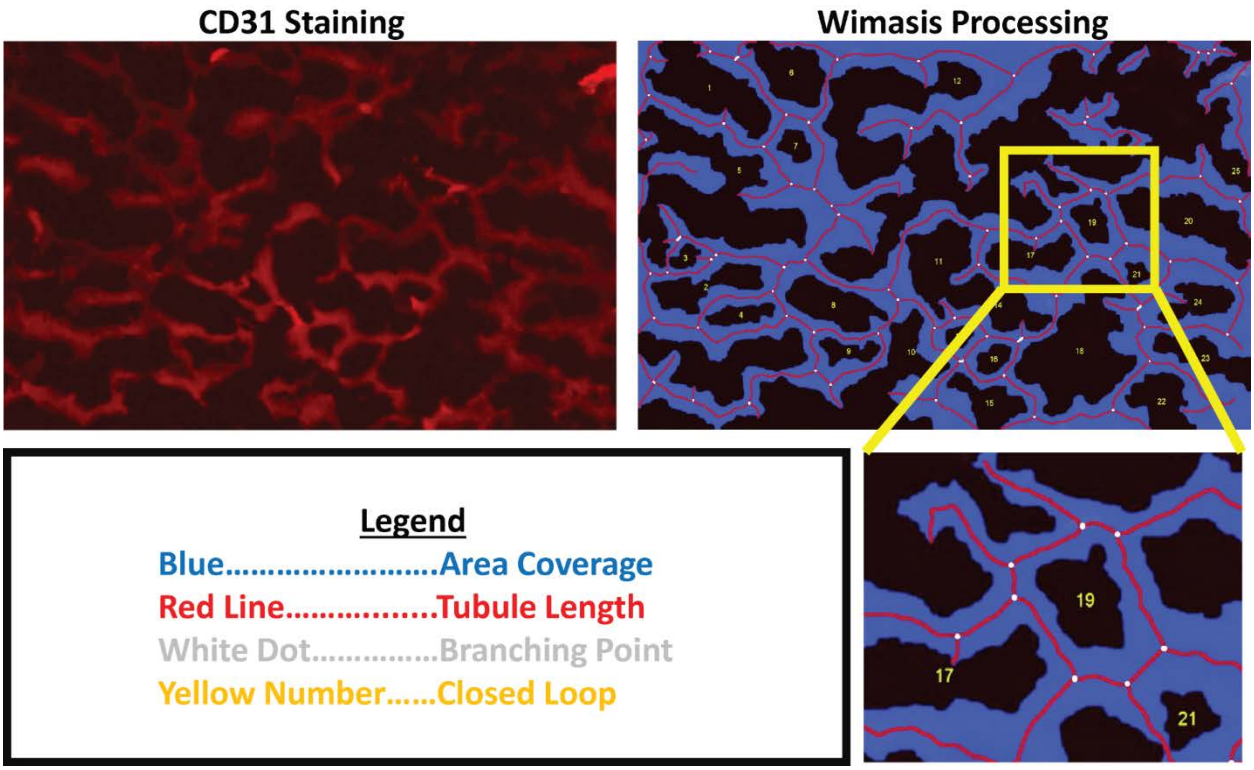

Figure 7. Legend demonstrating quantification parameters (area coverage, tubule length, branching points, closed loops) used in this study, and how they are represented in the Wimasis software processing system.

To assay for the potential of MSC differentiation towards a pericyte phenotype when exploring length of PDGF delivery, slides were incubated with primary antibody rabbit anti-alpha smooth muscle actin (ab5694, Abcam) and secondary antibody goat anti-rabbit IgG H&L (Alexa Fluor 488, Abcam). Images of slides were taken at 20X using a Nikon inverted light microscope. Alpha-smooth muscle actin (α-SMA) staining was quantified by analyzing fluorescent intensity of the resulting using ImageJ software. Image files were converted to 8-bit formatting, then automatically thresholded using the triangle thresholding method in ImageJ. Resulting binary images were quantified with the ImageJ “analyze particles” method with default settings.

4.2.4 PCR for Expression of Collagen-1

RNA was extracted from Matrigel plugs using an RNeasy mini kit (Qiagen Inc.) following the manufacturer's instructions. Extracted RNA samples were then concentrated using an RNA Clean & Concentrator-5 kit (The Epigenetics Company, Zymo Research.) Concentration and quality of RNA samples was verified using a NanoDrop analyzer (ThermoFisher Scientific). Real time quantitative PCR was then performed using a StepOne Real Time PCR system and software (V2.3) (ThermoFisher Scientific). TaqMan inventoried probes and primers (Invitrogen) were used in the mRNA analysis. Results, represented as relative level of gene expression, were calculated using the threshold cycle (Ct) method and comparative Ct ($2^{-\Delta\Delta Ct}$) calculation. These calculations were performed using eukaryotic 18S expression as the endogenous control, and the BMP-2 experimental group as the reference sample.

4.2.5 Statistical analysis

Multivariate ANOVA was performed using GraphPad 5.0 software to identify statistically significant differences (p less than 0.05) across multiple experimental groups for each set of *in vitro* growth factor delivery data. Post-hoc multiple comparison testing was performed to compare means using Tukey's test. Each experimental growth factor delivery group (PDGF, BMP, PDGF + BMP, etc.) contained N=3 samples. For every N, measured outcomes of n=3 cryoslices were first averaged to better represent each sample.

4.3 RESULTS

Using a three-dimensional *in vitro* Matrigel plug model, we observed how various presentation schedules of PDGF and BMP-2 influenced microtubule formation by human mesenchymal stem cells and human umbilical vascular endothelial cells. We observed that sequential presentation of PDGF to BMP-2 led to increased tubule formation over simultaneous delivery of these growth factors. Importantly, a 2-4 day overlap in the sequential presentation of PDGF and BMP-2 increased tubule formation as compared to groups with zero or complete growth factor overlap, suggesting that a moderate amount of angiogenic and osteogenic growth factor overlap may be beneficial for processes associated with angiogenesis.

4.3.1 Tubule Formation in Response to Sequential Treatment Schedules

In order to explore the variable space related to the sequence of PDGF/BMP for induction of vascular structures, we explored the growth factor delivery of (1) PDGF alone, (2) BMP alone, (3) PDGF + BMP [10 days of PDGF and BMP together], (4) PDGF to BMP [5 days of PDGF alone, followed by 5 days of BMP alone], (5) BMP to PDGF [5 days of BMP alone followed by 5 days of PDGF alone], (6) “blank” media with no added growth factors (Figure 8). The “blank” experimental group, which was supplemented with neither PDGF or BMP, served as a negative

control. All growth factor delivery schedules were assayed using the HUVEC/hMSC co-cultures seeded in Matrigel plugs. As a baseline, CD31 staining of Matrigel sections revealed at least some degree of tubule formation in each experimental group (Figure 9). The greatest amount of CD31 staining, as quantified by tubule area coverage and tubule length, was observed in samples treated with PDGF alone (Figure 10). However, CD31 staining also showed that the sequential delivery of PDGF to BMP outperformed other treatment groups in terms of tubule density (quantified by area coverage and tubule length per frame) and tubule organization (quantified by number of branching points.)

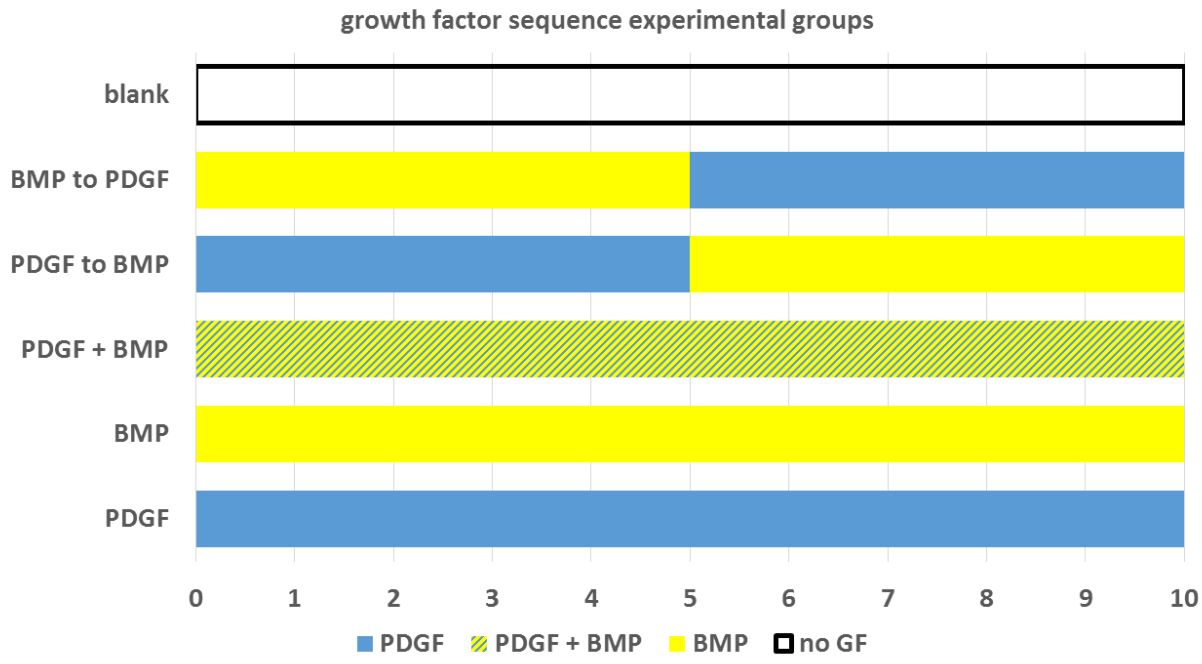

Figure 8. Sequential growth factor delivery regimens showing type of growth factor delivery per day over 10 days. Growth factors were delivered by pipetting 20 μL of media with concentrations of 10 ng/mL PDGF and/or 100 ng/mL BMP.

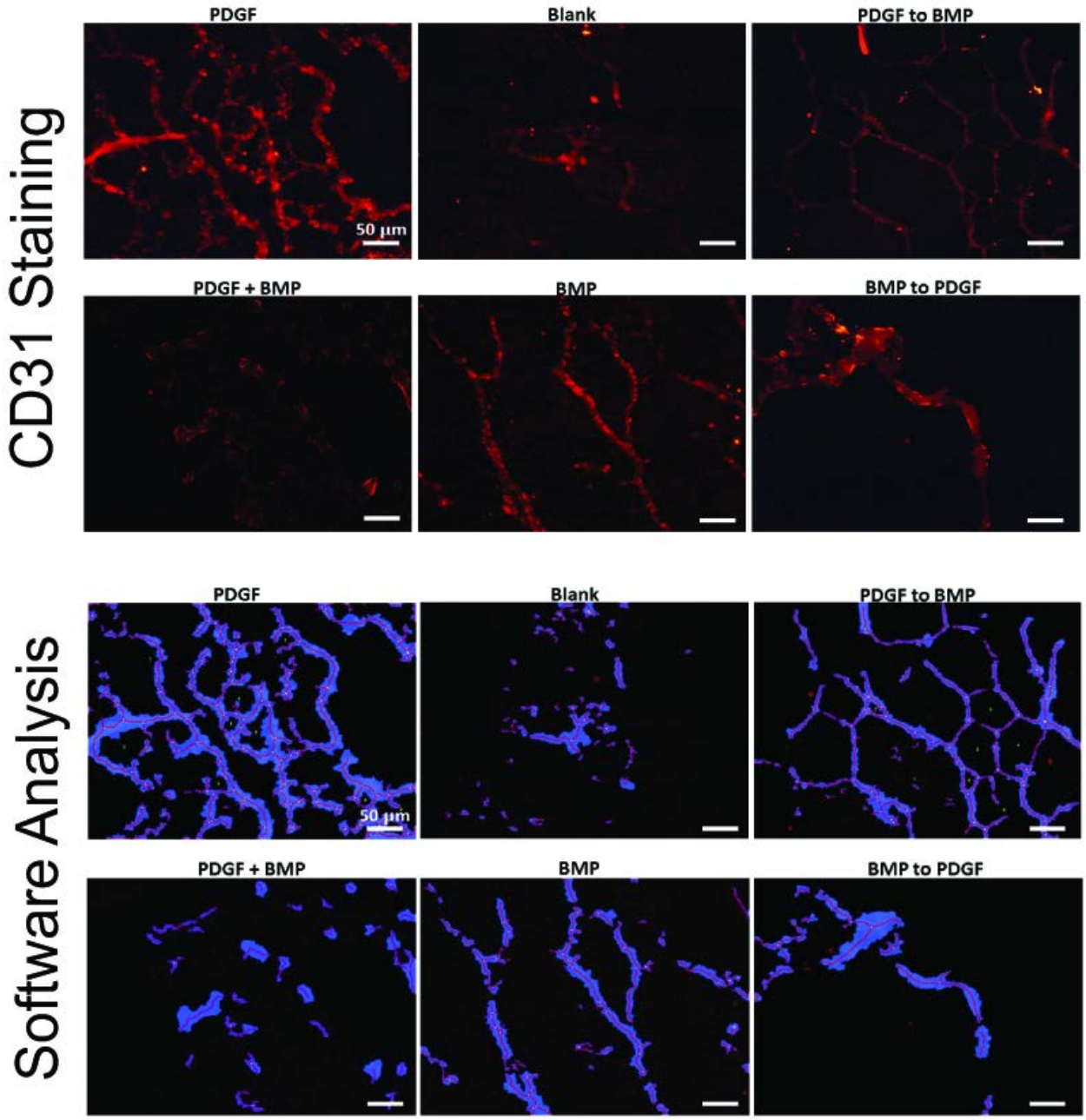

Figure 9. Sequential delivery of PDGF to BMP and delivery of PDGF alone results in organized tubule formation *in vitro*. A) CD31 staining of growth factor delivery groups, and B) software analysis overlay of the same images, showing quantification methods for tubule area, tubule length, branching points, and loops. All scale bars = 50 µm.

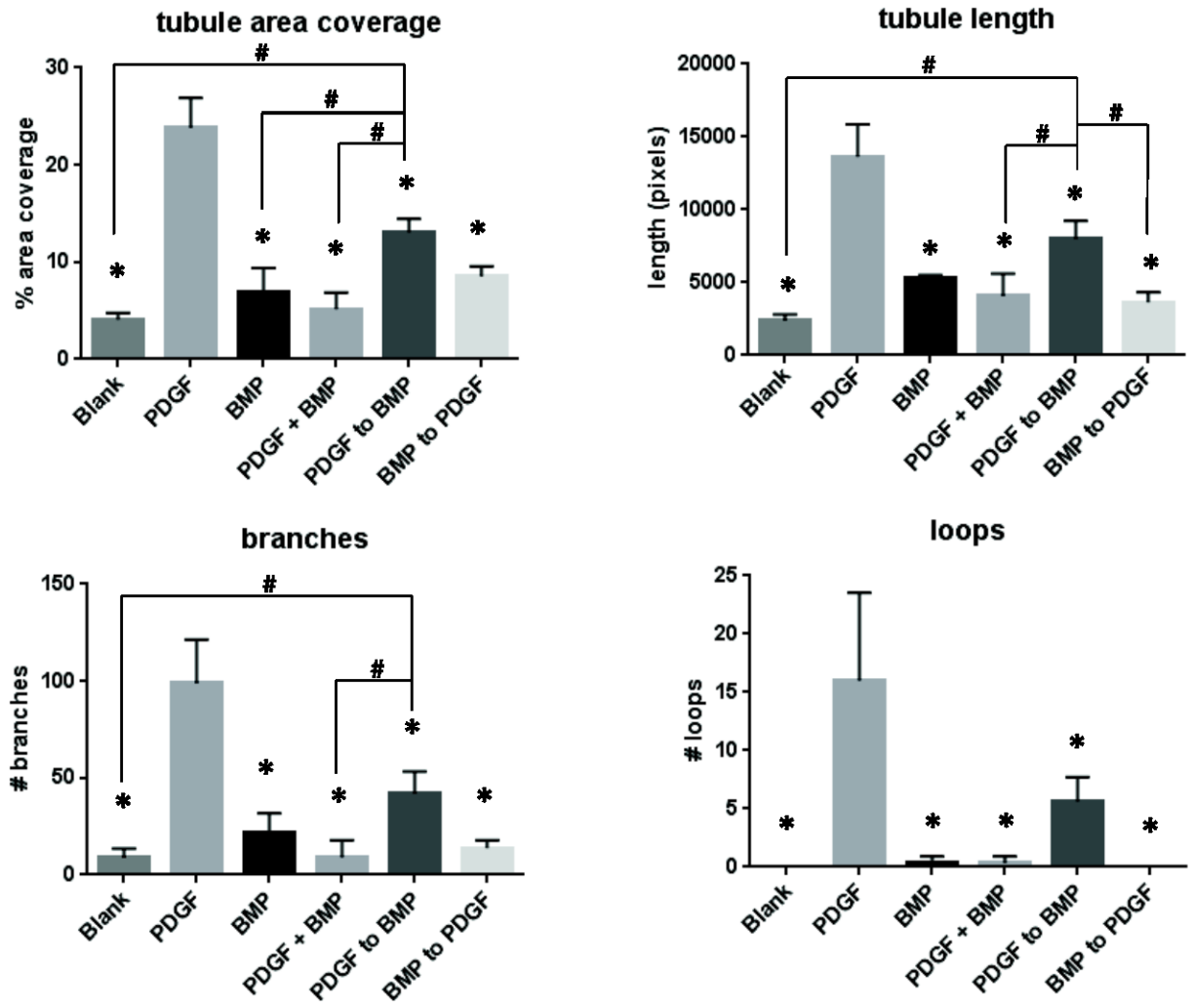

Figure 10. Quantification of tubule area, tubule length, branches, and loops for sequential growth factor delivery groups showing that PDGF delivery alone (positive control) results in significantly greater tubule formation when compared to all other treatment groups at each parameter. Sequential PDGF to BMP delivery results in significantly greater tubule area coverage, tubule length and branching points when compared to several other treatment groups. # indicates significant difference from PDGF to BMP treatment group, * indicates significant difference from PDGF treatment group.(ANOVA followed by post-hoc multiple comparison testing using Tukey's test. A=0.05.

4.3.2 Tubule Formation in Response to Length of PDGF Delivery

Three-dimensional Matrigel plugs in transwell plate inserts were seeded with a 1:1 co-culture of hMSCs and HUVECs to evaluate tubule formation and α-SMA expression in response to various lengths of PDGF delivery when sequentially delivering PDGF and BMP-2. Within the 10-day experimental timeframe, we explored 5 variations in length of PDGF to BMP delivery, with the sequential switch occurring after 1, 3, 5, 7, or 9 days of PDGF delivery (Figure 11). Matrigel sections treated with longer PDGF delivery before the switch to BMP-2 exhibited greater amounts of tubule formation (CD31 staining) and a-SMA expression (Figure 11). As shown in Figure 11, when PDGF was delivered for 7 days before the switch to BMP-2, sections of Matrigel plugs displayed significantly more a-SMA expression as compared to 1, 3, and 5 days of PDGF delivery. When PDGF was delivered for 9 days before the switch to BMP-2, significantly more a-SMA staining was observed as compared to 1, and 3 days of PDGF delivery. Greater amounts of CD31 staining were also observed for 9 days of PDGF delivery as compared to 1, 3, and 5 days. Although tubule lumens were not specifically assayed for in this study, they can be longitudinally observed in “7 days PDGF/3 days BMP” and “9 days PDGF/1 day BMP” frames of Figure 11, and are similar in appearance to longitudinally oriented tubule lumens in similar 3D *in vitro* studies [167, 168].

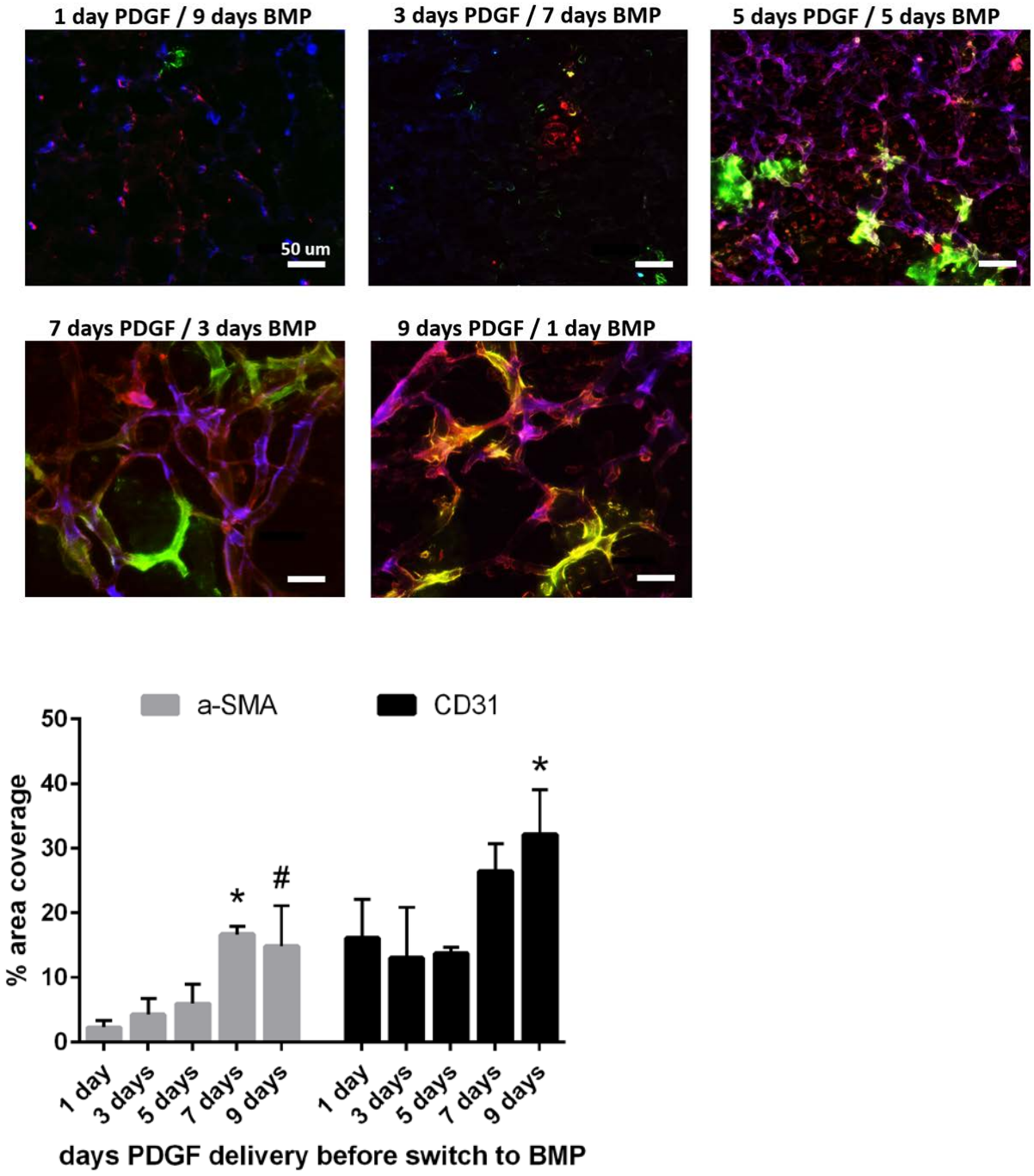

Figure 11. Immunofluorescent staining of CD31 (red), α-SMA (green), and nuclei (blue) of matrigel cross sections suggest that longer PDGF delivery before switch to BMP (7 days, 9 days) results in greater amounts of tubule formation and presence of pericytes * indicates significantly more area coverage vs. days 1,3 and 5. # indicates significantly more area coverage vs. days, 1,3

when compared using ANOVA and Tukey's test for post-hoc comparisons, $\alpha = 0.05$. All scale bars = 50 μm.

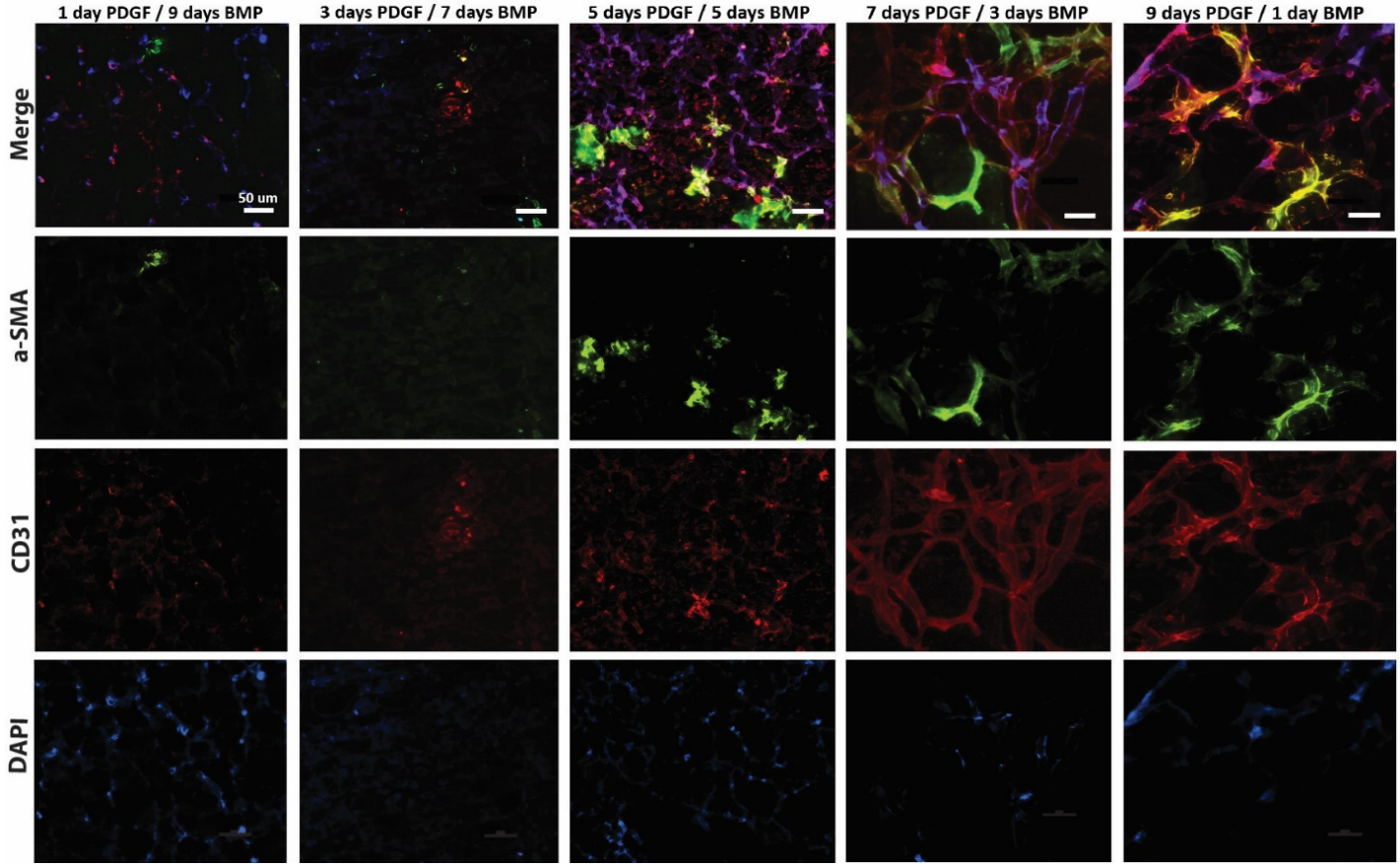

Figure 12. Independent channels for DAPI, CD31 and a-SMA staining for the formation of tubules in response to length of PDGF delivery (merge images comprise Figure 11.)

4.3.3 Tubule Formation in Response to Growth Factor Delivery Overlap

Three-dimensional plugs of Matrigel in transwell plate inserts were seeded with a 1:1 co-culture of hMSCs and HUVECs to evaluate tubule formation in response to treatment groups representing various degrees of growth factor presentation overlap *in vitro* over the 10 day experimental

timeframe. CD31 staining of Matrigel sections revealed that the greatest amount of tubule formation occurred in groups with moderate growth factor overlap (2-4 days of overlap) as shown in Figure 14. In sections representing 4 days of growth factor overlap, a significantly higher amount of tubules (tubule area, length) and greater level of tubule organization (loops, branching points) was observed than in any other experimental group (Figure 14). Sections representing 2 days of overlap were observed to have significantly more tubule area coverage and length than sections representing longer periods of growth factor overlap (8 and 10 days). For purposes of comparison, the 0-day overlap group in Figure 13 corresponds to the same treatment schedule as the "PDGF to BMP" group in Figure 9, and the 10-day overlap group corresponds to the same treatment schedule as the "PDGF + BMP" group in Figure 9.

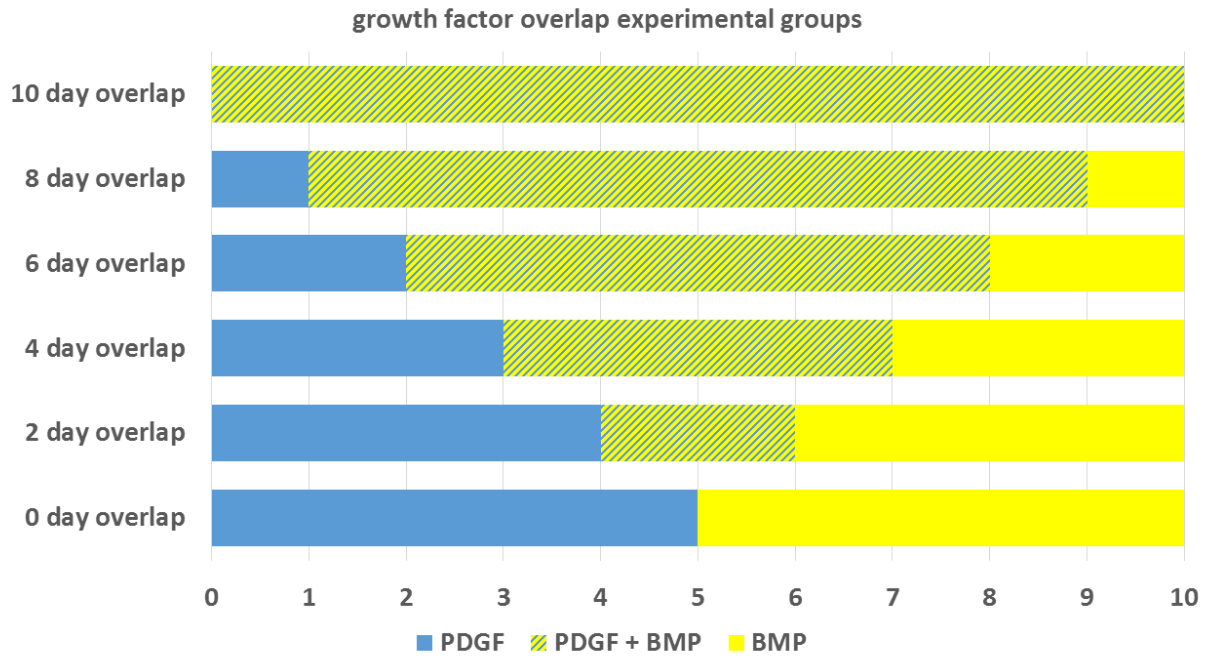

Figure 13. Overlapping growth factor delivery regimens showing type of growth factor delivery per day over 10 days. Growth factors were delivered by pipetting 20 μL of media with concentrations of 10 ng/mL PDGF and/or 100 ng/mL BMP.

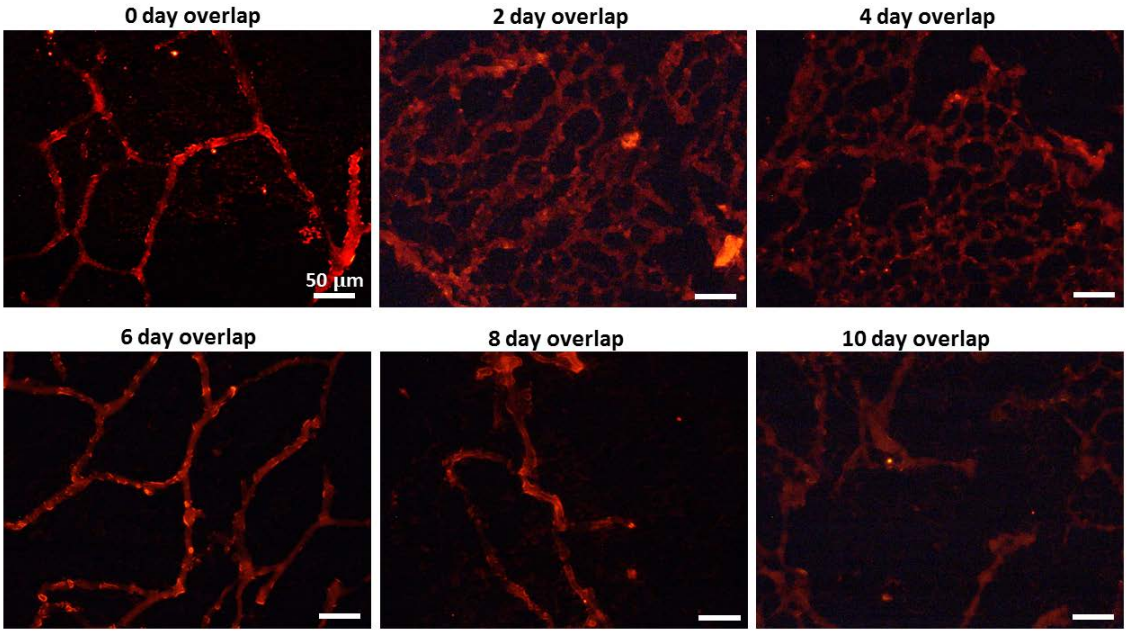

Figure 14. Moderate overlap (2-4 days) in PDGF and BMP delivery results in greater tubule formation (CD31 staining). All scale bars = 50 µm.

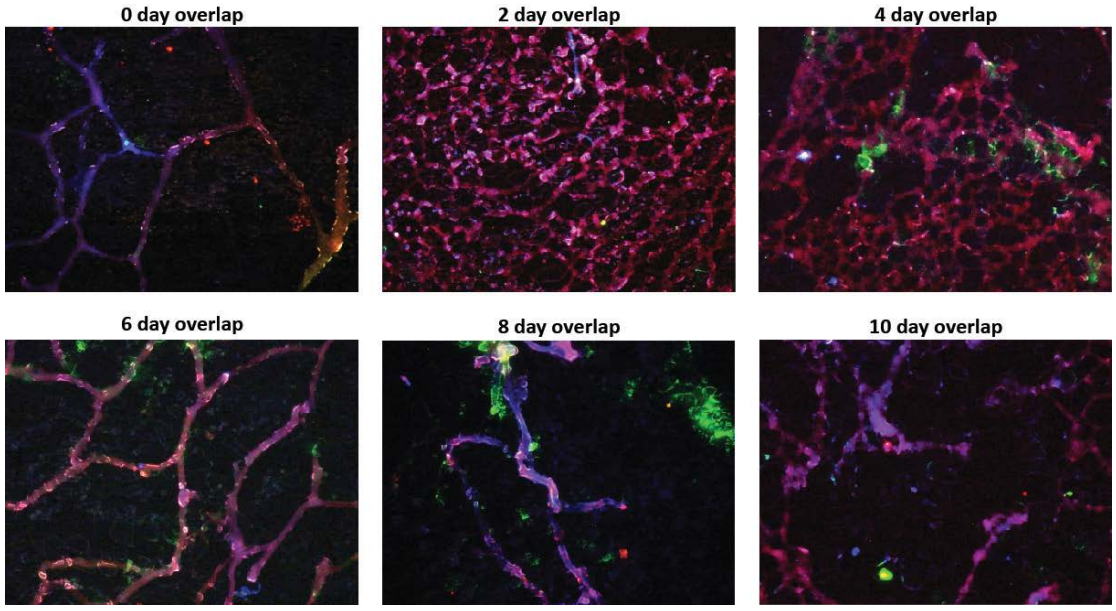

Figure 15. Merged images showing DAPI (blue), CD31 (red) and a-SMA (green) staining of tubule formation in response to degree of overlap in PDGF and BMP delivery (CD31 staining channel comprises Figure 15.)

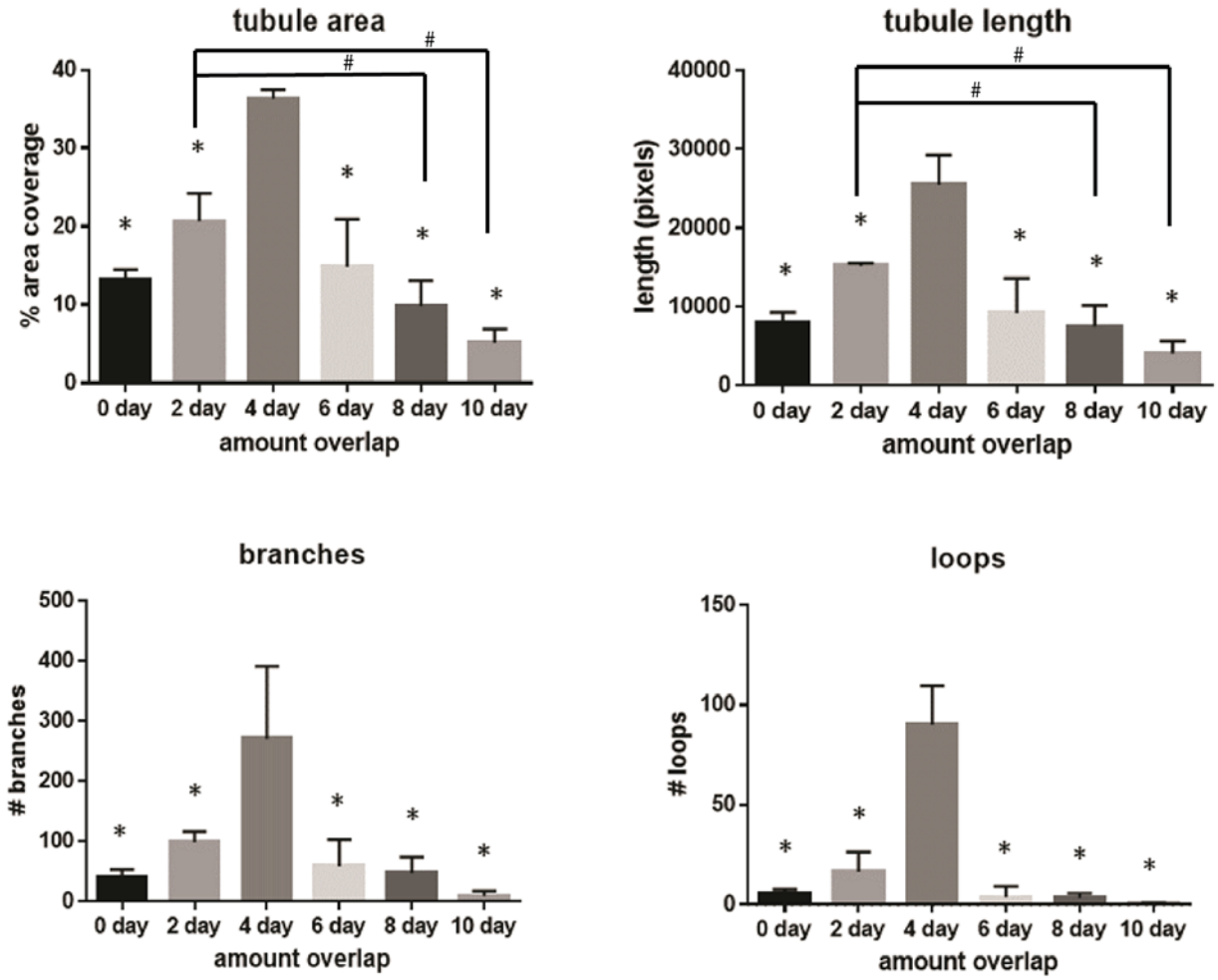

Figure 16. Tubule quantification (area, length, branches loops) of groups represented in Figure 14 showing that 4 days of overlap in growth factor delivery results in significantly greater tubule formation when compared to all other groups for every measured parameter. Additionally, 2 days of overlap in growth factor delivery results in significantly greater tubule area coverage and length vs. 8 days and 10 days of overlap. * indicates significant difference from 4 days overlap, # indicates significant difference from 2 days overlap when compared using ANOVA followed by post-hoc multiple comparisons with Tukey's test. $\alpha = 0.05$.

4.3.4 Tubule Formation in Response to PDGF Dosage

A range of soluble PDGF dosages were delivered to co-cultures of HUVECs and hMSCs over the course of a 5 day experimental time-frame. PDGF dosages ranged from concentration of 0.1 ng/mL to 1000 ng/mL, and were delivered in daily aliquots of 20 μL. In 10 μm slices imaged using a Confocal microscope, it was found that tubules appeared to form best under dosages between 1 ng/mL and 100 ng/mL. Interestingly, both low (0.1 ng/mL) and high (1000 ng/mL) dosages resulted in poor tubule formation.

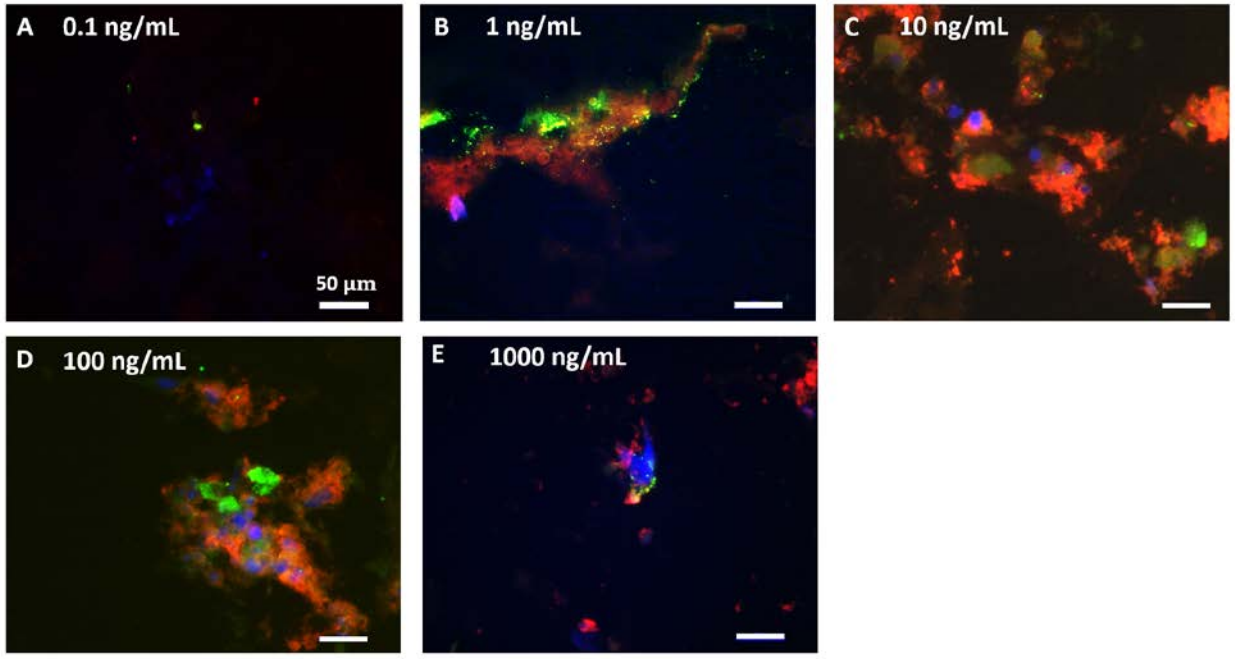

Figure 17. Tubule formation in response to PDGF dosages ranging from 0.1 ng/mL to 1000 ng/mL showing tubule forming in the range of 1 ng/mL to 100 ng/mL.

4.3.5 Collagen-1 Expression in Response to Growth Factor Delivery

Real time qualitative PCR was performed on sequential growth factor delivery groups to assay for the presence of early bone formation indicators. (Supplementary Figure 18). Relative mRNA expression for collagen-1 was found to be significantly lower in every growth factor delivery group as compared to the BMP delivery group (Supplementary Figure 18). Importantly, Matrigel alone (without cells or growth factor delivery) was also tested to investigate possible background levels of collagen-1 present in the Matrigel matrix. For these samples, no collagen-1 mRNA expression was detected, and no amplification was shown over the course of 40 PCR cycles (data not shown.) Additionally, alkaline phosphatase expression was assayed, but not detected in any of the experimental groups (data not shown.)

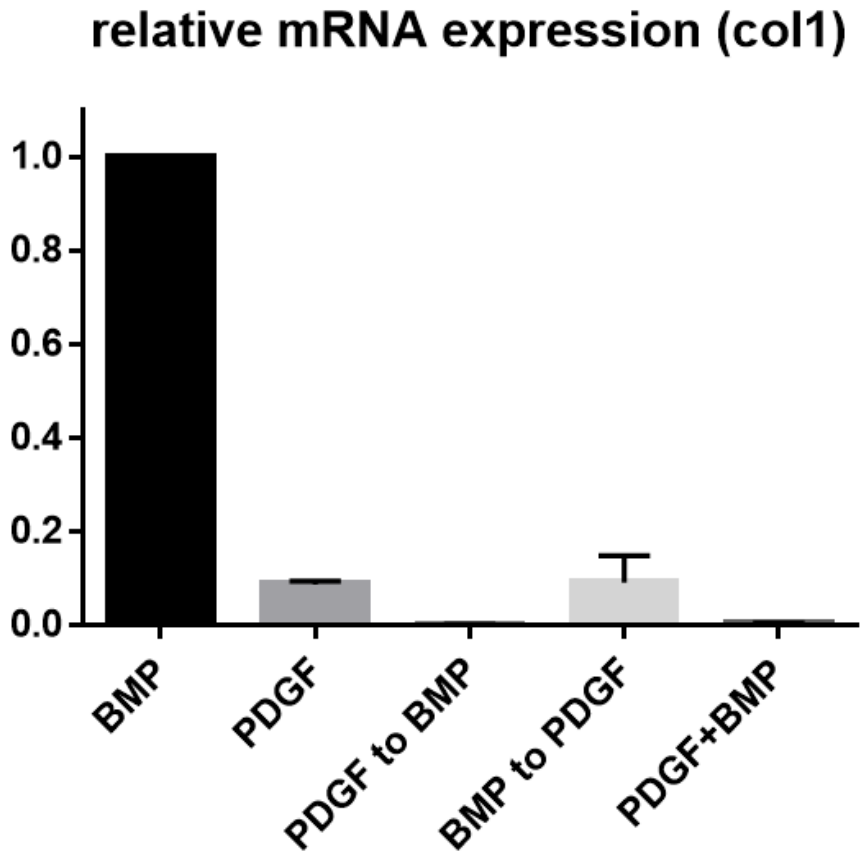

Figure 18. Relative levels of mRNA expression for collagen-1 using 18S as an endogenous control and BMP-2 as the reference sample showing that BMP-2 delivery results in greater collagen one expression compared to other growth factors delivery regimens.

4.4 DISCUSSION

The objective of this study was to determine how the pattern of presentation of angiogenic and osteogenic growth factors affect vascular formation in the context of bone regeneration. While some recent bone regeneration studies design controlled release systems for temporal separation

of growth factors [102, 119, 121], cellular responses to multiple growth factor timing and overlap are otherwise largely uncharacterized. For the purposes of this study, we utilized a 3D Matrigel plug model in order to focus on the sequence, timing, and overlap of two growth factors involved in bone regeneration that influence both angiogenesis (PDGF) and osteogenesis (BMP-2) in co-culture with endothelial cells and mesenchymal stem cells.

The known, potent effect of PDGF on angiogenesis was apparent in our study, which suggests that PDGF delivery alone (for the entire course of the study) results in the greatest amount of tubule formation (Figure 8). Consistent with this, when delivered in sequence with BMP-2, longer PDGF delivery results in greater amount of tubule formation, as expected (Figure 12). PDGF is known to modulate angiogenesis both directly (via endothelial cell PDGFβ receptors)[169] and indirectly (via stimulation of VEGF production from other cell types)[44], mechanisms which have both been observed *in vitro*[169, 170]. In addition to the role of PDGF in supporting angiogenesis, there is also evidence suggesting that PDGF is capable of acting as a chemoattractant for vasculature-stabilizing pericytes, or mural cells [43, 59]. Additionally, it has been shown that MSCs are capable of differentiating into this pericyte phenotype and supporting the maturation of vasculature [164]. In accordance with this information, we observed that when delivering a sequence of PDGF to BMP-2, with increasing length of PDGF delivery, a greater amount of α-SMA+ cells were present (Figure 11), suggesting that some MSCs present in the cell cultures may be acting phenotypically as pericytes, supporting tubule integrity [164]. This is significant, given that the colocalization of α-SMA+ cells with CD31+ cells indicates mature tubule formation [171]. Importantly, the positive α-SMA staining of hMSCs does not conclusively determine their differentiation into perictyes. While positive α-SMA staining coupled with the colocalization of hMSCs in proximity to tubules suggests the possibility of hMSCs acting as

pericytes, microscopic images depicting the presence of cellular projections wrapping the endothelial cells would more definitively indicate a pericyte cellular phenotype [172-174]. By co-culturing HUVECs and MSCs in this model, we add a layer of complexity over single cell culture, including an additional cell type and providing a platform for cellular crosstalk to occur. The HUVEC/MSC co-culture may also be useful in exploring cellular tendency towards bone formation at later timepoints, as MSCs may serve as osteoblast precursors [175].

Due to the stage-wise nature of bone repair, involving early steps of vascular infiltration and cell recruitment (coordinated by PDGF), followed by osteoblast proliferation and mineralization (upregulated by BMP-2) [58], we hypothesized that PDGF delivery followed by BMP-2 delivery would most effectively promote tubule formation. The results illustrated in Figure 9 demonstrate that the PDGF to BMP sequence did indeed result in greater tubule formation than either the reverse sequence (BMP to PDGF) or simultaneous delivery of PDGF and BMP. These results agree with existing studies that also suggest the importance of order in growth factor delivery for stage-wise regeneration [38, 85, 176]. For example, it has been shown that to promote specific, ordered stages of angiogenic repair, certain growth factors must be delivered in a particular sequence (not in reverse or simultaneously) for optimal results [38, 85]. Importantly, it appears that an antagonistic effect may exist between PDGF and BMP signaling, as the simultaneous delivery of these growth factors results in significantly less tubule formation when compared to sequential growth factor delivery (Figure 10.) This is not surprising, given evidence that a molecular antagonism (regulation of microRNA-24 expression) has been observed between PDGF and BMP signaling that controls cellular phenotypes, particularly vascular smooth muscle cell phenotypes [153]. Specifically when considering bone repair, these results are consistent with a previous study that suggests temporal or spatiotemporal separation of angiogenic and

osteogenic growth factors is beneficial for both the vascularization and mineralization stages of healing [176].

While complete overlap in PDGF and BMP-2 delivery resulted in poor tubule formation, we observed that some degree of overlap in the transition from PDGF to BMP-2 delivery may be beneficial for tubule formation (Figure 12). Greater amounts of tubule formation were observed when there was a 2-4 day overlap in growth factor delivery as compared to a "hard transition" in growth factor delivery, with no overlap in the sequence of PDGF to BMP-2 (Figure 12). This observation may be explained, in part, by how biological cascades of growth factors are regulated and expressed *in situ*. In the general wound healing model, there is evidence that growth factors are expressed in a cascading fashion, with overlapping waves of expression that may coincide for a few hours to days [177, 178]. Likewise, it has been shown that phases of bone healing and remodeling are not discrete stages, but instead, have some amount of overlap in transition [90, 179]. In addition to these observations, moderate overlap (2-4 days) in PDGF and BMP-2 delivery resulted in greater tubule formation than longer periods of overlap (6-10 days, Figure 12), which agrees with literature suggesting that the prolonged expression of PDGF may be deleterious for mineralization stages bone formation [65, 180, 181], and therefore, may be most effective when restricted to earlier healing stages.

Importantly, a baseline amount of CD31+ staining was observed in each experimental group, including Matrigel constructs with no delivered PDGF or BMP-2. This may be explained by the minor amount of growth factors found in Matrigel, including transforming growth factor beta (TGF-β) and insulin-like growth factor 1 (IGF-1) [182]. However, these low levels of background growth factors are not predominantly responsible for tubule formation, as there were statistically significant differences observed across experimental groups based on the presence or

absence of PDGF and BMP-2 (Figure 10). Additionally, according to the manufacture's analysis (Corning), concentrations of growth factors in the Matrigel used in these experiments range from 0.1 pg/mL - 5 ng/mL (one to six orders of magnitude less than the quantities of PDGF and BMP-2 used). In addition to Matrigel, additional biomaterials were considered as matrices for conducting cell-based assays, including collagen-1 and hyaluronic acid. Collagen-1 (Rat tail collagen-1, Fisher Scientific) was investigated as a possible alternative three-dimensional matrix for tubule formation. However, it was found to considerably shrink in size over the course of the ten day study (data not shown), limiting the experimental time-frame, and prohibiting endpoint assays for tubule formation. This shrinkage in size of the hydrogel has been observed in other studies, and is attributed to the contraction of collagen via cellular activity during successful wound healing [183]. In addition to these hindrances, collagen-1 is major component of avascular tissues *in vivo,* such as cartilage, ligament and fascia [184-187], suggesting it may not be the optimal material for conducting tubule formation assays. A hyaluronic assay matrix (Hystem, Sigma Aldrich) was also investigated for potential use as a template for 3D cell assays. During immunofluorescent analysis of tubule formation, it was found that the hyaluronic acid-based matrix had a tendency to autofluoresce, confounding results (data not shown). Like collagen-1, hyaluronan too, is commonly found in avascular tissues, including cartilage and connective tissues [188-190]. Another downfall of using a single component of ECM, such as collagen or hyaluronan is the oversimplification of the complex extracellular matrix [191]. A potential method for avoiding this oversimplification is to incorporate several matrix components through the use of decellularized matrix as a three-dimensional cell-culturing system. However, while decellularized matricies represent native ECM composition and structure, its procurement requires biological, chemical, and physical methods of treatment to fully remove cellular

material [191]. In comparison to decellularized ECM, Matrigel may more accurately recapitulate a native healing environment because of its combination of ECM components and low levels of growth factors [161, 192]. Given the challenges and limitations associated with alternative matrix materials, Matrigel was chosen as the biomaterial to be used in all *in vitro* three-dimensional assays.

Our current investigation of growth factor presentation on tubule formation suggests that PDGF and BMP-2 presentation patterns do indeed play a role in angiogenesis, by affecting the quantity and organization of tubules. Due to the flexibility of our model, further studies to explore the effects of growth factor timing on a variety of cell types is possible. To assess the impact of growth factor delivery schemes on the expression of bone markers and later stages of mineralization, future studies will focus on later timepoints (14-28 days) when these effects become apparent. Importantly, the evaluation of later time-points may provide additional information on how earlier growth factor timing patterns affect downstream healing activity, such as the eventual mineralization of bone. Additional cell types and growth factors can also be explored, along with *in vivo* validation, as there are many factors involved in fracture healing aside from those explored in this study. While this model provides a controllable *in vitro* system to evaluate cellular responses, the complexity of the system can be increased to better recapitulate an *in vivo* environment. Ultimately, *in vivo* validation studies must be performed in the future to confirm these results.

4.5 CONCLUSIONS

In summary, in this chapter, we have demonstrated the utilization of a three dimensional, *in vitro* model that permits the exploration of the effects of growth factor timing on vascularization in the context of bone repair with a large degree of variables. Specifically, with this system, we were able to evaluate resulting tubule formation from variations in sequence, length, and degree of overlap in growth factor delivery. We observed that the sequence of angiogenic (PDGF) to osteogenic (BMP-2) presentation resulted in greater tubule formation that the reverse presentation or co-delivery of these growth factors. Additionally, moderate overlap (2-4 days) in the sequence of PDGF to BMP-2 delivery resulted in greater tubule formation in comparison to the absence of overlap as well as prolonged overlap. This approach may be further applied to investigate the effects of growth factor timing, overlap, and sequence on additional cell types, later time points to gather information that may lead to improved *in vivo* outcomes. The resulting information could serve as a valuable contribution to our understanding of the effects of growth factor timing and sequence in the bone regeneration niche, and ideally, advance the development of growth factor therapies for fracture repair.

5.0 FABRICATION OF CONTROLLED GROWTH FACTOR DELIVERY SCAFFOLDING

5.1 INTRODUCTION

In previous chapters, we have discussed several strategies for improved bone regeneration. Currently, the gold standard treatment of fracture non-unions is currently autografting [193]; because these grafts are taken from the patient's own body, it serves as a non-immunogenic, osteogenic, osteoconductive, osteoinductive graft, delivering osteoblast precursors and growth factors to the site of healing [10, 194]. However, although autografts are an effective, gold-standard treatment, there are several drawbacks associated with them, including secondary surgical sites, and increased likelihood for blood loss and infection [195, 196]. To overcome these limitations while still providing instructive cues from growth factors to jumpstart fracture repair, biomaterials (such as collagen sponges) loaded with bone morphogeneic protein 2 (BMP-2) have been approved for clinical use in 2004 [197]. Delivering exogeneous BMP-2 stimulates bone healing through the proliferation and differentiation of pre-osteoblasts [48], and in the past 12 years of its clinical use, has proven very effective. However, due to short half-life of BMP-2 (~6.7 minutes) [197], to achieve results, the concentrations of BMP-2 delivered using these methods is approximately 1 million times physiological concentrations [197], and therefore may lead to complications, such as presentation to neighboring tissues and ectopic bone formation [198]. To mitigate these complications, a variety of methods for more controllably delivering BMP-2 have been explored,

one of which is its encapsulation in polymers [45]. Through these methods, BMP-2 may be delivered in lower concentrations to the target tissue over an extended period of time.

While the extended, controlled delivery of BMP-2 has shown to be effective for stimulating the proliferation and differentiation of pre-osteoblasts for the ultimate formation and mineralization of bone tissues [31], another critical stage of fracture healing, angiogenesis, may also benefit from the programmed release of an angiogenic factor. If an angiogenic growth factor could be controllably delivered alongside BMP-2, angiogenesis may increase in synthetic scaffolding, and lead to more successful healing outcomes. Because recent evidence is starting to show that recreating the biological cues that orchestrate the regenerative process is not as simple as delivering two (or more) growth factors simultaneously (Chapter 3), the spatiotemporal separation of angiogenic and osteogenic growth factor through controlled release may represent a reasonable approach for manipulating growth factor presentation. In support of this idea, the work of Chapter 4 demonstrates that the timing, dosage, sequence and overlap of PDGF and BMP-2 delivery impacts early angiogenic tubule formation. These recent results are fascinating because they suggest that the absence of a signal at a given period of time may be equally important to the presence of that signal at another time. To translate these findings into a system capable of further testing and potential clinical application, it is essential to engineer a system of autonomously delivering the growth factors according to the parameters in Chapter 4. Additionally, to provide a substrate for new bone growth, it is important to incorporate these growth factor delivery systems within a scaffolding construct.

To explore the possibility of creating such a scaffold, we employed the use of three biomaterials in combination to fabricate a scaffold capable of controllably releasing a desired series of growth factors. For the main structure of the scaffold, we used a formulation of calcium

phosphate, a biomaterial that is well-recognized for its osteoconductive properties, biocompatibility, and chemical similarity to bone composition (among other attributes) [199-201]. By combining calcium phosphate cement with PLGA microspheres, we were able to create a three dimensional scaffold with an interconnected porous network. Alginate hydrogels and microspheres were used to release a schedule of PDGF and BMP-2 delivery, previously found to effectively promote the formation of robust, organized, angiogenic tubules *in vitro* (Chapter 4). In addition to characterizing this scaffold and its release properties, further *in vitro* studies explored the capability of this scaffolding system to stimulate cellular infiltration of the scaffold, induce tubule formation and organization, and promote osteogenic differentiation. We hypothesize that releasing a programmed schedule of PDGF and BMP-2 (rather than an unorganized presentation of growth factors) will have the potential to promote both the formation of angiogenic tubules by HUVECs and the osteogenic differentiation of hMSCs. Further, the incorporation of this controlled release schedule from an osteoconductive calcium phosphate scaffold may encourage cell infiltration of the scaffold. This, together with the promotion of angiogenic tubule formation and osteogenic differentiation, will aid in the creation of a scaffold capable of orchestrating both the angiogenic and osteogenic phases of bone regeneration.

5.2 MATERIALS AND METHODS

In the following experiments, we aimed to characterize growth factor release behaviors from microsphere and hydrogel formulations and fabricate a porous, three-dimensional hybrid alginate-calcium phosphate scaffold capable of controllably releasing a schedule of PDGF and BMP-2

delivery. Additionally, we aimed to assess cellular responses to growth factor release schedules from this hybrid scaffold.

5.2.1 Scaffold Fabrication

To fabricate the porous, three-dimensional hybrid alginate-calcium phosphate scaffold, we first custom-fabricated spherical poly-lactic-co-glycolic PLGA microspheres as a porogen. Alginate microspheres and hydrogels were fabricated to controllably release PDGF and BMP-2. These components were then incorporated into the porous calcium phosphate scaffolding as follows:

5.2.1.1 PLGA Particle Fabrication for Scaffold Porogen

Blank PLGA microspheres (not containing any growth factor) were fabricated using a double emulsion evaporation procedure. 200 mg of PLGA polymer (poly(D,L-lactide-co-glycolide), 24-36 kD, 50:50 lactide:glycolide, ester terminated, Sigma-Aldrich) was dissolved in 4 mL dichloromethane (Sigma-Aldrich). Dissolved PLGA was then sonicated with 200 μL of deionized water, then pipetted dropwise through a 250 μm sieve into a solution of 1% polyvinyl alcohol in deionized water (Polysciences, Inc.) spinning at 400 rpm. Following dichloromethane evaporation (3 hrs), microspheres were collected via centrifugation, washed four times with deionized water, frozen, and lyophilized.

5.2.1.2 Hydrogel Fabrication for PDGF Release

Alginate hydrogels were fabricated by mixing 30 mg of medium viscosity sodium alginate (MP Biomedicals, LLC) into 3 mL of deionized water until alginate was fully dissolved to constitute a 1% solution. A 30 μL aliquot 200 μg/mL of soluble PDGF-BB (Thermo Fisher) was then gently, homogeneously stirred into each 200 μL of alginate solution. Once the aliquot of growth factor was homogenously mixed into the alginate solution, the hydrogel was chemically crosslinked with 1 mL of 700 mM calcium chloride (Fisher Scientific) for 10 minutes. Following crosslinking, the hydrogels were washed with deionized water to remove excess crosslinking solution.

To produce a hydrogel with a reasonably consistent thickness and shape, 200 μL aliquots of 1% alginate + PDGF were transferred to a flat-bottom 96-well plate (Corning). A rounded disk of medium porosity, medium flow rate filter paper (Fisher Scientific) was place atop the alginate hydrogel, and 700 mM calcium chloride crosslinker was added dropwise on top of the filter paper to allow slow, even crosslinking of the hydrogel. Several other methods of creating hydrogels of consistent thickness were explored (Figure 27), however, the above described method was found to produce hydrogels most consistently.

Release behavior was assayed for three different conditions: from a 1% alginate hydrogel, from a 1% alginate hydrogel applied as a coating the ReCaPP scaffold.

5.2.1.3 Microsphere Fabrication for BMP-2 Release

Single emulsion alginate microspheres were fabricated by mixing 300 mg of sodium alginate in 10 mL of deionized water until alginate was fully dissolved to constitute a 3% alginate solution.

A 200 μL aliquot of 100 μg/mL soluble BMP-2 (Shenandoah) in deionized water was homogeneously mixed into the alginate solution. The BMP-2 -alginate solution was then placed into 5 mL syringes and left undisturbed for 30 minutes to remove air bubbles from the solution. Once bubbles were removed from the alginate solution, alginate was added dropwise into 2.5% solution of Span 80 in iso-octane and homogenized at 5000 RPM. Next, 3 mL of 30% Tween 80 in iso-octane was added and homogenized at 5400 RPM. 700mM calcium chloride solution was then used to crosslink the particles, which were further cured with 2-propanol. Following fabrication, the particles were collected via centrifugation, washed twice with 2-propanol, then washed 3 times with deionized water. Collected particles were then frozen and lyophilized.

5.2.1.4 Preparation of Cement Powders and Liquid

To produce ReCaPP cement powder, alpha-tri-calcium phosphate (α-TCP, pure phase, Sigma-Aldrich), calcium carbonate (99%+, Acros Organics), calcium sulfate di-hydrate (99%+, Acros Organics) and disodium hydrogen phosphate (99%+, Sigma-Aldrich) were mixed in an agate mortal-pestle for 30 minutes and stored in 50 mL Falcon Tubes for use. The composition of the cement powder consisted of ratios of 72.7% α-TCP, 9.1% calcium carbonate, 9.1% calcium sulfate di-hydrate, and 9.1% disodium hydrogen phosphate, by weight.

The liquid component of the cement (nano-CaPs) is a colloidal solution of nano-sized calcium phosphate homogeneously dispersed in a buffer solution. On a per-millileter basis, this solution is created by adding 500 μL of 0.75 M CaCl2 dropwise into 500 μL of phosphate precursor solution. Phosphate precursor solution consisted of 0.357 M NaCl (99.5%+, Fisher Scientific), 13 mM KCl (99%+, Fisher Scientifict), 15 mM dextrose monohydrate (Fisher

Scientific), 64 mM HEPES free acid (99.5%+, Sigma-Aldrich), and 1.91 mM Na3PO4.12H2O (98%+, Acros Organics).

5.2.1.5 Hybrid Scaffold Fabrication

To fabricate hybrid, three-dimensional scaffolding consisting of calcium phosphate cement, BMP-2-releasing microspheres, and PDGF-BB-releasing hydrogel, first a porous cement scaffold was created by mixing 100 μm PLGA microspheres with ReCaPP cement powder in a ratio of 20 mg microspheres to 30 mg ReCaPP. When used in cell-culturing assays, the cement ReCaPP powder and microsphere mixture was sterilized via UV light for 30 minutes. To form scaffolds 33 uL of liquid nano-CaPs was mixed into the ReCaPP-microsphere powder. This slurry was then compressed in a cylindrical mold to create disks. After initial setting, the resulting tablet was dried at 37^{O}C overnight. The 50 mg tablet scaffolds were then placed in three successive washes of dichloromethane for 10 minutes each to completely dissolve PLGA microspheres from the scaffold. After the last wash of dichloromethane evaporated, scaffolds were then rinsed in deionized water three times to remove residual dichloromethane and dried at room temperature.

To infiltrate the ReCaPP cement scaffold with BMP-2-alginate microspheres, scaffolds were placed in a glass Pyrex dish with a solution of 10 mg of BMP-2-alginate microspheres in 500 μL deionized water. Pyrex dishes were then placed in the water bath of a Bronson 1510 sonication bath, and sonicated at full power for 30 minutes. Following BMP-2-alginate microsphere infiltration, scaffolds were frozen and lyophilized for 24 hours.

A PDGF-BB-releasing hydrogel was applied to the scaffolds as an outer coating by submerging scaffolds for 10 minutes in a 1% alginate solution, which was fabricated as described previously

in “Hydrogel Fabrication for PDGF-BB Release.” For scaffolds used in cell culture, 10 μL of 200 μg/mL PDGF-BB was mixed into each 100 μL solution of alginate coating. Alginate solutions and calcium chloride crosslinking solutions were both UV sterilized prior to cell culture use. Once PDGF-BB alginate coatings were applied to porous ReCaPP scaffolds, they were crosslinked by submerging the scaffolds in a 700 mM calcium chloride solution for an additional 10 minutes. Completed, crosslinked scaffolds were rinsed in deionized water to remove residual calcium chloride solution.

5.2.2 Scaffold Degradation Analysis

To determine degradation rates of the scaffold, particularly the growth factor-containing alginate components, scaffolds were fabricated by mixing 40 mg alginate microspheres with 60 mg ReCaPP cement powder. For purposes of the degradation study, BMP-2 was not encapsulated in the alginate microspheres. The ReCaPP/alginate microsphere mixture was then mixed with 150 μL of liquid nano-CaPs, compressed in a cylindrical mold, and allowed to dry overnight at 37^{O}C. The following day, a 1% alginate hydrogel was applied as a coating to the scaffolds, as described in “Hybrid Scaffold Fabrication.” Scaffolds were placed in 1.5 mL lo-bind Eppendorf tubes with 1 mL phosphate buffered saline (PBS) and subject to end-over-end rotation at 37^{O}C. PBS solution was removed daily and replaced with fresh PBS. Scaffolds were removed from solution at experimental timepoints (days 1-10, 15, 20, 40) and frozen in liquid nitrogen, and lyophilized for dry weight measurement.

5.2.3 Controlled Growth Factor Release Assay

To determine the release rate of BMP-2 from alginate microspheres, 10 mg of alginate microspheres were suspended in 1 mL of PBS in a lo-bind Eppendorf tube and subject to end-over-end rotation at 37^{O}C. At predetermined experimental time-points, particle suspensions were centrifuged at 1000 RPM and supernatant was collected and frozen at -20^{O}C. Fresh PBS was added, particles were re-suspended, and again end-over-end rotated at 37^{O}C. At the conclusion of the study, all frozen supernatant samples were thawed and assayed for BMP-2 concentration using a human BMP-2 ELISA assay (R&D Systems).

To determine the release rate of PDGF-BB from alginate hydrogels, 200 μL hydrogel samples were submerged in 1 mL of PBS release solution in a lo-bind Eppendorf tube and subject to end-over-end rotation at 37^{O}C. PBS release solution consisted of PBS supplemented with SDS (50mM) and 0.1% BSA to further prevent released PDGF-BB from sticking to the Eppendorf tube. At predetermined experimental time-points, hydrogel samples were either removed and/or centrifuged to separate the samples from the PBS solution supernatant. Collected supernatant samples were frozen at -20^{O}C until the conclusion of the experiment, whereupon they were thawed and analyzed for PDGF-BB content using a PDGF-BB ELISA assay (R&D Systems).

5.2.4 Tubule Formation in Repsonse to Controlled Release Growth Factor Delivery

Well inserts of 8 μm, 24-well transwell plates (Sigma-Aldrich) were filled with 250 μL of growth factor reduced, phenol-free Matrigel (LDEV free, Fisher Scientific). Human umbilical vascular endothelial cells (HUVECs, Lonza) and human bone marrow-derived mesenchymal stem cells (BM hMSCs, Life Technologies) were seeded at a density of 1.5 x 10^5 cells per well, in a 1:1

(hMSC : HUVEC) ratio. The lower reservoirs of MSC-HUVEC co-cultures we filled with 500 μL of a 1:1 ratio of endothelial basal media (Lonza) and minimum essential media (Life Technologies) supplemented with 1% penicillin-streptomycin (Life Technologies) and 1% antibiotic-antimycotic (Life Technologies) to provide hydration to Matrigel plugs.

For positive control experimental groups, soluble growth factors were delivered by daily hand-dosing of PDGF-BB and BMP-2 concentrations to closely match growth factor release profiles of PDGF-BB and BMP-2 delivered by controlled release mechanisms. For controlled release experimental groups, 100 μL alginate hydrogels were embedded within the Matrigel to release PDGF-BB.

At the conclusion of the experimental timeframe (7 days), Matrigel plugs were removed from transwell inserts, embedded in TissueTek (Fisher Scientific) and snap frozen in liquid nitrogen. Frozen sections (10 μm) were incubated with primary antibody mouse anti-human CD31/PECAM-1 (R&D Systems) and secondary antibody donkey anti-mouse IgG (R&D Systems) to identify endothelial cell activity and vessel formation. Images of CD31-stained sections were taken at 20X and 10X using a Nikon inverted light microscope, then analyzed using WimTube software (Wimasis Image Analysis, GmbH). Images at a magnification of 10X were used for analysis to gain a larger representative sample area. WIMASIS software was used for analysis of four parameters for every image: total area covered by vessels, total length of vessels, number of branching points, and number of closed loops.

To identify MSC differentiation towards a pericyte phenotype when exploring length of PDGF delivery, slides were incubated with primary antibody rabbit anti-alpha smooth muscle actin (ab5694, Abcam) and secondary antibody goat anti-rabbit IgG H&L (Alexa Fluor 488, Abcam). Images of slides were taken at 20X using a Nikon inverted light microscope.

5.2.5 Cellular Infiltration of the Scaffold in Response to Growth Factor Delivery

Alginate hydrogels were prepared as described in Materials and Methods Section 5.1.1.4. Four growth factor delivery groups were explored: hydrogels releasing no growth factor (No GF), hydrogels releasing PDGF alone (PDGF), hydrogels releasing BMP-2 alone (BMP-2), and hydrogels releasing both PDGF and BMP-2 at the same time (PDGF+BMP) Hydrogels were placed in transwell inserts of an 8 μm 24-well transwell plate (Sigma Aldrich). Atop each hydrogel, porous ReCaPP scaffolds were placed into each transwell insert, and snugly fit to prevent liquid leakage between the scaffold and transwell insert wall. Prior to fitting ReCaPP scaffolds in transwell inserts, scaffolds were soaked in a solution of 1% BSA in PBS to encourage cell attachment to scaffold surfaces. A co-culture of HUVECs and hMSCs were then seeded atop porous ReCaPP scaffolds. Lower transwell reservoirs were filled with 500 μL of media () to provide hydration to the alginate hydrogels. At the end of the experimental time-frame (7 days) scaffolds were removed from transwell inserts, snap-frozen in liquid nitrogen and lyophilized. Subsequently, scaffolds were broken in half to image vertical cross-sections. Scaffolds were sputter coated and imaged with a Scanning Electron Microscope.

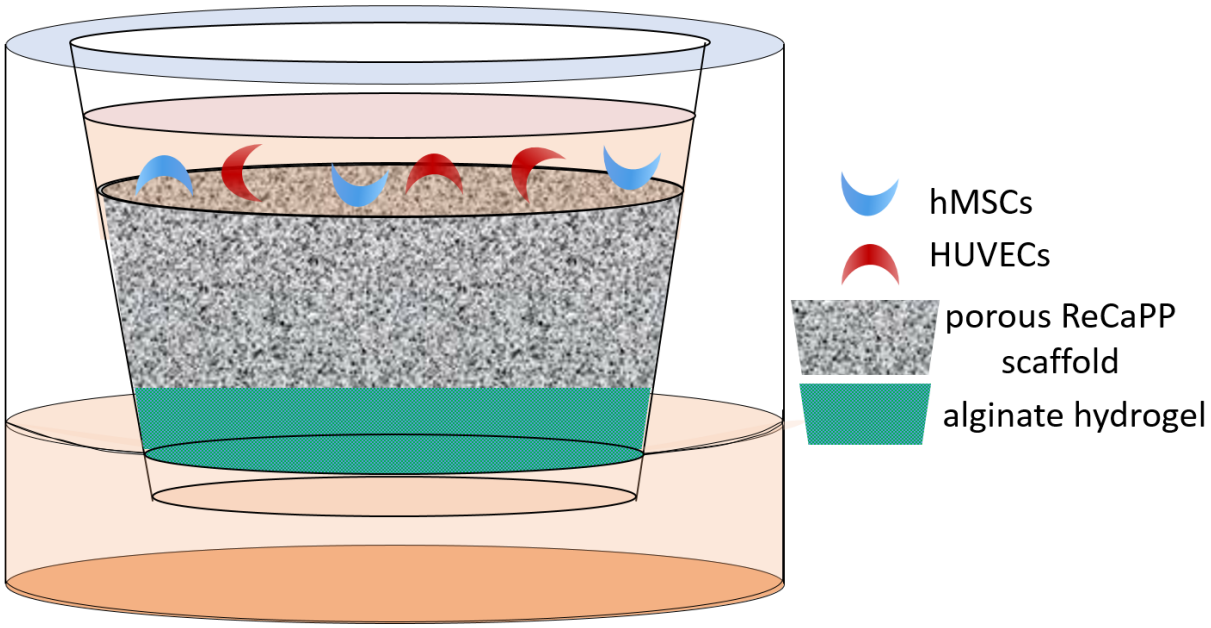

Figure 19. Schematic of transwell set up used to assay cell infiltration in response to growth factor releasing alginate hydrogels.

5.2.6 Alkaline Phosphatase Expression in Response to Growth Factor Delivery

Lower surfaces of a 8 μm 24-well transwell plate (Sigma Aldrich) were seeded with bone marrow-derived human mesenchymal stem cells (BM hMSCs, Life Technologies) at a density of $1x10^4$ cells per well. Each well was filled with 1 mL of α-MEM media (Life Technologies) supplemented with 1% penicillin-streptomycin (Life Technologies) 1% antibiotic-antimycotic (Life Technologies) and 10% fetal bovine serum (Fisher Scientific) which was changed every 2-3 days throughout the experiment. Transwell inserts contained the following experimental scaffold groups: ReCaPP scaffold with no additional growth factor (No GF), ReCaPP scaffold with PDGF-BB-eluting alginate hydrogel (PDGF), ReCaPP scaffold with BMP-2-eluting alginate microspheres (BMP), and ReCaPP scaffold with PDGF-BB-eluting alginate hydrogel and BMP-

2-eluting alginate microspheres (PDGF to BMP). After scaffolds we placed in transwell inserts, 100 µL of media was added to hydrate the scaffold and facilitate release of growth factors from hydrogels and miscropheres.

At each experimental time-point (7 days, 14 days, 21 days, 28 days) transwell inserts were removed, media was aspirated, and cells were assayed for alkaline phosphatase (ALP) expression using an AP Staining Kit (System Biosciences). Following staining, wells were imaged using a Nikon Inverted Light Microscope at 20X magnification.

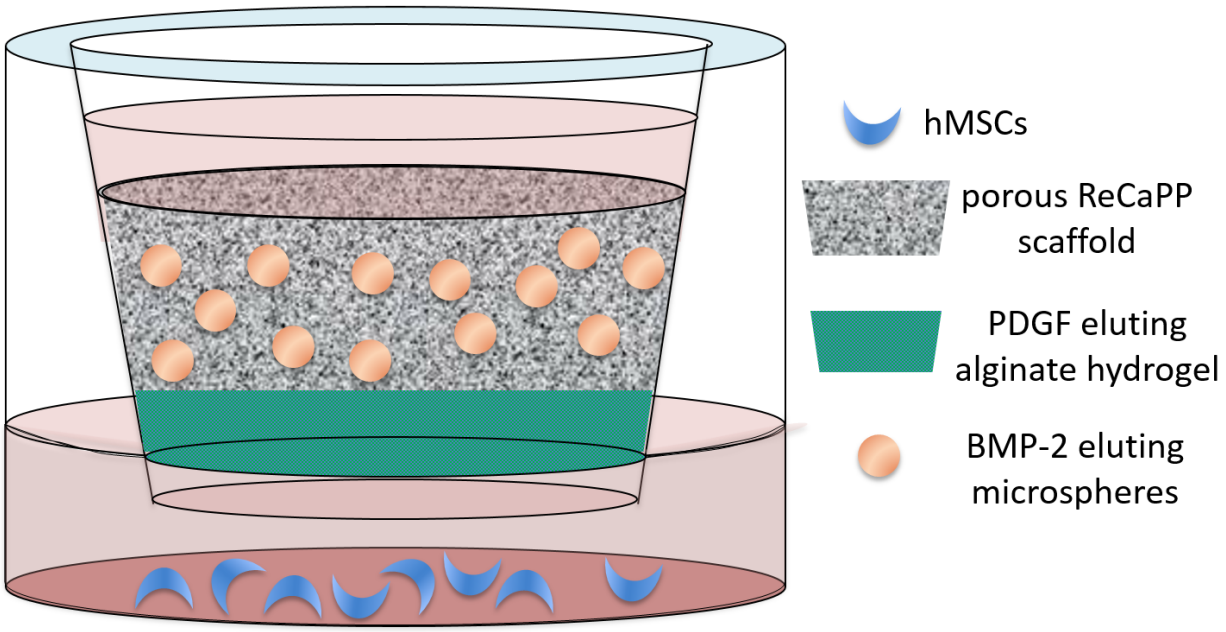

Figure 20. Schematic of transwell set-up used to assay alkaline phosphatase expression in response to PDGF eluting alginates hydrogels and BMP-2 eluting alginate microspheres.

5.3 RESULTS

Several biomaterials (calcium phosphate, alginate, and PLGA) and processing methods were used to fabricate a three-dimensional porous scaffold capable of controllably releasing a predetermined schedule of PDGF and BMP-2 release. We observed that a co-culture of HUVECs and hMSCs infiltrated the calcium phosphate scaffold in repsonse to a PDGF gradiant presented from an alginate hydrogel coating. Additionally, controlled PDGF release promoted similar angiogenic tubule formation in comparison to hand-delivered PDGF schedules. Scaffolds controllably releasing PDGF and BMP-2 stimulated the production of alkaline phosphatase, indicated the tendency of hMSCs towards an osteoblastic phenotype.

5.3.1 Hybrid Scaffold Fabrication

PLGA microspheres were fabricated to be morphologically spherical, with a smooth surface and average size of 90-100 μm in diameter (Figure 21). Miscrospheres were mixed with ReCaPP powders and liquids, compressed, and hardened overnight, resulting in a tablet-shaped ReCaPP scaffold with embedded PLGA microspheres (Figure 22). By mixing these miscropheres with ReCaPP cement powders in a ratio of 40 mg microsphere to 60 mg ReCaPP powder by weight, and subsequently dissolving PLGA microspheres with dichoromethane, porous ReCaPP scaffold were fabricated (Figure 23). To fabricate tablet scaffolds of various thicknesses, increasing amounts of PLGA microspheres and ReCaPP powder were mixed, from a total weight of 25 mg of 100 mg, while maintaining the same 2:3 weight ratio of microspheres to ReCaPP powder. As shown in Figure 24, by increasing amounts of microspheres and ReCapp powder, tablet scaffolds

varied in thickness from approximately 900 μm (25 mg total) to approximately 2.5 mm (100 mg). For all cellular experiments, 25 mg tablets were used.

Using 25 mg total weight scaffolds (10 mg PLGA microspheres + 15 mg ReCaPP powder), PLGA microspheres were dissolved from the scaffolds, and subsequently, the scaffolds were reinfiltrated with 10 mg of ~20 μm alginate microspheres (Figure 25) via sonication. Resulting scaffolds (Figure 25) show that alginate microspheres fully infiltrated porous ReCaPP scaffolding, filling pores in the center of the cross-sectioned scaffold.

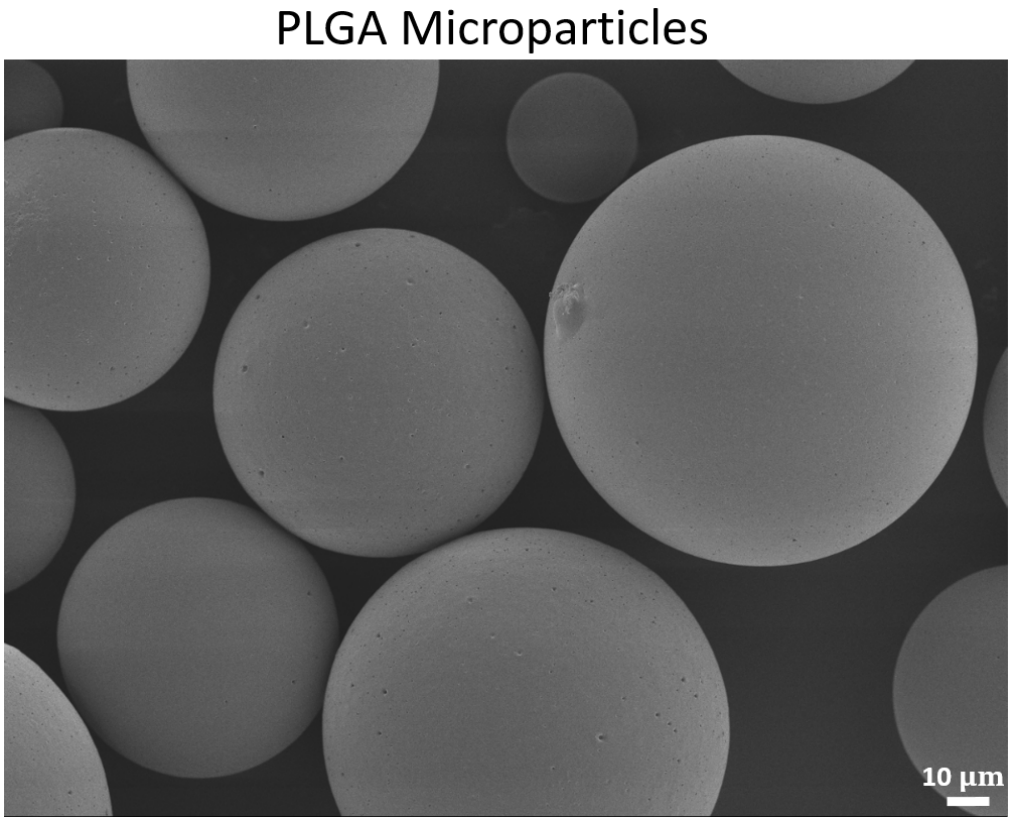

Figure 21. 100 μm PLGA microspheres used as a porogen in ReCaPP scaffolds.

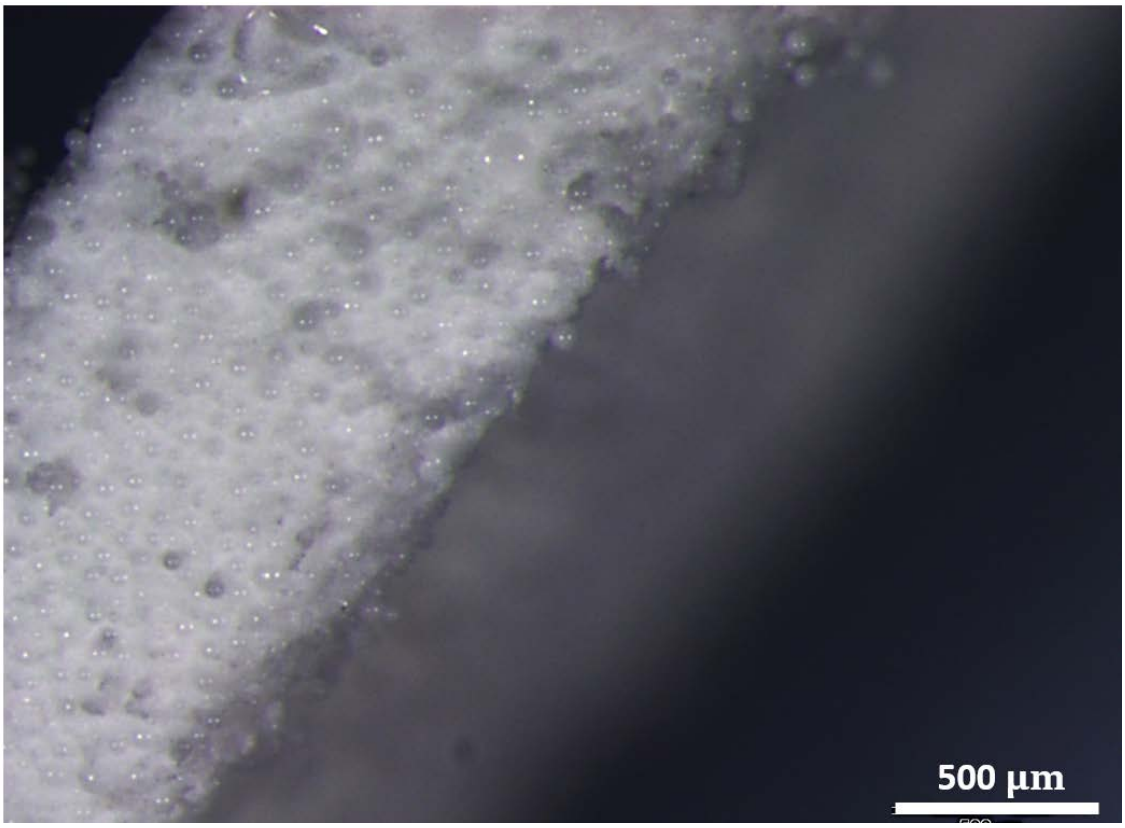

Figure 22. A ReCaPP/PLGA microsphere scaffold edge prior to PLGA microsphere dissolution showing distribution and density of PLGA microspheres embedded throughout the scaffold.

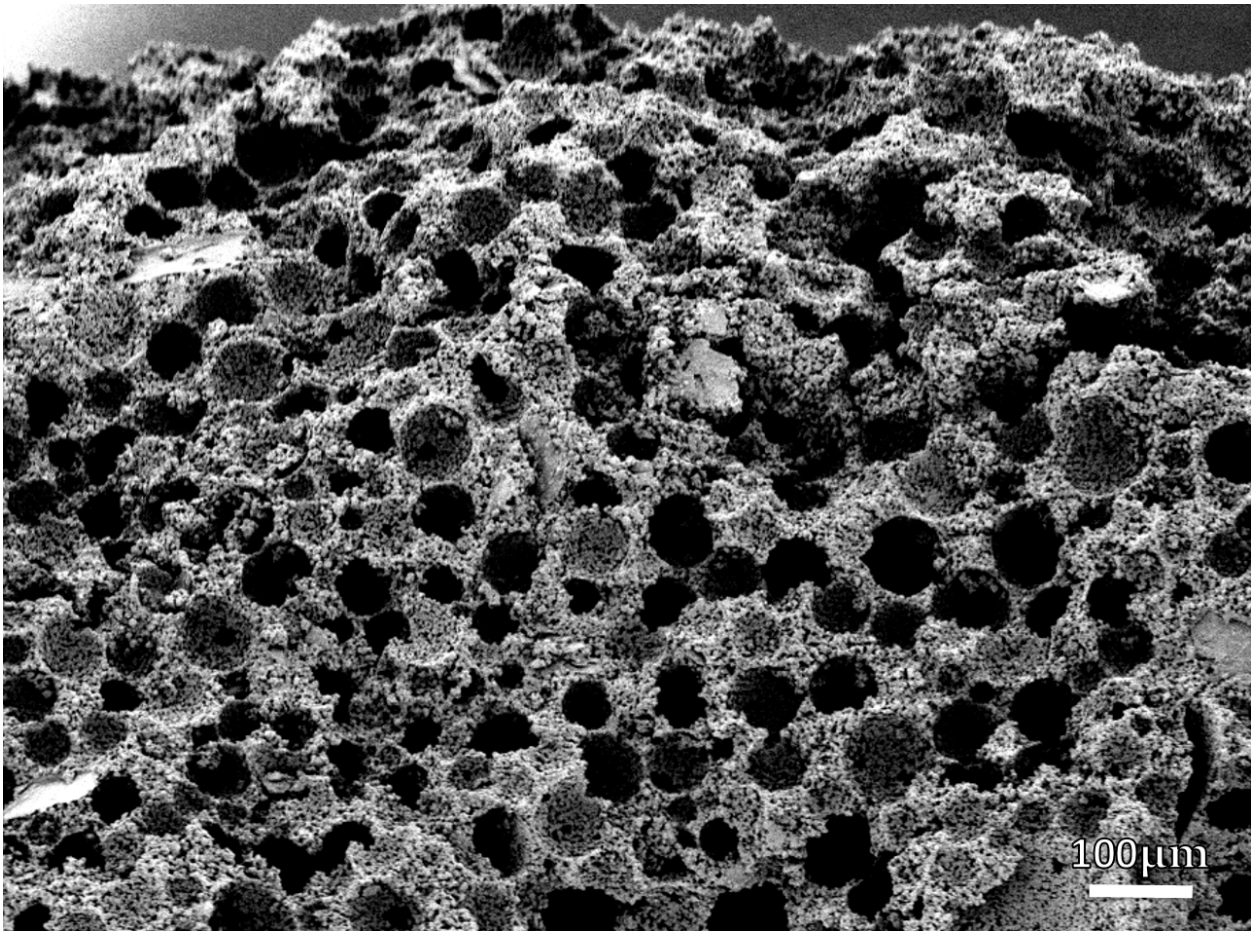

Figure 23. SEM showing porosity of ReCaPP scaffold after PLGA microspheres have been dissolved.

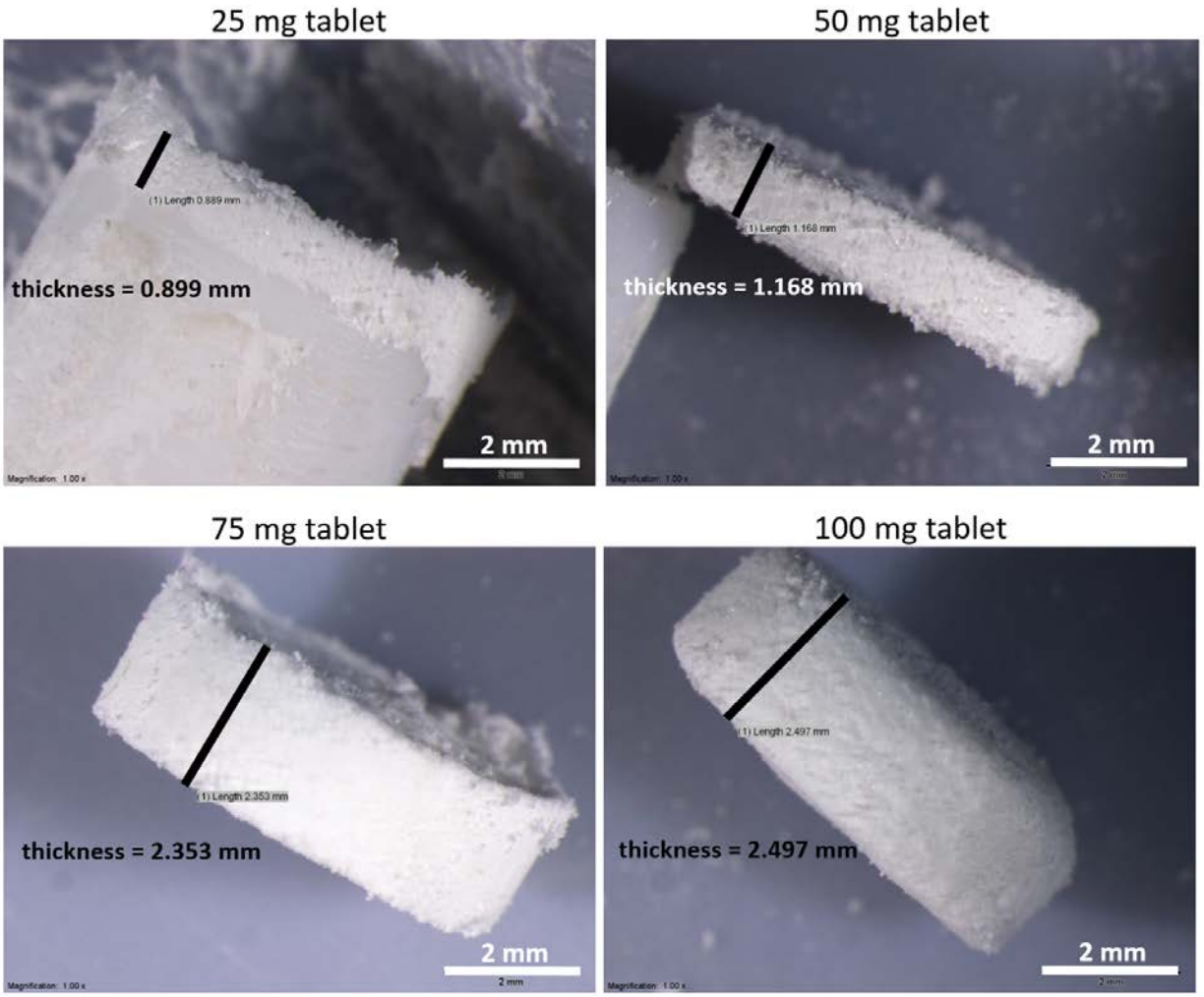

Figure 24. Tablet-shaped ReCaPP-PLGA microsphere scaffolds of various thickness, showing thickness increase with increasing amounts of PLGA microspheres and ReCaPP powders used to fabricate scaffolding.

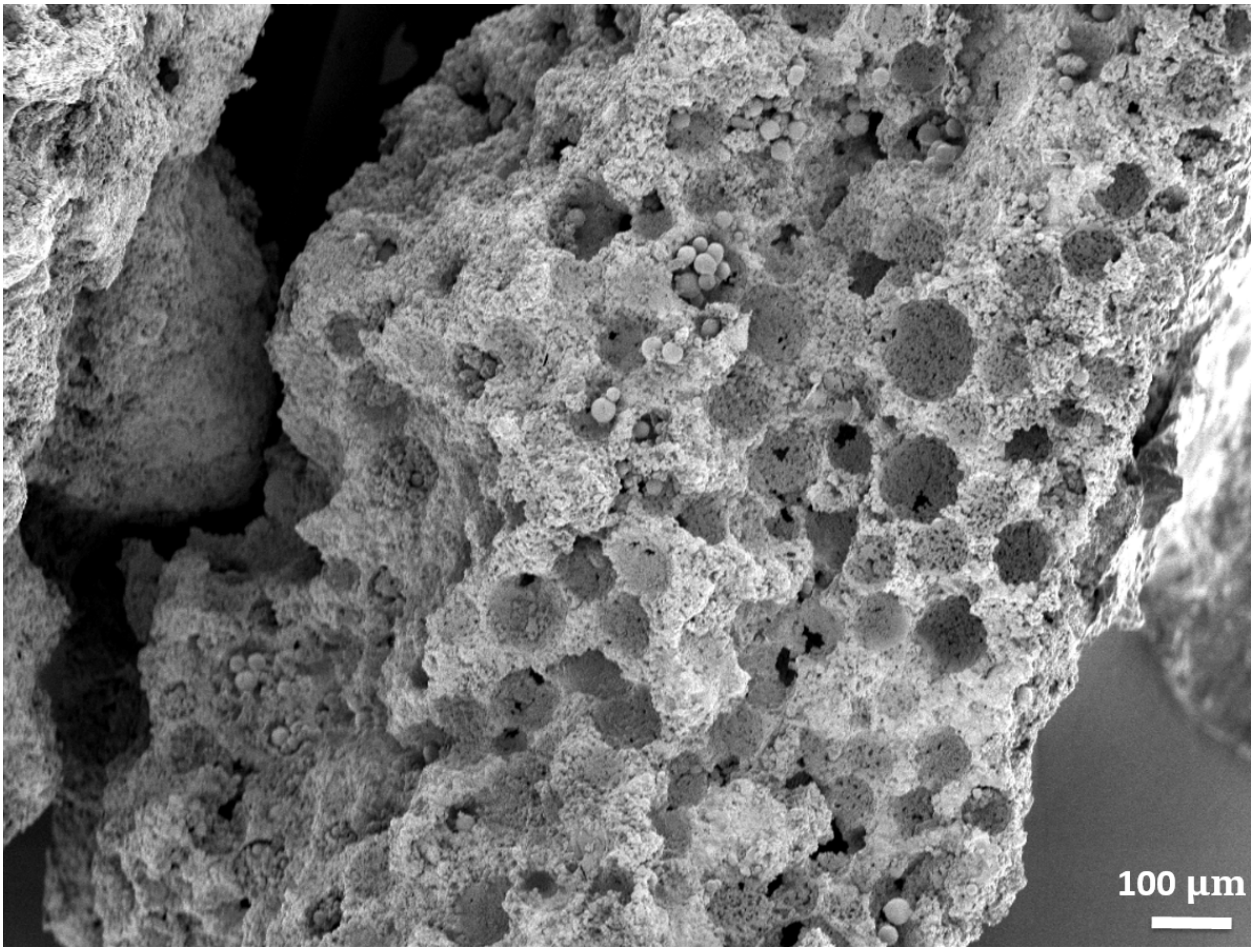

Figure 25. SEM of porous ReCaPP scaffold that has been reinfiltrated with BMP-2-alginate microspheres, showing that the BMP-2-alginate microspheres penetrate to the center of the scaffold.

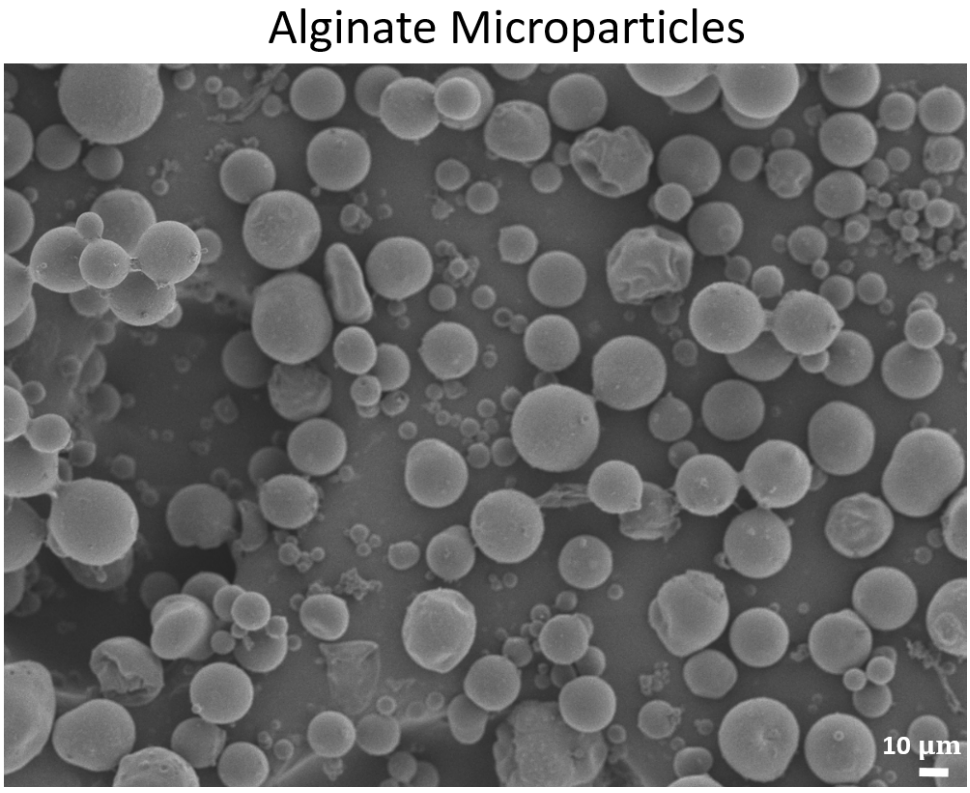

Figure 26. SEM of alginate microspheres showing that fabricating microspheres at speeds of 5400 RPM results in spheres approximately 20 µm in diameter that can be used to reinfiltrate the 100 µm pores of porous ReCaPP scaffolding.

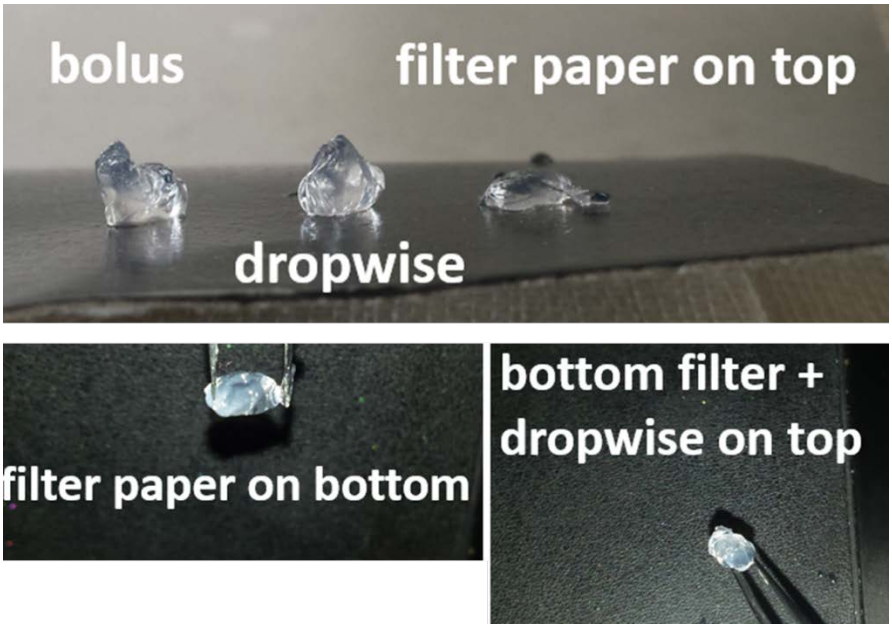

Figure 27. Different methods of adding calcium chloride crosslinker to alginate hydrogels, showing that hydrogels with the most consistent shape and thickness are generated through the addition of crosslinker through filter paper.

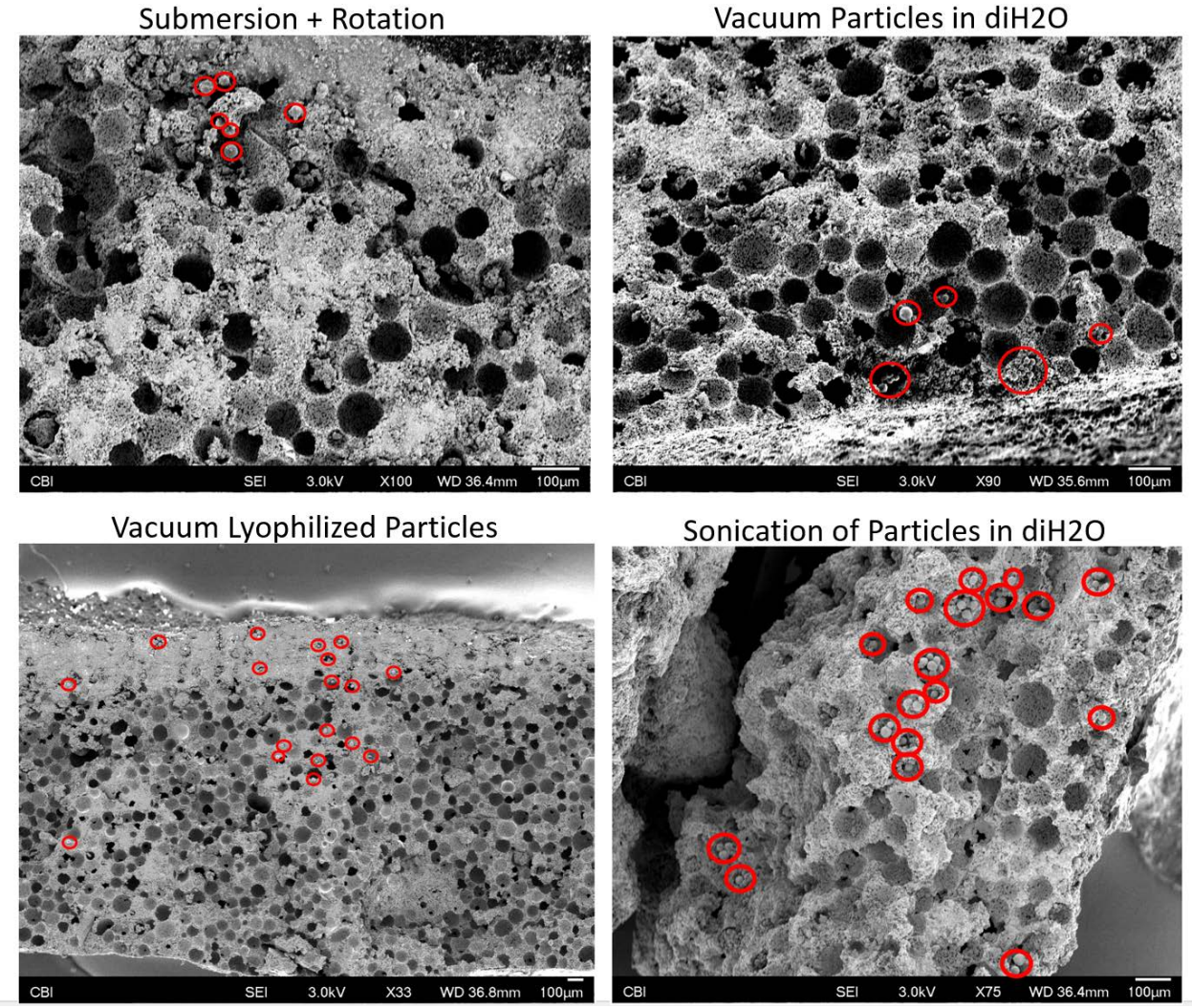

Figure 28. SEMs of porous ReCaPP scaffolds representing several methods of re-infiltrating the scaffolds with 20 µm alginate microspheres. Alginate microspheres are highlighted inside red circles. Of the four methods shown, sonicating the scaffold with a solution of microspheres suspended in diH2o most effectively distributed microspheres throughout the scaffold.

5.3.2 Scaffold Degradation

Degradation of scaffolds was measured over 40 days. Dry weights of three scaffolds comprised of ReCaPP cement, 3% alginate microspheres, and 1% alginate hydrogels were measured for each time-point. Degradation, measured by mass loss, occurred primarily over the first 20 days of the assay timeframe, with no additional significant mass loss measured at day 40.

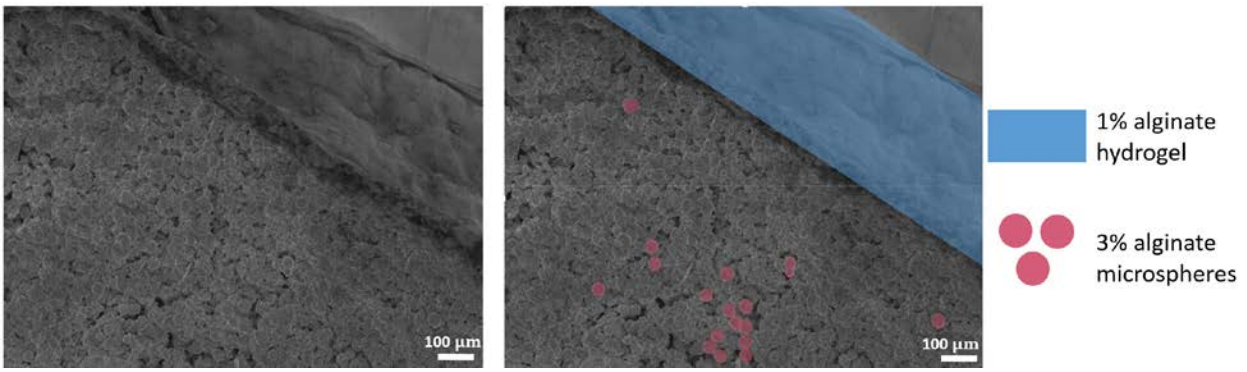

Figure 29. SEMs showing scaffolds prepared for the degradation study, showing 3% alginate microspheres embedded in a ReCaPP matrix with a 1% alginate hydrogel coating.

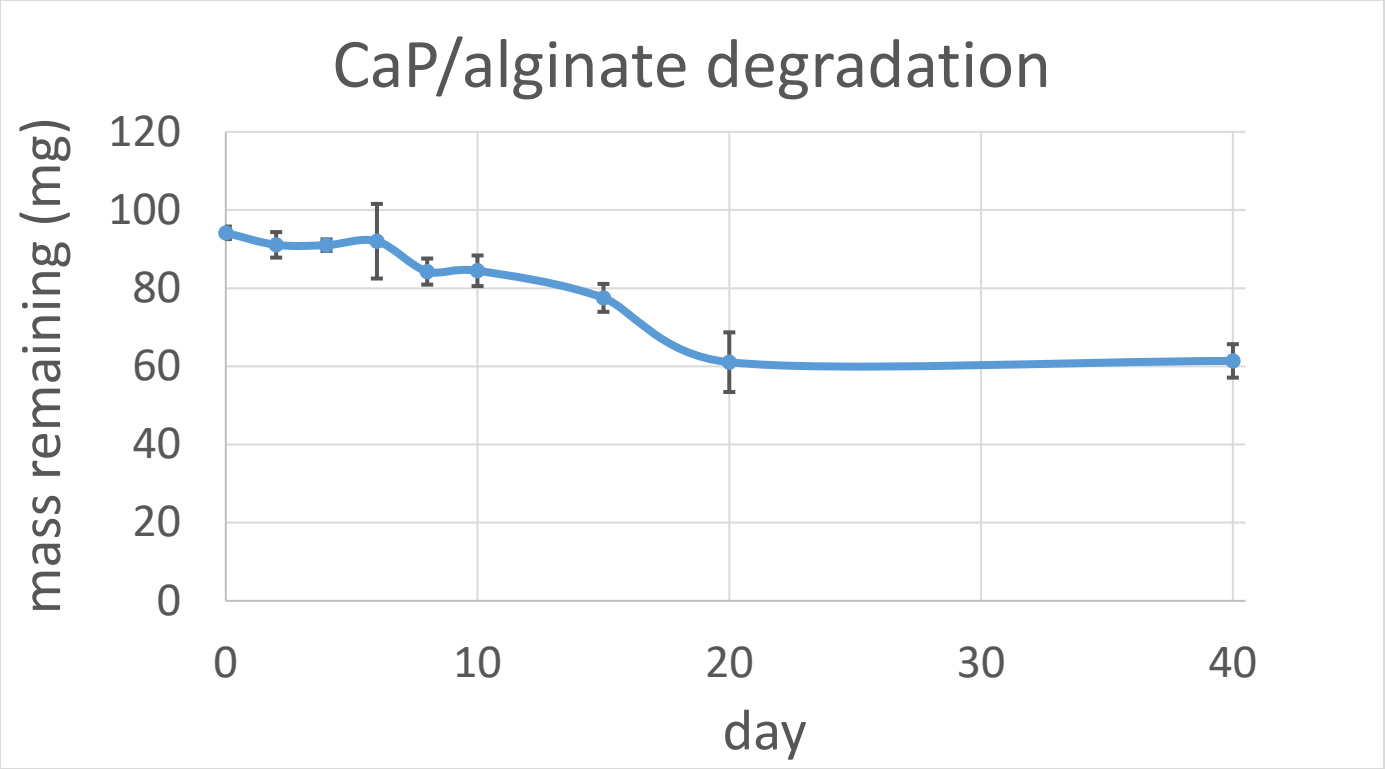

Figure 30. A graphical representation of the degradation of the alginate ReCaPP scaffold over 40 days, showing an approximate mass loss of 40 mg dry weight.

5.3.3 PDGF and BMP-2 Release Profiles

Three formulations of alginate hydrogels were assayed for PDGF release: a 1% hydrogel, a 1% hydrogel applied as a coating to ReCaPP scaffolding, and a 3% hydrogel applied to ReCaPP scaffolding (Figure 31). Over the first six days of release, the 1% alginate hydrogel exhibited fast burst release of PDGF, which was complete by day four. Both 1% and 3% hydrogels, when applied as a coating to scaffolds exhibited more steady, linear release of PDGF, with PDGF releasing more slowly from 3% alginate hydrogel coatings.

Release profiles of the PDGF from 1% alginate hydrogel coatings and BMP-2 from 3% alginate microspheres show early PDGF release, and later, delayed BMP-2 release (Figure 32). BMP-2 release begins on day 5, overlapping with PDGF release for 3 days (day 5-day 7).

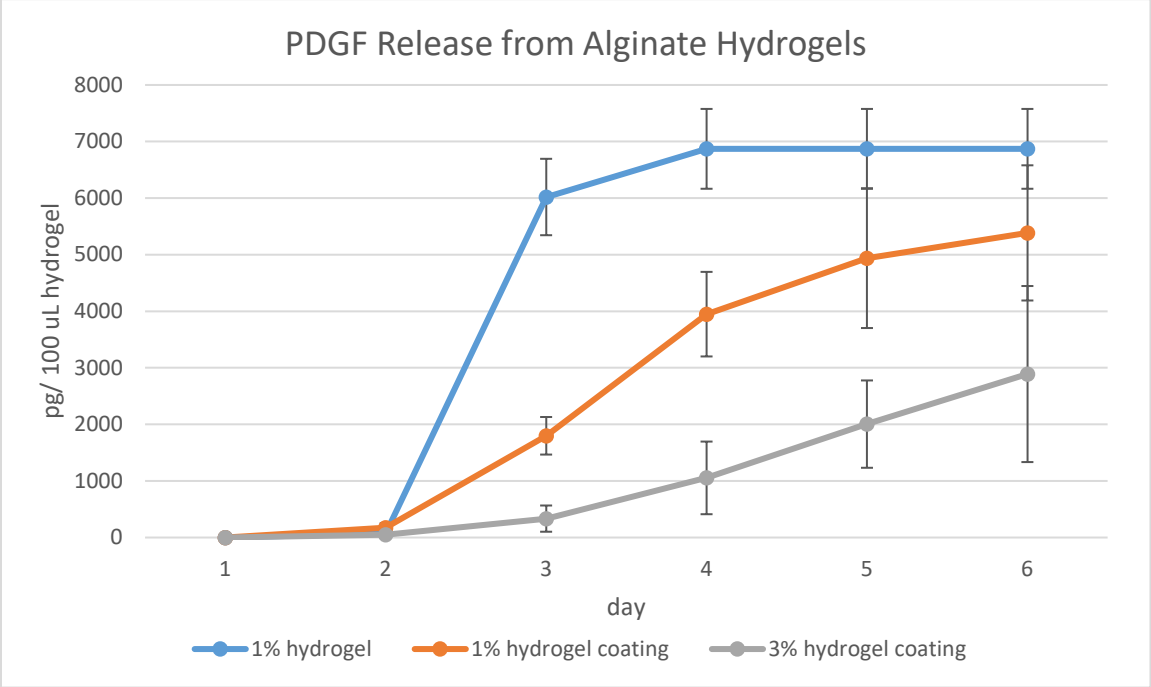

Figure 31. Release of PDGF from alginate hydrogel formulation showing burst release of PDGF from the 1% hydrogel. When hydrogels are applied as a coating to ReCaPP scaffolds, release profiles become relatively linear over the first 6 days of release, indicated a more steady release of PDGF.

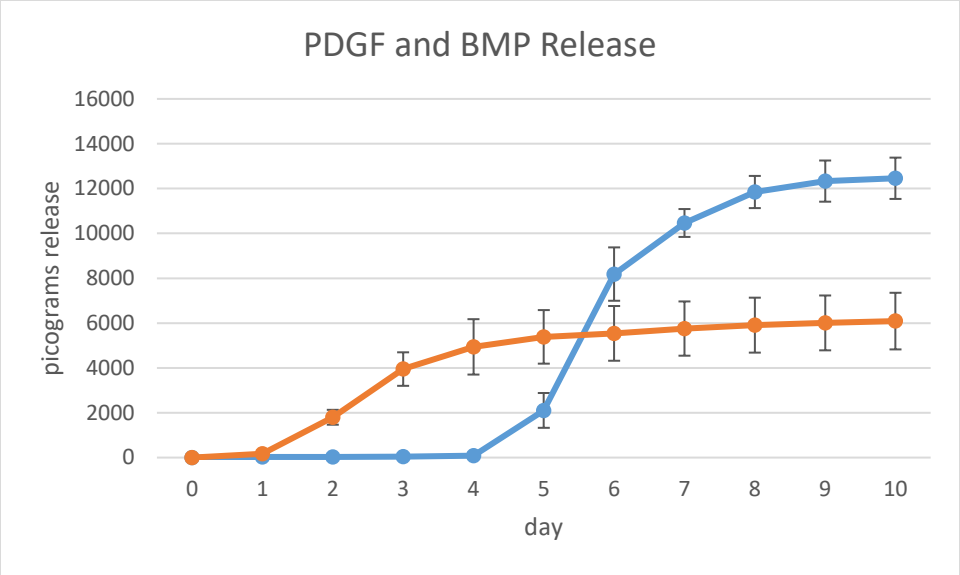

Figure 32. Release profiles of PDGF from 1% alginate hydrogels applied as a coating to ReCaPP scaffold, and BMP-2 from 3% alginate microspheres. PDGF release occurs over the first 7 days, while BMP-2 release subsequently begins on day 5, overlapping for three days with PDGF release.

5.3.4 Tubule Formation in Response to Controlled Release Growth Factor Delivery

PDGF was delivered to a co-culture of hMSCs and HUVECs in a Matrigel plug over the course of 7 days. Two methods of delivery were used: controlled delivery of PDGF from an alginate hydrogel and daily hand-dosing of PDGF via pipetting soluble aliquots into the Matrigel plug. As seen in Figure 34, both methods of PDGF delivery resulted in similar density and organization of tubules.

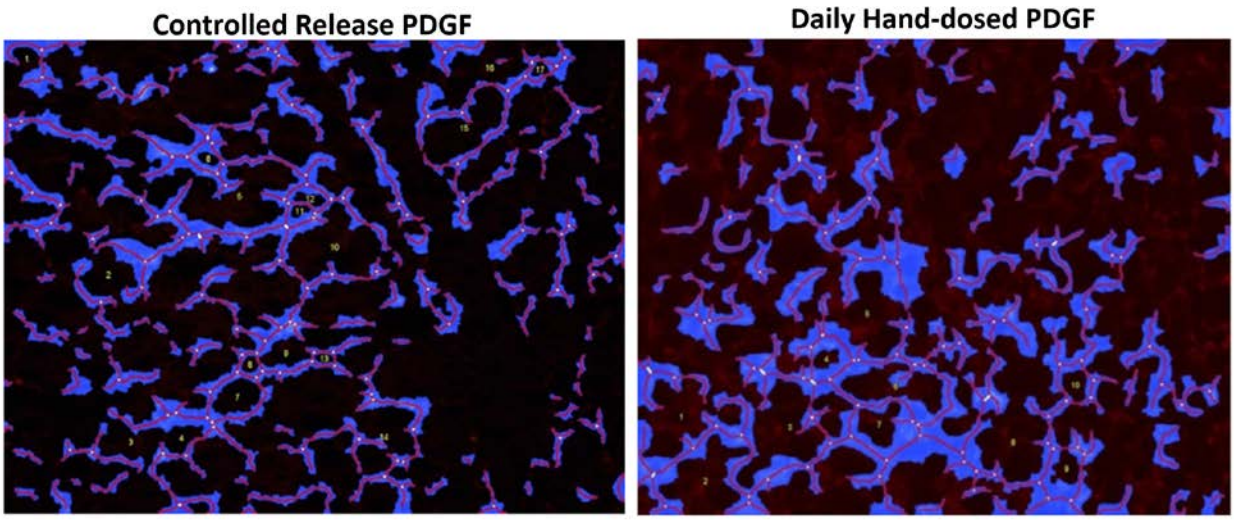

Figure 33. Wimasis software overlay of tubule formation in response to PDGF dosing techniques showing comparable tubule formation in response to controlled release PDGF delivery with tubule formation in response to daily hand-dosed cell cultures.

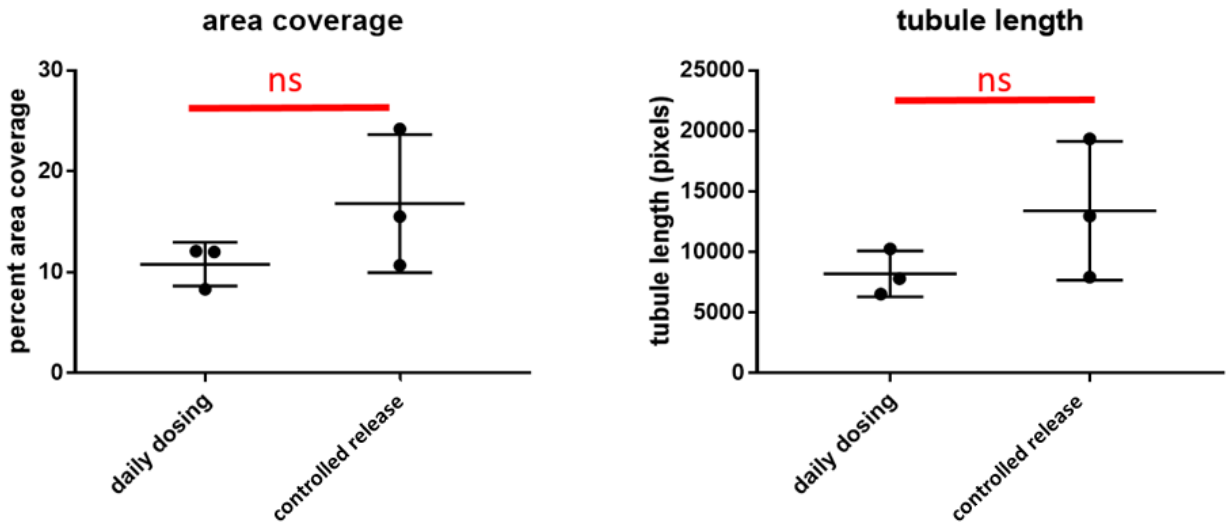

Figure 34. Results of unpaired students t-test with Welch's correction showing that there is no statistical significant difference in tubule area coverage or tubule length for daily dosing vs. controlled delivery PDGF.

5.3.5 Cellular Infiltration of Scaffold in Response to Growth Factor Delivery

To evaluate the efficacy of PDGF to recruit cells to the scaffold, PDGF hydrogels were applied to one side of the scaffolding (creating a gradient of growth factor release across the scaffolding), while a co-culture of HUVECs and hMSCs were seeded on the opposite side of the scaffolding. At the experimental endpoint, scaffolds were broken in half to reveal a vertical cross-section and imaged with a scanning electron microscope to identify cellular locations within the scaffolding (Figure 35). In response to PDGF release, cellular infiltration was observed through approximately 75% of the 900 μm thick, 3D scaffold over the course of 7 days (Figure 36). In comparison, when no growth factor was released from the hydrogel coatings, cell infiltration was only observed to penetrate approximately 25% of the way into the scaffold. Interestingly, when BMP-2 was released from the hydrogel coating, no cells were observed to infiltrate the scaffold. When PDGF and BMP-2 were delivered simultaneously from the hydrogel, cells penetrated through approximately 30% of thickness of the scaffold.

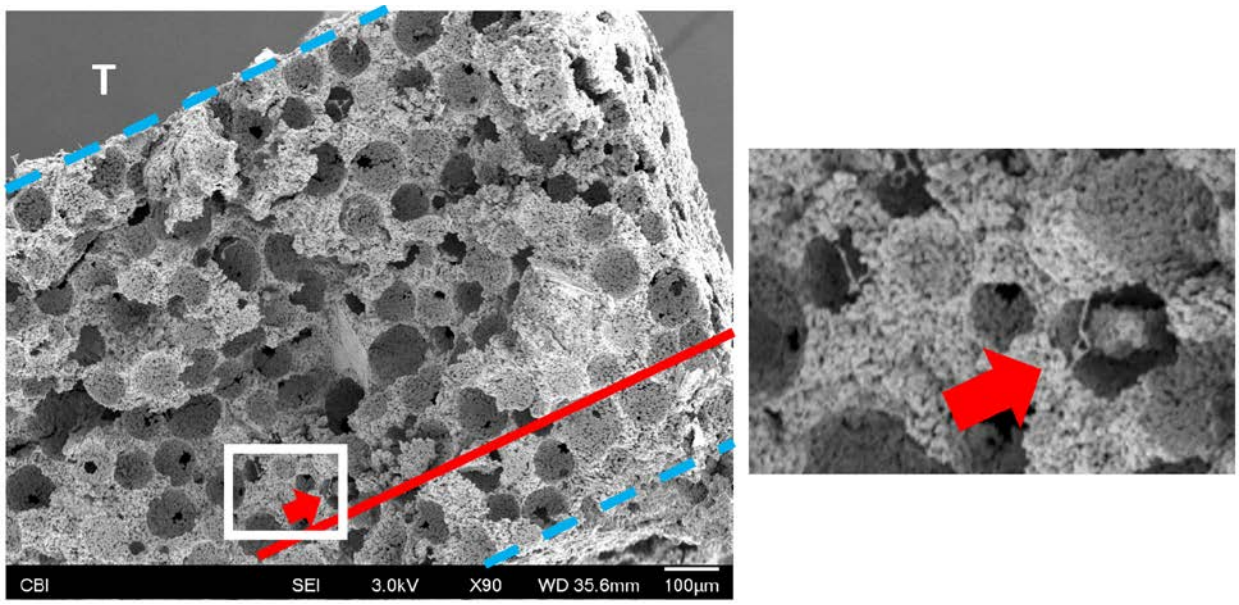

Figure 35. SEM of a cross-section of porous ReCaPP scaffolding indicating depth of cell infiltration. Blue dotted lines demarcate upper and lower boundaries of the cross-sectional slice; the letter "T" identifies the top surface of the scaffold where cells were seeded. Red lines and arrows indicate the furthest depth at which cells were found to penetrate the scaffold. Scaffolding within the white box is enlarged in the right-hand image to show an example of cells inside of scaffold pores.

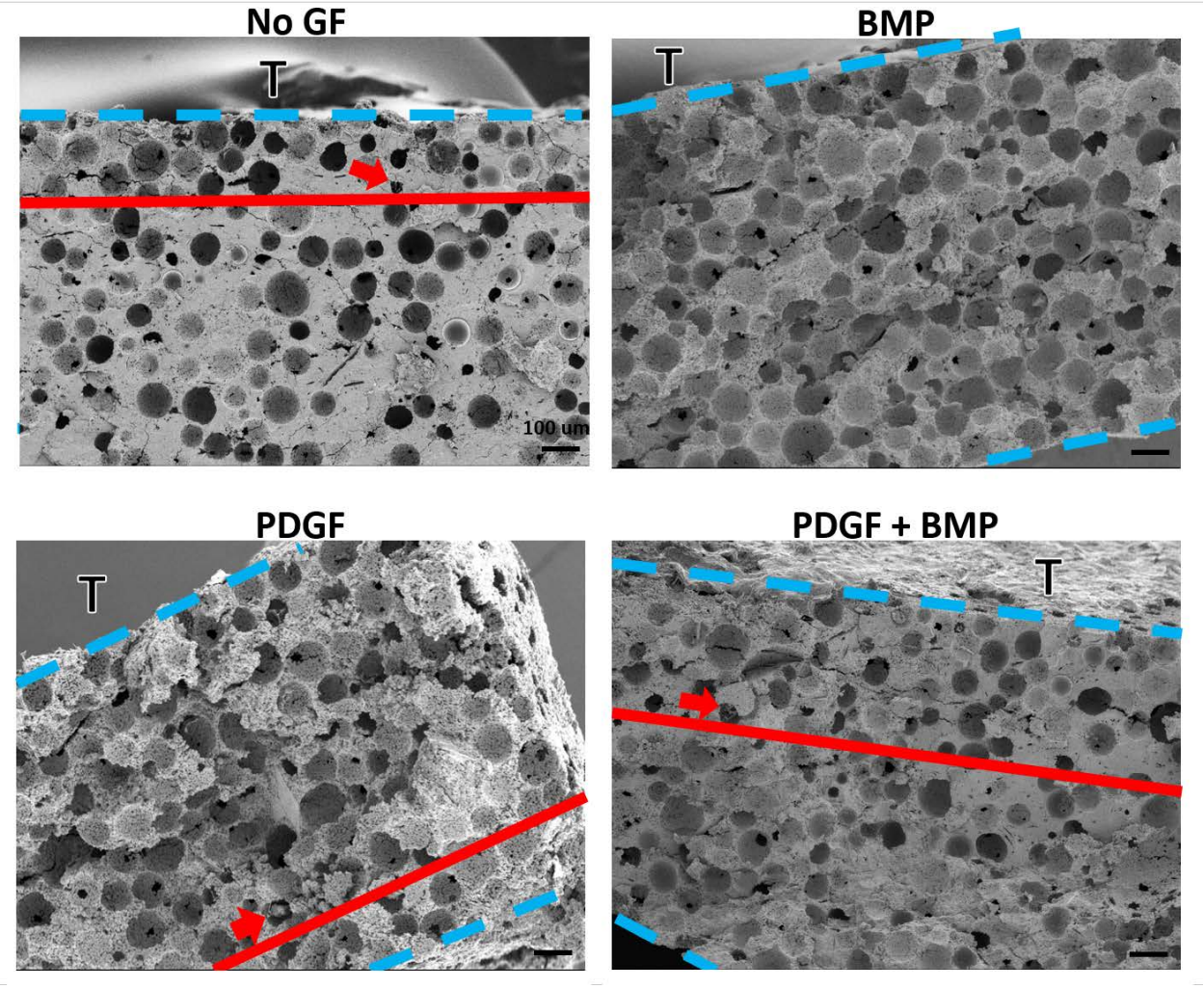

Figure 36. SEMs of porous ReCaPP scaffold cross-sections indicating penetration depth of infiltrating cells in response to growth factor gradients. Blue dotted lines demarcate upper and lower boundaries of the cross-sectional slice; the letter "T" identifies the top surface of the scaffold where cells were seeded. Red lines and arrows indicate the furthest depth at which cells were found to penetrate the scaffold.

5.3.6 Alkaline Phosphatase Expression in Response to Controlled Growth Factor Delivery

Programmed PDGF and BMP-2 delivery were presented to hMSC cultures as depicted in Figure 20. Cell cultures were assayed for ALP expression at three time-points: 7 days, 14 days, and 21 days. At the week 1 time-point (7 days) hMSC cultures with PDGF delivery and no growth factor delivery were absent of ALP staining. hMSC cultures with BMP-2 microspheres, as well as cultures receiving programmed PDGF to BMP-2 delivery stained positively for ALP expression. At day 14, cell cultures receiving BMP-2 and PDGF to BMP-2 treatments showing increased ALP staining (over staining amount at 7 days). Continuing with this trend, at day 21, cell cultures subject to BMP-2 release and PDGF to BMP-2 release again showed an increase in ALP staining compared to previous time-points. Interestingly, cell cultures receiving no growth factor treatment, as well as cultures exposed to PDGF release showed trace amounts of ALP staining at day 14, and increased ALP expression at 21 days (compared to the same treatment groups at earlier timepoints). Importantly, ALP staining in “No GF” and “PDGF” groups showed significantly less ALP staining than “BMP-2” and “PDGF to BMP” groups, when compared at the same time-point.

In Figure 37, ALP expression was assayed for at day 21 under three conditions: cells exposed to BMP-2 releasing ReCaPP scaffolding, cells exposed to ReCaPP scaffolding with no growth factor, and cells cultured in the absence of ReCaPP scaffolding and growth factors. Cells showed no positive ALP staining in the absence of ReCaPP scaffolding and growth factors, a moderate amount of ALP expression when cultured in the presence of ReCaPP scaffolding without growth factors, and the most ALP staining when subject to ReCaPP scaffolding releasing BMP-2 (Figure 38).

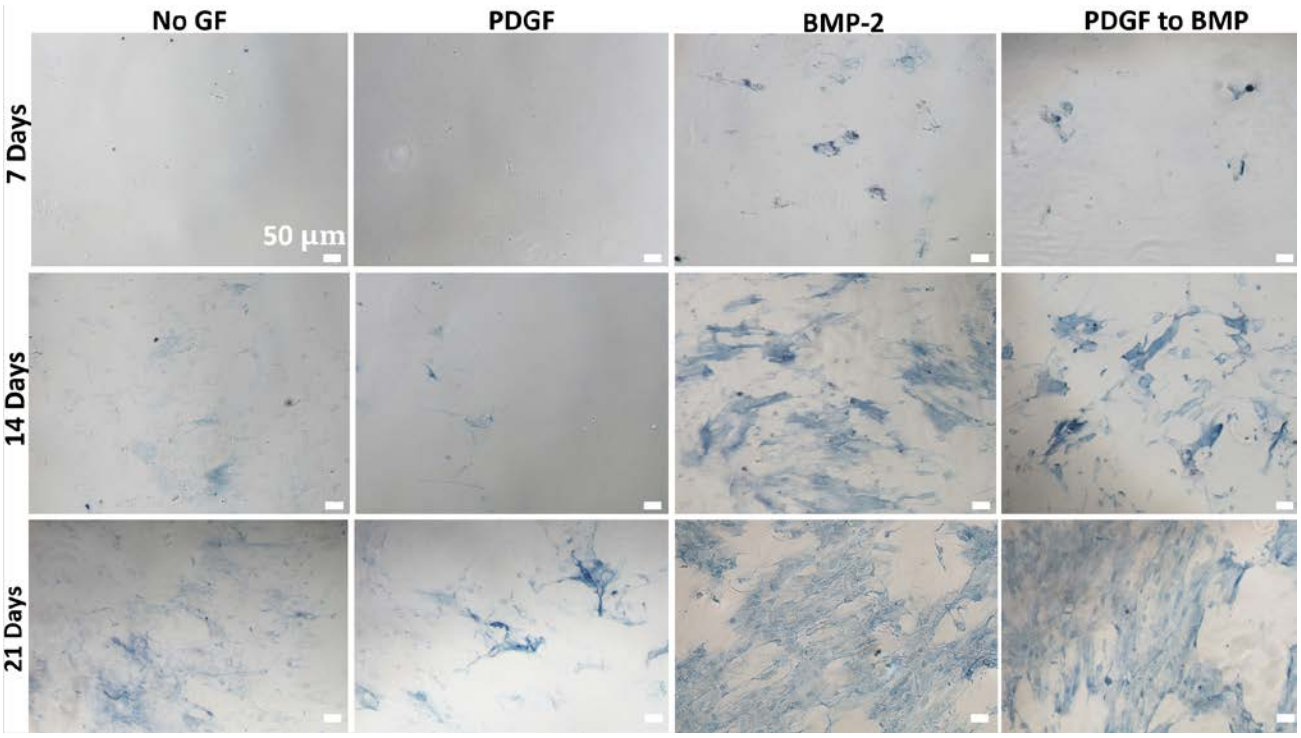

Figure 37. ALP expression (blue staining) at day 7, day 14, and day 21 showing that hMSCs with scaffolds releasing only BMP-2, as well as scaffolds releasing a schedule of PDGF to BMP-2 stimulate ALP expression. hMSCs receiving no growth factor or PDGF show less ALP expression at days 7, 14 and 21 versus groups receiving BMP-2 or PDGF to BMP-2.

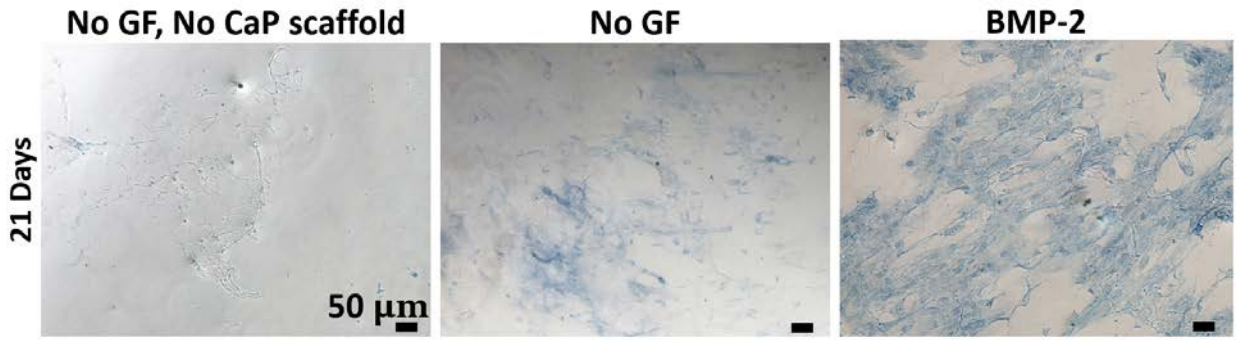

Figure 38. ALP expression at day 21 for cells cultured with no additional growth factor and no calcium phosphate scaffolding, cells cultured with calcium phosphate scaffolding releasing no growth factor, and cells cultured with calcium phosphate scaffolding releasing BMP-2. Scaffolds

releasing BMP-2 result in the most ALP staining, while scaffolds releasing no growth factor result in a moderate amount of ALP staining. Cells cultured in the absence of calcium phosphate scaffolding show no ALP staining.

5.4 DISCUSSION

Calcium phosphate cements have been widely investigated for use as synthetic bone scaffolding material due to their similarities in composition to bone mineral, biocompatibility, and tunable degradation/resorption rates [202-205]. Bioactive components, such as antibiotics and growth factors can also be released from calcium phosphate scaffolding, either by adsorbing the proteins or antibiotics to the surface of the scaffolding, or through the inclusion of a second biomaterial phase, such as synthetic or natural polymers to encapsulate bioactive agents [202, 206]. For example, by incorporated vancomycin-loaded PLGA microspheres into calcium phosphate scaffolding, it was shown that vancomycin could be released over the course of 100+ days from the scaffold [206]. Calcium phosphate cements can also be engineered to be highly porous through fabrications methods (such as sintering or salt leaching [207]) or by including degrading polymers [206], to form interconnected micro- and macro-porous networks. In this study, we aimed to combine these benefits of calcium phosphate scaffolding with a controlled release schedule of PDGF and BMP-2.

While calcium phosphate cements have been used in previous studies to deliver growth factors [202], metrics used for evaluating efficacy often focus primarily on mineralization, and largely overlook the capacity of a combination of growth factors to generate angiogenic formation. For the purposes of this study, we engineered a controlled delivery system capable releasing a

schedule of PDGF and BMP-2 that has shown to be effective in generating a robust, organized network of angiogenic tubules (Chapter 4). We have incorporated this controlled delivery system with a calcium phosphate matrix, and characterized the degradation, release profiles, and cellular responses to the resulting hybrid scaffold.

To fabricate a calcium phosphate scaffolding template with interconnected pores, we combined ReCaPP cement with PLGA microspheres at a 2:3 weight ratio of 100 μm microspheres to ReCaPP cement (by weight, 40 g microspheres to 60 g ReCaPP cement). In our previous studies, similar calcium phosphate constructs were fabricated with a lower ratio of PLGA microspheres (37.9 g microspheres to 62.1 g ReCaPP cement), and when evaluated with mercury porosimitery intrusion, were found to have a porosity of 73.7% when PLGA microspheres were fully dissolved from the scaffold [206]. To ensure at minimum this level of porosity for scaffolding used in this study, we increased the ratio of microspheres (of the same diameter) relative to the amount of ReCaPP cement. To create scaffolding with immediate porosity (versus porosity that is created over time via polymer degradation), PLGA microspheres were dissolved away with dichloromethane. For this reason, growth factors were incorporated into the scaffold following the creation of a porous network, in part to avoid possible denaturation in the presence of a harsh solvent. For the *in vitro* experiments conducted in this study, several scaffolding total weights were explored; ultimately, 25 mg tablets were used to generate scaffolds with an approximate thickness of 900 μm.

Medium viscosity sodium alginate, crosslinked with calcium chloride served as the base for both PDGF and BMP-2 controlled release systems. Alginate was chosen as the polymer for PDGF release, as other polymers, such as PLGA have been shown to have a “sticky” effect with PDGF due to their opposing electronegative (PLGA) and electropositive (PDGF) charges, leading

to unpredictable and hindered PDGF release [208]. Additionally, because PDGF is a heparin binding protein, it may reversibly bind to alginate hydrogels, enabling its sustained release, a phenomenon that has been demonstrated in studies investigating the release of other heparin binding growth factors (including VEGF and FGF) from alginate hydrogels [209-211]. Alginate hydrogels of 1% and 3% were investigated for PDGF release. When released from a 1% bulk hydrogel, PDGF exhibited burst release in the first 48 hours of the release assay. When the same 1% alginate hydrogel formulation was applied as a coating to ReCaPP scaffolding, linear release over 6 days was observed. This difference in release may be attributed to the fact that when the alginate hydrogel was applied as a coating, the same aliquot was spread more thinly over the scaffold, exposing more of its surface area to be more strongly, consistently crosslinked. This hypothesis agrees with known release behaviors of alginate hydrogels in the literature; a greater amount of crosslinking will slow protein release from the hydrogel [210, 212]. Similarly, when a 3% alginate hydrogel was applied as a coating to ReCaPP scaffolding, linear release was observed over the first 6 days, at a slower rate of release compared to 1% alginate hydrogels. This difference can be explained by the concentration of alginate used in the hydrogels; as the percentage of alginate increases, total release is slowed [212]. In addition to generating the desired PDGF release profile, alginate hydrogel were chosen for this application because of their ability to be applied as a coating. Segregating PDGF to the outside of the ReCaPP prevents potential adsorption (and potentially inactivation) of PDGF to the ReCaPP scaffolding, as it might be if it was embedding within the scaffold.

To generate delayed release of BMP-2, the protein was encapsulated in 3% alginate microspheres. Not only were we able to achieve delayed BMP-2 release that began on day 7 with BMP-2 alginate microspheres, but because they were fabricated at an average size of 20 μm, the

microspheres could be reinfiltrated throughout the porous ReCaPP scaffolding, creating local BMP-2 release throughout the scaffold, that will be presented to cells that have already infiltrated the scaffold in response to earlier PDGF release.

To evaluate the efficacy of PDGF to recruit cells to the scaffold, PDGF hydrogels were applied to one side of the scaffolding (creating a gradient of growth factor release across the scaffolding), while a co-culture of HUVECs and hMSCs were seeded on the opposite side of the scaffolding. In response to PDGF release, cellular infiltration was observed through approximately 75% of the 900 μm thick, 3D scaffold over the course of 7 days. In comparison, when no growth factor was released from the hydrogel coatings, cell infiltration was only observed to penetrate approximately 25% of the way into the scaffold. Interestingly, when BMP-2 was released from the hydrogel coating, no cells were observed to infiltrate the scaffold. When PDGF and BMP-2 were delivered simultaneously from the hydrogel, cells penetrated through only approximately 30% of thickness of the scaffold. It is possible that BMP-2 with PDGF may send conflicting signals to the cells and potentially inhibit their migration into the scaffold, giving further support the idea that early PDGF release following by later BMP-2 release is beneficial for the ordered regenerative stages of bone formation. This hypothesis is in line with evidence that while BMP-2 is a potent inducer of MSC differentiation to an osteoblastic phenotype, its activity blocked in situ by BMP-4 and noggin expression during times when osteoblast recruitment to the fracture site is most active [213].

To assaying for early tendency of hMSCs towards an osteogenic phenotype, fully assembled scaffolds of porous ReCaPP cement with PDGF-releasing alginate hydrogels and BMP-2-releasing alginate microspheres were assessed using a transwell system (Figure 20). At the day 7 time-point, groups delivering BMP-2 alone and a schedule of PDGF to BMP-2 both

stained positively for ALP expression. Groups delivering PDGF alone or no growth factor showed no ALP staining at day 7. At day 14, greater amounts of ALP staining were observed in cell cultures received BMP-2 and PDGF to BMP-2 growth factors. Cell cultures with no released growth factors, and those receiving only PDGF showed relatively small amounts of positive ALP staining (when compared with "BMP-2" and "PDGF to BMP" groups) on day 14 and day 21, which may be attributed to the osteoconductive (and potentially osteoinductive) effects of the calcium phosphate scaffolding [201, 214]. In support of this hypothesis, when cells were cultured in the absence of ReCaPP scaffolding and growth factors, no ALP expression was detected at day 21 (where as cells cultured in the presence of ReCaPP scaffolding with no releasing growth factors showed a moderate amount of ALP staining.) Importantly, these results indicate that while PDGF does not induce the expression of ALP (or the differentiation of hMSCs towards an osteoblastic phenotype), its early presentation does not inhibit the ability of later BMP-2 presentation to promote osteoblastic differentiation. These results are supported by evidence that PDGF is involved not only during the angiogenic phase of bone repair, but also plays an important role in stimulating the cellular events preceding osteogenesis, such as recruiting MSCs and stabilizing the blood vessels which guide the orientation of osteoblast sheets [87]. Additional staining techniques to assay for mineralization (such as Alizarin Red or Von Kossa staining) were not used in these experiments due to the false positive results that would be generated by the calcium phosphate scaffolding. As an alternative, to confirm the results indicated by ALP staining, osteocalcin staining could be performed on cells seeded in the same transwell configuration, as illustrated in Figure 20. Osteocalcin, a protein found in bone tissues is produced specifically by osteoblasts [215], and can be assayed for near day 14 of culture [216]. However,

osteocalcin is viewed as an indicator of bone turnover (not necessarily bone formation) as it is produced and incorporated into the matrix during bone resorption [217].

5.5 CONCLUSIONS

The present study demonstrates the use of degradable PLGA microspheres along with calcium phosphate cements to form scaffolds with interconnecting porous networks following the dissolution of PLGA microspheres with DCM. Further, these scaffolds can be reinfiltrated with smaller, BMP-2-releasing alginate microspheres and coated with PDGF-releasing alginate hydrogels to deliver a programmed schedule of these growth factors to cell cultures. The chosen delivery schedule of PDGF and BMP-2 has shown to be effective in stimulating cell infiltration of the scaffold, generating angiogenic tubule network formation, and promoting alkaline phosphatase expression, indicating the potential for this hybrid scaffold system to supply the cues to orchestrate vascularized bone regeneration. With further *in vivo* studies of these materials, the translation of this technology from a proof-of-concept model to the development of a new approach for fracture healing may be realized.

6.0 ORDERED COLLOIDAL CRYSTAL SCAFFOLDING

The work in this chapter began in collaboration with Melissa Lash, PhD. Materials and Methods for crystalline templates and cement-based inverted colloidal crystals were developed in this collaboration and adapted from her thesis.

6.1 INTRODUCTION

The use of porous scaffolding for bone regeneration provides a template for cellular infiltration and attachment, allows vascular infiltration to bring circulating cells into the scaffold, removes waste, and provides nutrients. In the work described in Chapter 5, scaffolds with interconnected porosity were fabricated using high enough ratios of porogen volume to scaffolding material (ReCaPP cement) volume to ensure porous networks. While these scaffolds can be fabricated with a high degree of porosity (~74%), when pore networks are unorganized, resulting scaffolds may have regions without pore interconnectivity, and varying, unpredictable mechanical strength [218]. Another approach to creating scaffolding with interconnected pores is through the colloidal crystal arrangement of porogens. Using monodisperse microspheres arranged into a colloidal crystal formation as a template, scaffolding material can be infiltrated through the crystal and hardened. Subsequently, by dissolving away the organized microsphere template, the resulting scaffold bears

the structure of an inverted colloidal crystal (ICC). This highly organized ICC structure has several benefits over scaffolding with random porous networks, such as a high degree of organization, uniform pore size, and predictable mechanical strength [218, 219]. Additionally, scaffolding with an ordered porous network allows for microarchitecture reproducibility with reliably interconnected pores [218, 220-222].

In this work, we used microsphere self-assembly techniques to explore the creation of an ICC scaffold for bone tissue engineering using ReCaPP cement. Further, we fabricated monodisperse PLGA microspheres loaded with PDGF for the potential future use a growth factor eluting porogen in ICC scaffolding.

As a proof of concept model to refine our fabrication techniques, we first fabricated PLA and PLGA ICCs, as several groups have done [219, 223]. In contrast to other porous CaP scaffolds with ordered pore structures or those that incorporate the controlled release of biological factors, we have incorporated controlled drug release within an ordered ICC composite scaffold to biomimetically promote ordered tissue regeneration [110, 220, 224]. By designing a bioactive scaffold with an ordered macroporous network, we aim to homogeneously release growth factors from localized pockets within the scaffold to recruit cell that will infiltrate the scaffold and create new tissue throughout.

6.2 MATERIALS AND METHODS

Monodisperse soda lime and polystyrene microspheres were used to fabricate non-Brownian colloidal crystals templates. These templates were then fused and combined with PLGA and ReCaPP to produce three-dimensional inverted colloidal crystal scaffolds. Subsequently, we investigated the production of monodisperse PLGA microspheres as a growth factor delivery component of colloidal crystal scaffolding for potential applications in bone repair.

6.2.1 Soda Lime Particle Crystalline Templates

Glass vials (1 mL capacity) containing 150 μg SL particles and 200μL DIW were suspended in the sonication bath for 90 minutes. Following sonication, the fluid was allowed to fully evaporate. The soda lime crystals were then fused together via calcination for 3 hrs at 680 °C with a ramping rate of 15 °C/min in air. Fusion temperatures and times were varied in method development from 670-690 °C for 2-5 hrs.

6.2.2. Polymer-based Inverted Crystals

Solutions of PLA and 75:25 PLGA in dichloromethane (DCM) (10 wt%) were respectively added to the soda lime particle crystals post-fusion and cooling. The solution was added until the crystal was fully submerged (~200 µL). After the DCM fully evaporated, the glass vials were cracked and the samples were removed and transferred to a Nalgene container containing a 5% HF solution. Samples were rotated end-over-end until complete removal of SL particles was achieved as monitored on a stereomicroscope. Washing generally occurred over ~8-10 days with a daily exchange of wash fluid and end-over-end mixing. On days 4 and 7, the Nalgene container with sample was submerged for 10 s in sonication bath, the wash fluid changed and was then returned to mixing. On day 8, the sample was washed 5-10X in deionized water, immersed in deionized water for 24 hours of mixing and dried for further use. *Note: PS particle-crystals would not work in this combination due to the PS's solubility in DCM.

6.2.3 Polystyrene Particle Crystalline Templates

Polystyrene (PS) microspheres (90 and 200 µm in diameter) were organized by agitating a solution of polystyrene microspheres in deionized water via sonication. Briefly, 600 µL of particles in solution (10 wt% in diH2O) were deposited and sonicated in stainless steel molds (as pictured in Figure 40) for 90 minutes. Samples were then fused at 165 °C for 48 hrs and 220 °C for 8 hrs respectively.

6.2.4 Cement-based Inverted Crystals

A cement slurry was added with pressure to infiltrate it throughout the particle bed. The cement powder (ReCaPP) was prepared by mixing calcium salts and disodium hydrogen phosphate. Alpha-tri-calcium phosphate (α-TCP, pure phase, Sigma-Aldrich, USA), calcium carbonate (99+%, Acros Organics, USA), calcium sulfate di-hydrate (99+%, Acros Organics, USA), and disodium hydrogen phosphate (≥99%, Sigma-Aldrich, USA) were mixed in an agate mortar-pestle for 30 min. *Note: SL particle-crystals would not work in this combination due to the cements inability to withstand HF washing.

6.2.4.1 Preparation of ReCaPP Liquids

The liquid component of the ReCaPP consisted of a colloidal solution of nano-sized calcium phosphate (nano-CaPs) homogeneously dispersed in a buffer solution. Details of the nano-CaPs preparation can be in Chapter 5. Briefly, for each milliliter of nano-CaPs solution, 250 µl of 0.75 M $CaCl_2$ was added drop wise to a 250 µl of phosphate precursor solution, pH 7.5, comprised of 0.357 M NaCl (>99.5%, Fisher Scientific, USA), 13 mM KCl (>99%, Fisher Scientific, USA), 15 mM dextrose monohydrate (Fisher Scientific, USA), 64 mM HEPES free acid (99.5%, Sigma-Aldrich, USA) and 1.91 mM of $Na_3PO_4 \cdot 12H_2O$ (98+%, Acros Organics, Thermo Fisher Scientific, USA).

6.2.4.2 Cement Preparation and Scaffold Fabrication

Each of the cement samples was prepared by mixing 250 mg of the cement powder with 150 µl of the nano-CaPs solution in a polystyrene pour boat. Once mixed, the cement slurry was loaded into a 1.0 mL syringe and deposited on top of cooled PS crystals. A tamping device was then used to compress the cement encouraging infiltration through the crystal, filling its voids. Samples of cement and PS crystals were then placed in an incubator and allowed to harden for a minimum of 24 hours while incubated at 37 °C. PS particles were removed via calcination in air at 500 °C for 3 hrs with a ramping speed of 2.77 °C/min.

6.2.5 Scaffold Imaging

Samples were cut using a razor blade for imaging cross-sections. An Olympus ZS100 microscope was used to visualize the pore structure of the sample and to watch the cement infiltration prior to drying. SEM was also used to image the scaffolds and a sputtercoat thickness ~5 nm was applied for imaging.

6.2.6 PLGA Particle Fabrication for Growth Factor Eluting Colloidal Crystal Construct

Double emulsion PLGA microspheres were fabricated by dissolving 200 mg of 50:50 PLGA in 4 mL of dichloromethane. A 100 µL aliquot of 200 µg/mL soluble PDGF-BB (R&D Systems) was mixed with a 100 µL aliquot of NaCl in deionized water to make aqueous solutions with salt

concentration ranging from 5 mM to 50 mM. This 200 μL aqueous aliquot, containing both salt and PDGF, was sonicated with the dissolved PLGA for 30 seconds at 25% to create a water-in-oil emulsion. The resulting solution was then pipetted dropwise through a 250 μm sieve into a spinning solution of 1% PVA in deionized water to create water-in oil-in water microspheres of approximately 100 μm in diameter. Following fabrication, the particles were collected via centrifugation, washed five times with deionized water. Collected particles were then frozen and lyophilized.

6.2.7 Growth Factor Release from PLGA Particles

To determine the release rate of PDGF from PLGA microspheres, 10 mg of PLGA microspheres were suspended in 1 mL of PBS release solution in a lo-bind Eppendorf tube and subject to end-over-end rotation at 37^{O}C. PBS release solution consisted of PBS supplemented with SDS (50mM) and 0.1% BSA to further prevent released PDGF-BB from sticking to the Eppendorf tube. At experimental timepoints, particle suspensions were centrifuged at 1000 RPM and supernatant was collected and frozen at -20^{O}C. Fresh PBS was added, particles were re-suspended, and again end-over-end rotated at 37^{O}C. At the conclusion of the study, all frozen supernatant samples were thawed and assayed for PDGF concentration using a human PDGF-BB ELISA assay (R&D Systems).

6.2.8 Arrangement and Fusion of PLGA Particles

Poly-lactic-co-glycolic (PLGA) microspheres (with 25 mM and 50 mM NaCl aqueous phases) were organized by agitating a solution of PLGA microspheres in deionized water via sonication. Briefly, 600 μL of particles in solution (10 wt% in diH2O) were deposited and sonicated in stainless steel molds (as pictured in Figure 40) for 90 minutes. Excess water was allowed to evaporate overnight. Samples were then fused at 40°C for 10 hrs and for 8 hrs, respectively.

6.2.9 Monodisperse PLGA Microsphere Fabrication

Monodisperse microparticles were fabricated using a microfluidics system (Micronit Fluidics) in combination with two syringe pumps (New Era Syringe Pumps, Inc.) The first syringe pump was loaded with a 50 mL syringe (Norm-Ject) containing a solution of 1% PVA in deionized water. The second syringe pump was outfitted with a solution of 800 mg of 50:50 PLGA dissolved in 16 mL of dichloromethane. The PLGA/dichloromethane solution was sonicated with 800 μL of 25 mM and 50 mM sodium chloride in deionized water for 60s at 25% power prior to syringe loaded to create the first water-in-oil emulsion. The syringe pumps were then connected to the microfluidics system, which housed a focussed flow microfluidics chip. With the appropriate connections, the PLGA emulsion phase passed through two converging channels of 1% PVA solution, creating double emulsion microspheres, which were collected in a 200 mL beaker of

static 1% PVA. Several pumping speeds for each phase were evaluated, ultimately, the 1% PVA in deionized water was pumped at a rate of 4 mL/hr, while the PLGA emulsion was pumped at 1 mL/hr. Following collection, resulting microspheres were imaged using a Nikon inverted light microscope, then frozen in liquid nitrogen and lyophilized for further use and analysis.

6.3 RESULTS

To generate proof-of-concept ICC scaffolding for bone repair, sonication was used to organize monodisperse microspheres in the micron size range (diameters of approximately 100 μm) for the fabrication of three-dimensional colloidal crystal templates. After optimizing fusion methods, these colloidal crystals were infiltrated with PLGA and ReCaPP. Crystal templates were then dissolved away, leaving behind highly porous, inverted colloidal crystal scaffolds. Additionally, the production and characterization of monodispersed PLGA microspheres was investigated for the potential release of growth factors from colloidal crystal scaffolding.

6.3.1 Inverted Colloidal Crystal Calcium Phosphate Scaffold

Prior to using calcium phosphate to create inverted colloidal crystals, PLA and PLGA were used as infiltration media to create ICCs (Figure 39). Fabrication of ICCS formed using these (ond other) polymers is described in detail in the literature, and allowed us to refine our methods

before exploring the creation of ICCs using calcium phosphate. SEM imaging of ICCS created with PLA and PLGA show a uniform structure and interconnected porous network (Figure 39).

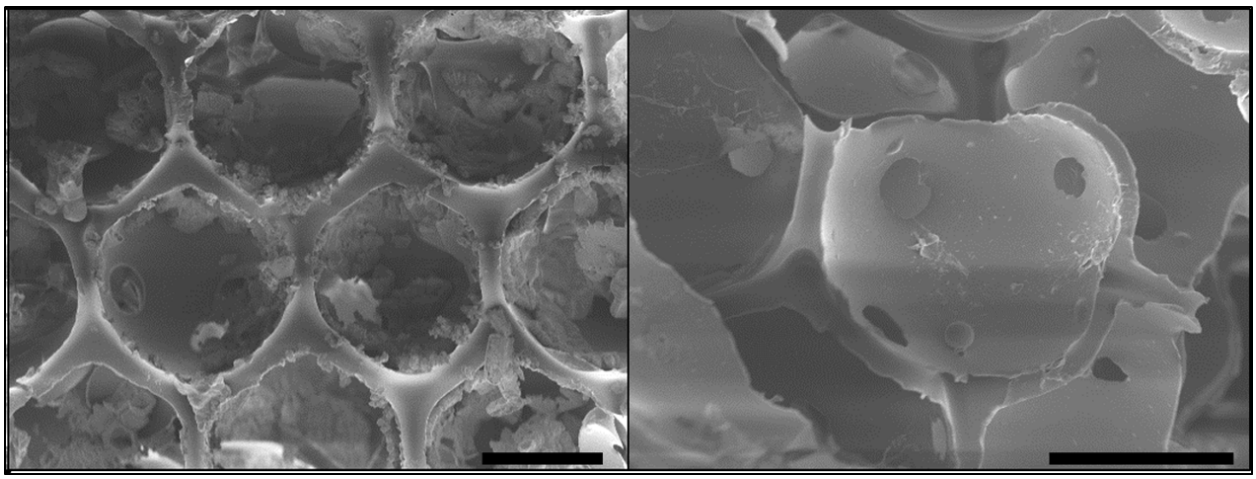

Figure 39. PLA ICC scaffolding, showing a uniform interconnected porous network. Scale bars = 100 μm.

Calcium phosphate inverted colloidal crystals (CP ICCs) were produced by first arranging monodisperse polystyrene microspheres within a stainless steel mold (Figure 40, A) and fusing the resulting hexagonally-packed crystal (Figure 40, B). Once the crystal cooled, calcium phosphate was added to the mold and allowed to set (Figure 40, C.) Following CaP setting, infiltrated crystals were calcinated for 3 hours at 500^{o}C for 3 hours, leaving behind an the calcium phosphate inverted colloidal crystal (Figure 41). Interestingly, differing microstructures were observed in the same CP ICC (Figure 42).

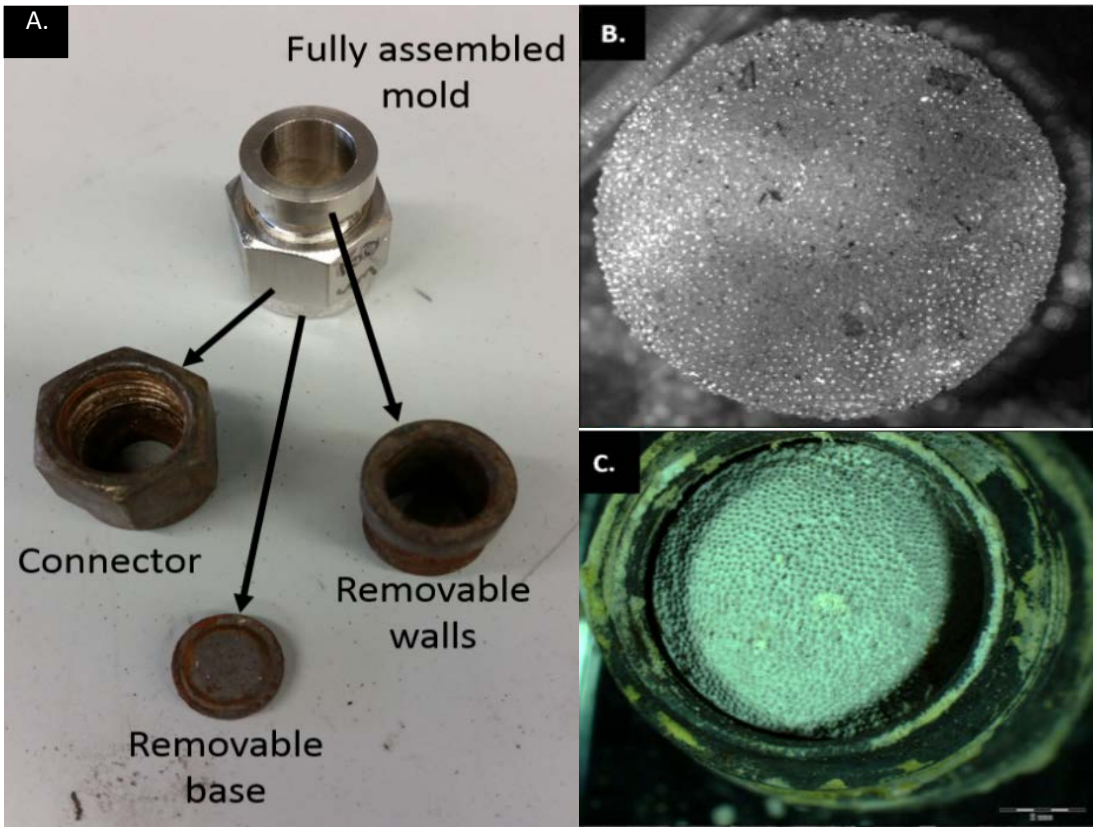

Figure 40. A) Depiction of steel mold used to fabricate polystyrene particle colloidal crystals, B) Resulting colloidal crystal removed from mold following fusion, and C) PS colloidal crystal following infiltration with ReCaPP cement.

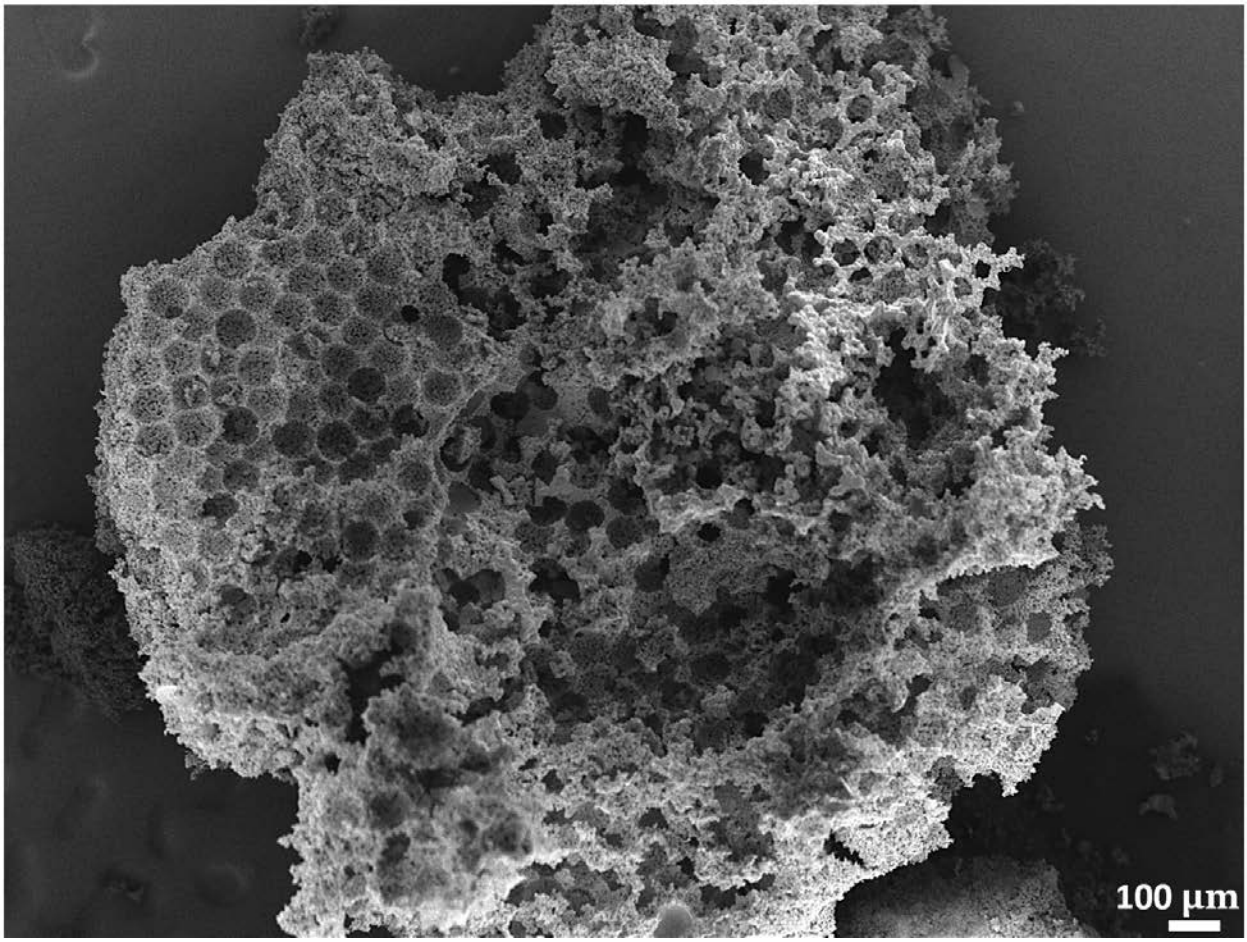

Figure 41. SEM of ReCaPP inverse colloidal crystal following calcination of polystyrene particles.

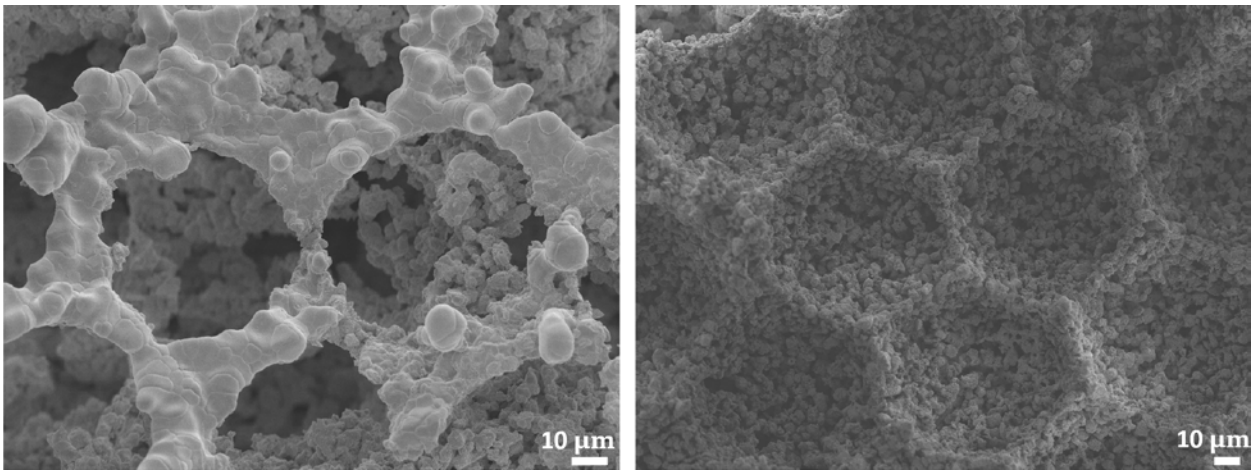

Figure 42. SEMs showing regions of the CP ICC in Figure 33, revealing regions of differing microstructures

6.3.2 PLGA Microspheres for Growth Factor Release

PLGA microspheres were fabricated with a range of NaCl concentrations in the inner aqueous phase to create porous microspheres for the facilitation of PDGF release. Examples of the creation of porous microspheres via salt concentrations ranging from 5 mM NaCl to 50 mM NaCl (Figure 43) show that microspheres are increasingly porous with increasing salt concentrations. In Figure 44, an SEM of a microsphere fabricated with a 50 mM inner aqueous salt concentration shows resulting porosity across the surface of the microsphere.

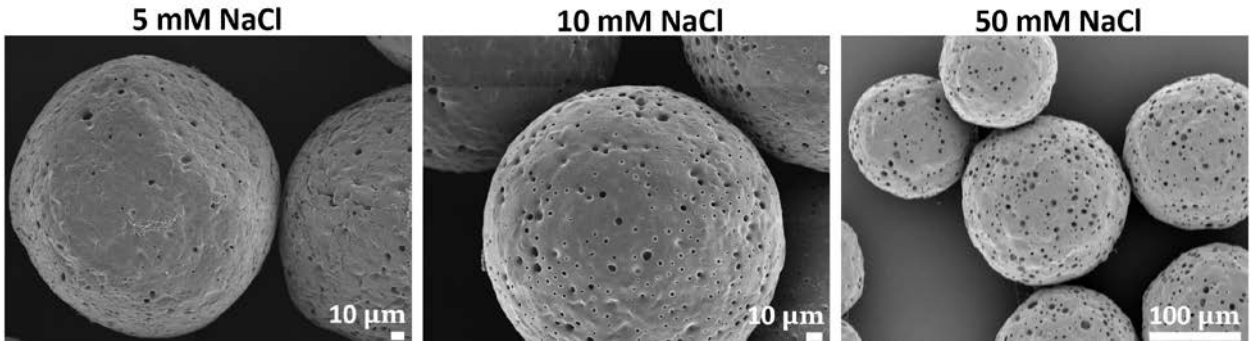

Figure 43. SEMs of PLGA particles fabricated using different concentrations of salt in the water phase, resulting in increasing porosities with increasing salt concentrations

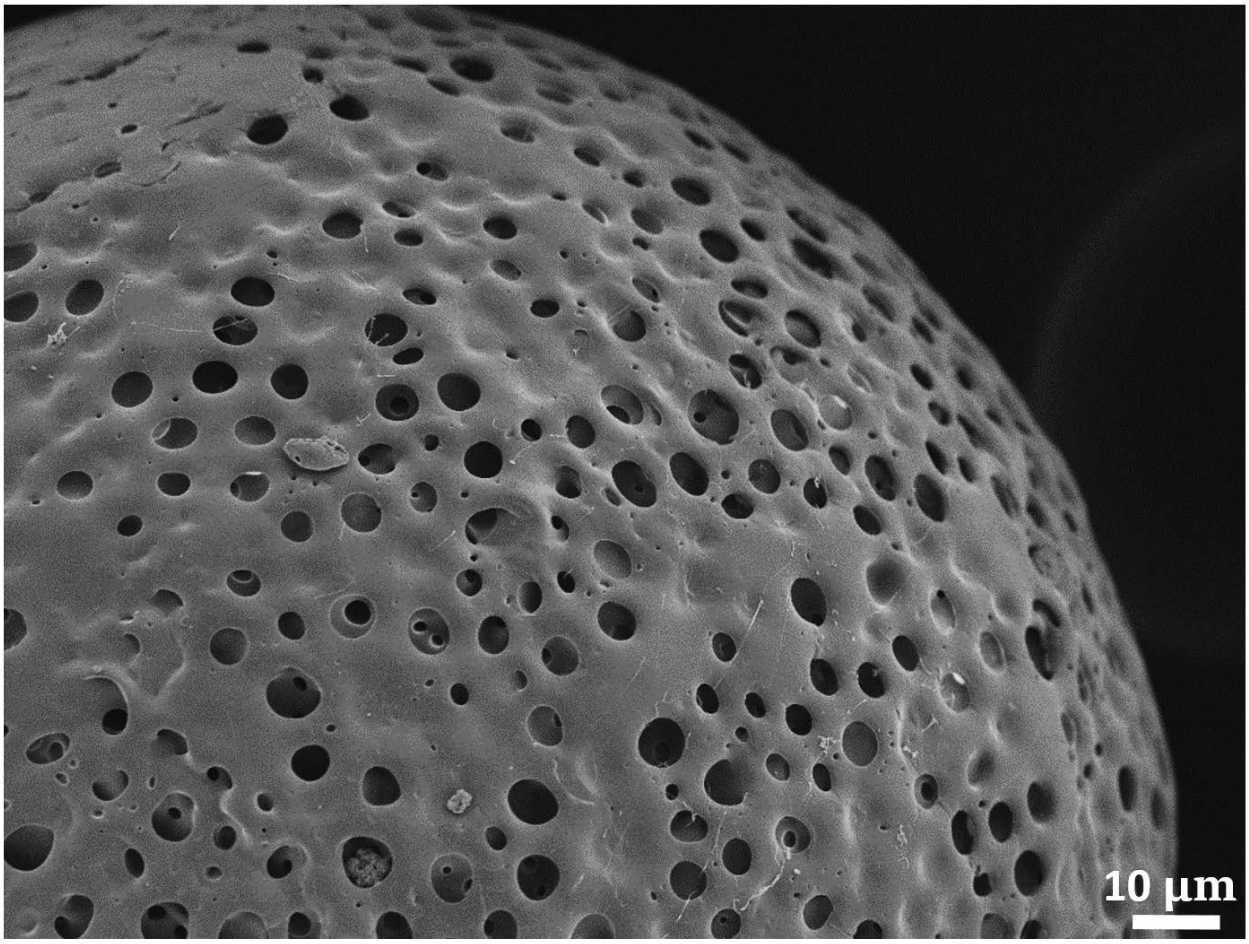

Figure 44. SEM of surface architecture porosities of PLGA microsphere produced using a 50 mM NaCl concentration in the inner aqueous phase.

6.3.3 PDGF Release from PLGA Microspheres

PDGF release was assayed from microspheres fabricated with inner aqueous phases of varying salt concentrations (0 mM – 50 mM) PDGF release from microspheres was assayed over the course of 10 days. As shown in Figure 45, all microsphere formulations had a burst release over the first 2-3 days of the assay, after which no further release was detected. Additionally, the magnitude of

the burst observed increased with increasing inner acqueous salt concentration/microsphere porosity.

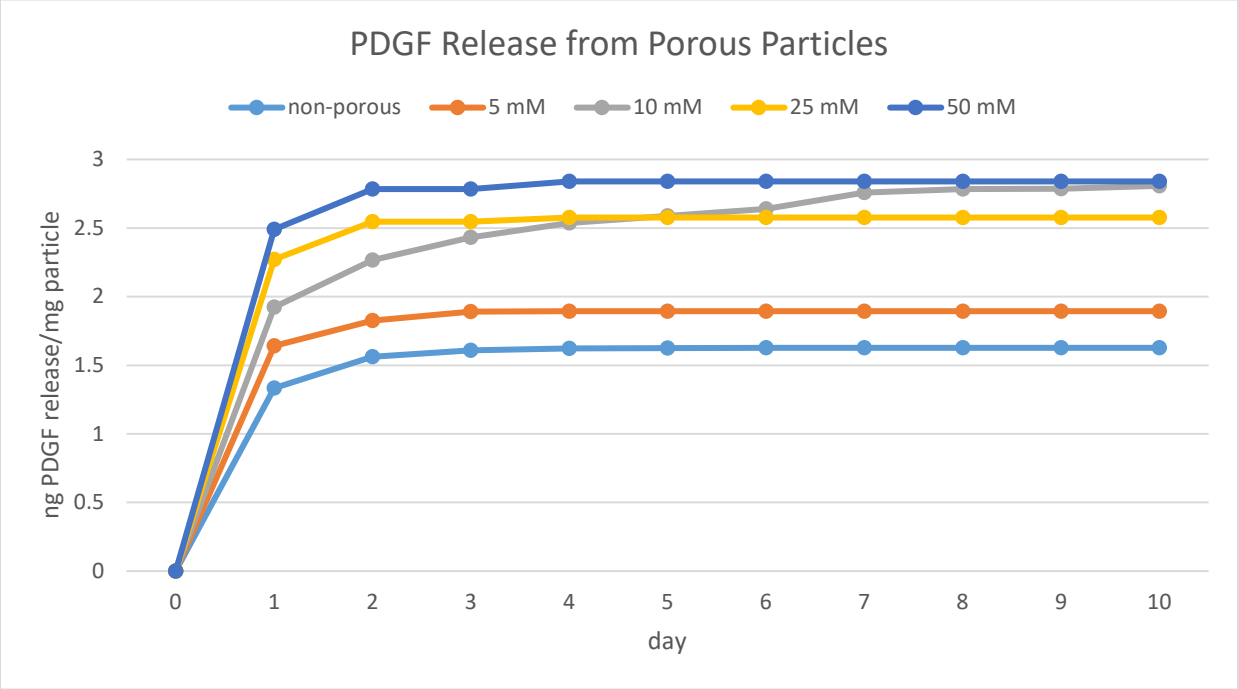

Figure 45. PDGF release profiles of PDGF particles with varying salt concentrations in the water phase, showing that increasing salt concentration increase the burst release of PDGF.

6.3.4 Arrangement and Fusion of PLGA Microspheres

Microspheres with 25 mM and 50 mM inner aqueous NaCL concentration were used in fusion experiments. Less porous microspheres (with 25 mM NaCl inner aqueous concentration) were fused at 40^{O}C for 10 hours, while microspheres with greater porosity (50 mM NaCl inner aqueous concentration) were fused at 40^{O}C for 8 hours. Resulting crystals were imaged (Figure 46),

showing that microspheres lost their shape and structure when fused for 10 hours, and at 8 hours were no longer spherical, but maintained their surface architecture and porosity.

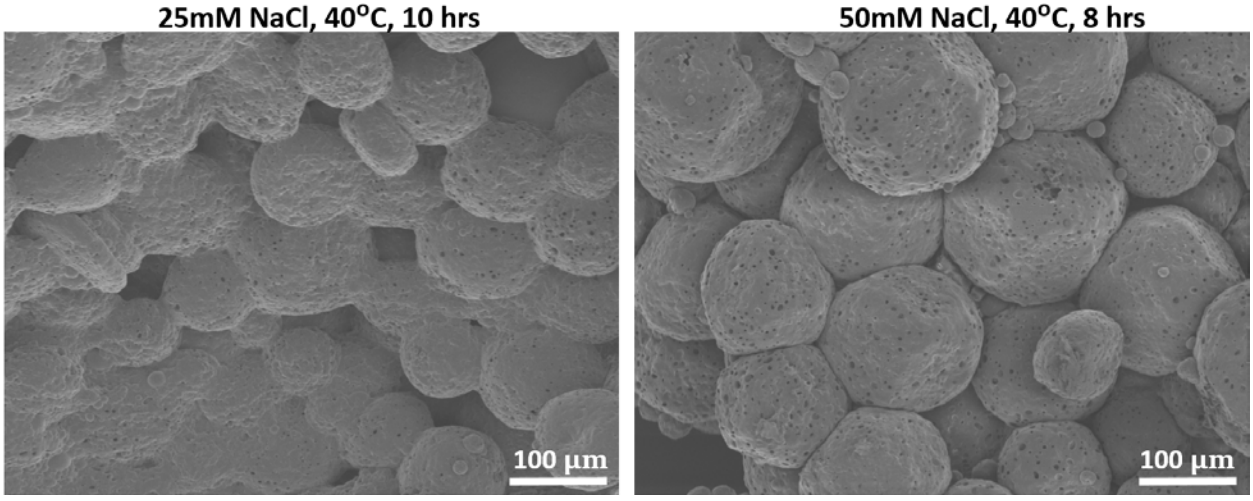

Figure 46. SEM micrographs of PLGA microsphere fusion attempts at 40°C for 10 hours and 8 hours, showing that microspheres begin to melt at 10 hours, and begin to deform at 8 hours, suggesting a midpoint in this time range may be more ideal for fusion.

6.3.5 Monodisperse PLGA Microsphere Fabrication

Monodisperse PLGA microspheres were fabricated using a focussed flow microfluidics chip (Micronit Fluidics) in combination with two syringe pumps – one to pump the water-in-oil growth factor/PLGA emulsion, and one to pump a 1% PVA phase. Resulting microspheres of approximately 175 µm (when wet) were produced as shown in Figure 47.

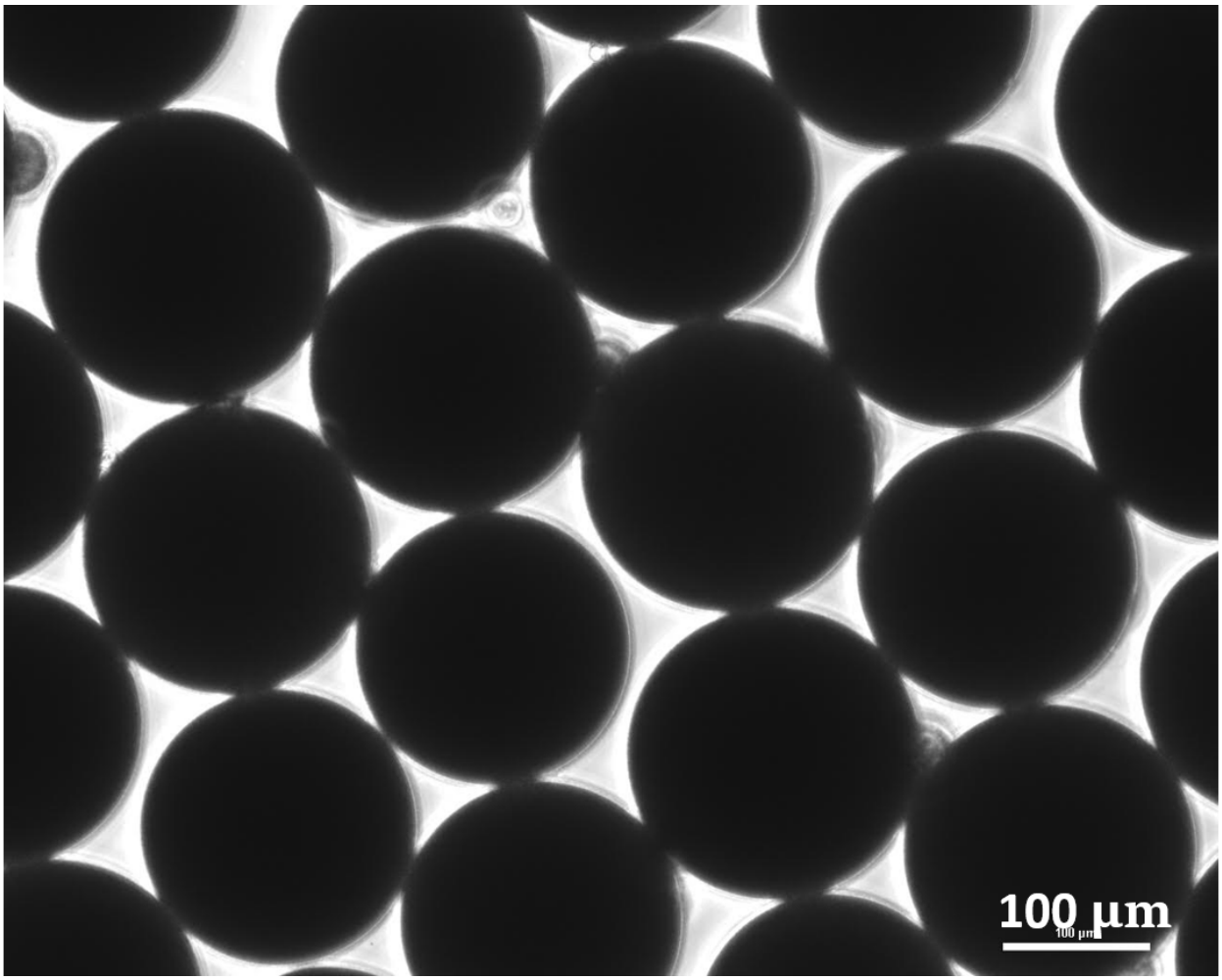

Figure 47. A microscopic image of monodisperse PLGA microspheres immediately following fabrication showing consistently sized microspheres approximately 175 µm in diameter prior to freeze-drying.

6.4 DISCUSSION

To create a CP ICC, various methods of dissolving microspheres (polystyrene, PLGA) away from the scaffold were investigated, including dichloromethane, hydrofluoric acid, dimethyl sulfoxide,

and tetrahydrohydrofuran. However, these methods resulted in uneven dissolution of the microspheres, and unpredictable swelling of the microspheres during dissolution, which at times, compromised the structural integrity of the scaffolding. As an alternative method of microsphere removal, scaffolds were heated to temperatures of 500-700^{O}C over time periods ranging from 30 minutes to 3 hours. Ultimately, it was found that heating the scaffolds at lower temperatures for longer time-frames resulted in more complete microsphere removal, and therefore, a more porous, organized three-dimensional structure. Interestingly, when the resulting CP ICC was imaged with a scanning electron microscope, it was found to have distinct regions of differing microstructures (Figure 42). In regions where microsphere imprints are observed, this is likely a result of incomplete microsphere fusion, which allowed CaP infiltration fully around the surface of the microsphere. Where "bridges" of CaP scaffolding are observed, microspheres had likely fused to a greater degree, leaving behind little room for CaP to infiltrate, and resulting in large pore "windows." Ideally, a more consistent microsphere fusion would result in more standard CaP infiltration, creating an organized, predictable pore structure throughout the scaffold.

To incorporate growth factor release into the colloidal crystal template, double emulsion PLGA microspheres were fabricated with salt (NaCl) in the inner aqueous phase to create porous particles that facilitate PDGF release. Microspheres with inner aqueous salt concentrations of 25 mM and 50 mM were ultimately chosen for incorporation in ICC scaffolding, as they had the greatest porosity of microspheres generated (Figure 44). With increasing microsphere porosity, we expected greater growth factor release, which was indeed observed in the magnitude of burst release of PDGF (Figure 45). Interestingly, no PDGF release was observed in porous microspheres following burst release, indicating that positively-charged PDGF may have bound to the negatively-chardged degrading PLGA [208]. Another explanation for this behavior may be that

the swelling of inner pockets of the microspheres containing PDGF caused rupture of the microsphere, resulting in immediate burst release of its contents [225, 226].

To fuse PLGA microspheres and create the template for the colloidal crystal scaffolding, a low temperature (40^{O}C) was chosen for several reasons: 1) the known melting point of PLGA ranges from 60^{O}C to over 200^{O}C, (depending on molecular weight and polymer ratio)[227, 228] 2) growth factors such as PDGF become inactivated at higher temperatures (in excess of 100^{O}C [229]), and 3) as found in our previous experiments, both the fusion and calcination of microspheres occurs more uniformly at lower temperatures over longer time periods. In addition to choosing to fuse microspheres at 40^{O}C, two time periods were explored for fusing PLGA microspheres: 8 hours and 10 hours. Microspheres with high porosity (50 mM inner aquous salt concentration) were fused for less time (8 hours) in anticipation of their high porosity speeding fusion. It was found that while microspheres began to deform after 8 hours, they did not fuse to one another, indicating a longer fusion period may be necessary (Figure 46). However, when microspheres were fused for 10 hours, they deformed greatly, melting to the point of losing their spherical structure (Figure 46). Together, these results indicate that a midpoint between 8 and 10 hours of fusion at 40^{O}C may be more appropriate for fusing PLGA microspheres in this application.

As shown in Figure 47, when generating monodisperse PLGA microspheres, pumping speeds of 4 mL/hr for the 1% PVA phase and 1 mL/hour for the PLGA single emulsion phase were found to generate microspheres of approximately 175 μm in diameter immediately following fabrication (before dehydration and freezing.) Microspheres of this size are acceptable for use in the fabrication of an ICC scaffold, as microspheres ranging from 100-200 μm are recognized to generate pores of a size that will allow angiogenesis formation and diffusion throughout the scaffold [230-232].

6.5 CONCLUSIONS

In these experiments, we have shown the possibility of creating an inverted colloidal crystal scaffold with calcium phosphate cement. Additionally, we have fabricated our own monodisperse PLGA microspheres capable of releasing PDGF in a predictable manner and explored the fusion of these microspheres into a colloidal crystal template. Together, these results can be further optimized and combined to create a CP ICC capable of controllable releasing growth factors. The work performed in this chapter demonstrates the potential for the fabrication of a calcium phosphate-based inverted colloidal crystal scaffold capable of releasing growth factors to promote cell infiltration, and ultimately, the regeneration of new tissue. Through continued collaboration, fabrication techniques may be refined to create a more consistent porous network and to explore cellular responses to growth factor release from this hierarchically organized structure.

7.0 CONCLUSIONS AND FUTURE OUTLOOK

We have utilized a three dimensional, *in vitro* model that permits the exploration of the effects of growth factor timing on vascularization in the context of bone repair with a large degree of variables. Specifically, we were able to evaluate resulting tubule formation from variations in sequence, length, and degree of overlap in growth factor delivery. We observed that the sequence of angiogenic (PDGF) to osteogenic (BMP-2) presentation resulted in greater tubule formation than the reverse presentation or co-delivery of these growth factors. Additionally, moderate overlap (2-4 days) in the sequence of PDGF to BMP-2 delivery resulted in greater tubule formation in comparison to the absence of overlap as well as prolonged overlap. Using PLGA microspheres, alginate hydrogels, alginate microspheres, and ReCaPP cement, we fabricated an osteoconductive, three-dimensional, porous scaffold capable of controllably releasing a programmed schedule of PDGF and BMP-2 delivery. With this combination of materials, we stimulated the infiltration of ReCaPP scaffolding by hMSC and HUVEC co-cultures in response to a PDGF gradient. Additionally BMP-2 that was controllably released from alginate microspheres in the ReCaPP scaffold promoted ALP expression in hMSCs cultures on both day 7 and day 14 time-points. Using alginate microspheres, ReCaPP cement, polystyrene microspheres, and PLGA microspheres, we have begun to explore additional scaffolding and assaying techniques that may lead to greater advances in the efficacy of these controlled release systems. These approaches may be further applied to investigate the effects of growth factor timing, overlap, and sequence on additional cell

types, later time points to gather information that may lead to improved *in vivo* outcomes. The resulting information could serve as a valuable contribution to our understanding of the effects of growth factor timing and sequence in the bone regeneration niche, and ideally, advance the development of growth factor therapies for fracture repair.

Traditional methods used clinically for fracture repair, on a daily basis, are something you may expect of more primitive times; hammers, chisels, and saws are used to cut bone from one location in the living human body, that is then nailed into the site of fracture to promote healing. Even recent technologies, like the incorporation of BMP-2 into synthetic scaffolding still has many limitations; it is currently broadly delivered in large quantities, and while sometimes effective, has also led to complications such as ectopic bone formation and fused spinal vertebrae. At this moment, we are at the beginning of understanding the complex *in vivo* healing processes, that is, how cells and growth factors communicate with each other over space and time to orchestrate a multi-stage cascade of cellular event. This body of work serves to bring the field a step closer in understanding these complex behaviors, and in response, creating new biomaterials that begin to take these complexities into account when designing a new generation of growth factor delivery scaffolding for bone repair.

The future testing and development of these growth factor technologies for regeneration intersects with a fascinating moment in the US government's classification and regulation of biologically active medical devices. While both BMP-2 and PDGF-BB have been approved for different applications in clinical use, there remain serious side effects and complications associated with growth factor delivery for regeneration. Particularly in the case of BMP-2 delivery, overproduction of bone growth (and in some cases, undesired bone fusion) has soured the enthusiasm once held for these therapies. Additionally, there has yet to be a product approved for

clinical use that elutes multiple recombinant growth factors. Although products such as platelet–rich plasma, which contain a variety of growth factors are approved for some clinical applications, they fall under the “biologics” classification of the FDA, and are regulated by the Center for Biologics Evaluation and Research. When combining multiple biologically active agents (particularly recombinant proteins) with scaffolding material engineered to provide controlled release, we reach an undefined, grey area between “medical device” and “biologic” FDA classification. While controlled release technologies may assuage some of the drawbacks of multiple growth factor release in clinical applications (such as mitigating ectopic bone formation and cutting costs by delivering lower growth factor concentrations) there still remain unanswered questions in the approval and implementation processes of such products.

APPENDIX

CONFIRMING CELLULAR STRUCTURES WITH SCANNING ELECTRON MICROSCOPY

While cells are sometimes difficult to identify within scaffolds using scanning electron microscopy, several studies have validated the use of SEM to analyze cells specifically within calcium phosphate scaffolds [233-236]. For the purposes of identifying cell infiltration in these studies, calcium phosphate scaffolds were imaged from the top (where cells were seeded), from the bottom (opposite side from where cells were seeded), and along a top-to-bottom vertical cross-section at approximately the diameter of the cylindrical scaffold. Cells were identified to be spindle-like structures within the pores of the scaffolds that are visually similar to the appearance of cells identified via SEM in calcium phosphate scaffolds of comparable studies [233, 234]. Spindle-like cell structures observed in the cross-sections of scaffolds can be more clearly seen in Figure 48, which depicts the top of a scaffold in the PDGF + BMP treatment group. These structures were absent from the bottom images of all scaffolds, an example of which can be seen in Figure 49. Other methods of microscopically identifying cells within the scaffold are limited because calcium phosphate is opaque, and therefore, cannot be penetrated by a light source that is

required by most microscopy methods. As a potential alternative to SEM, a top-lit confocal microscope, however, this resource is not currently available for use at our imaging facilities.

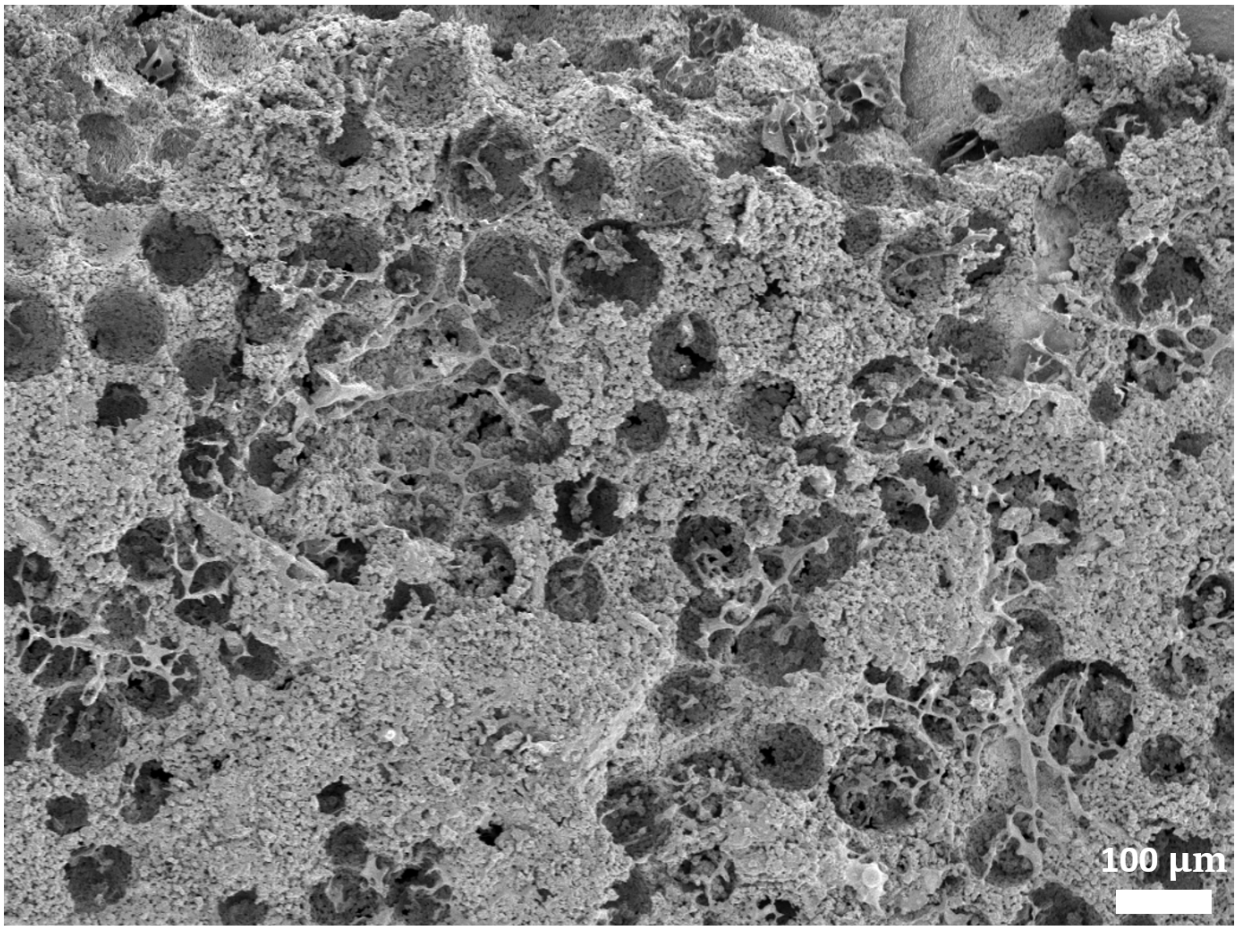

Figure 48. The top surface of a scaffold at experimental day 10, where a co-culture of HUVECs and hMSCs were seeded on day zero, showing spindle-like cellular structures within the surface pores of the scaffold.

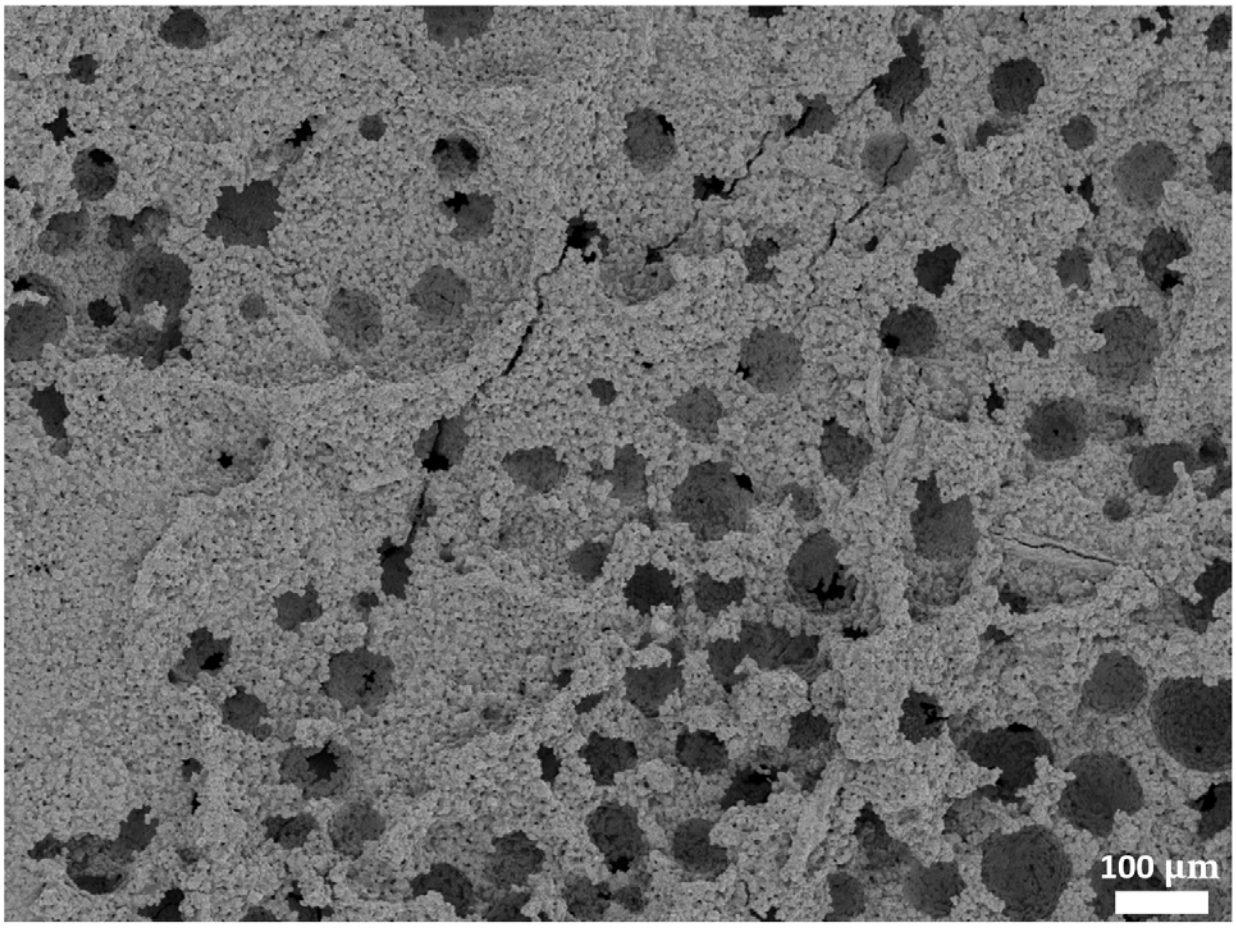

Figure 49. The bottom surface of a scaffold on experimental day 10, opposite the site of cell seeding, showing an absence of spindle-like cellular structures from the surface or pores of the scaffold.

BIBLIOGRAPHY

[1] Bone Graft: Iliac Crest Bone Harvest, EBSCO Publishing, Icahn School of Medicine at Mount Sinai, 2016.

[2] R. Dimitriou, E. Jones, D. McGonagle, P.V. Giannoudis, Bone regeneration: current concepts and future directions, BMC Med, 9 (2011) 66.

[3] J.N. Fisher, G.M. Peretti, C. Scotti, Stem Cells for Bone Regeneration: From Cell-Based Therapies to Decellularised Engineered Extracellular Matrices, Stem Cells Int, 2016 (2016) 9352598.

[4] G.K. Michalopoulos, Liver regeneration, J Cell Physiol, 213 (2007) 286-300.

[5] X. Feng, J.M. McDonald, Disorders of bone remodeling, Annu Rev Pathol, 6 (2011) 121-145.

[6] A. Sood, S. Chung, P.J. Therattil, E.S. Lee, Reconstruction of a Complex Metacarpal Shaft Fracture With Segmental Bone Loss Using Autologous Iliac Crest Bone Graft, Eplasty, 15 (2015) ic47.

[7] C. Hasselman, G. Gruen, Principles of operative fracture stabilization and fixation, in: R. Fitzgerald (Ed.) Orthopaedics, Mosby, St. Louis, USA, 2004, pp. 2228-2238.

[8] G.F. Rogers, A.K. Greene, Autogenous bone graft: basic science and clinical implications, J Craniofac Surg, 23 (2012) 323-327.

[9] Z. Fedorowicz, M. Nasser, J.T. Newton, R.J. Oliver, Resorbable versus titanium plates for orthognathic surgery, Cochrane Database Syst Rev, (2007) CD006204.

[10] C.G. Finkemeier, Bone-grafting and bone-graft substitutes, J Bone Joint Surg Am, 84-A (2002) 454-464.

[11] M.K. Sen, T. Miclau, Autologous iliac crest bone graft: should it still be the gold standard for treating nonunions?, Injury, 38 Suppl 1 (2007) S75-80.

[12] R. Dimitriou, G.I. Mataliotakis, A.G. Angoules, N.K. Kanakaris, P.V. Giannoudis, Complications following autologous bone graft harvesting from the iliac crest and using the RIA: a systematic review, Injury, 42 Suppl 2 (2011) S3-15.

[13] B.P. Chan, K.W. Leong, Scaffolding in tissue engineering: general approaches and tissue-specific considerations, Eur Spine J, 17 Suppl 4 (2008) 467-479.

[14] M. Hosseinkhani, D. Mehrabani, M.H. Karimfar, S. Bakhtiyari, A. Manafi, R. Shirazi, Tissue engineered scaffolds in regenerative medicine, World J Plast Surg, 3 (2014) 3-7.

[15] R. Marsell, T.A. Einhorn, The biology of fracture healing, Injury, 42 (2011) 551-555.

[16] C. Sfeir, L. Ho, B.A. Doll, K. Azari, J.O. Hollinger, Fracture Repair, in, Humana Press, Inc., Bone Regeneration and Repair: Biology and Clinical Applications, 2005, pp. 21-44.

[17] R. Dimitriou, E. Tsiridis, P.V. Giannoudis, Current concepts of molecular aspects of bone healing, Injury, 36 (2005) 1392-1404.

[18] D.R. Marsh, G. Li, The biology of fracture healing: optimising outcome, Br Med Bull, 55 (1999) 856-869.

[19] T.A. Einhorn, L.C. Gerstenfeld, Fracture healing: mechanisms and interventions, Nat Rev Rheumatol, 11 (2015) 45-54.

[20] B. Beale, Orthopedic clinical techniques femur fracture repair, Clin Tech Small Anim Pract, 19 (2004) 134-150.

[21] J.P. Waddell, D.W. Johnston, A. Neidre, Fractures of the tibial plateau: a review of ninety-five patients and comparison of treatment methods, J Trauma, 21 (1981) 376-381.

[22] E. Gómez-Barrena, P. Rosset, D. Lozano, J. Stanovici, C. Ermthaller, F. Gerbhard, Bone fracture healing: cell therapy in delayed unions and nonunions, Bone, 70 (2015) 93-101.

[23] E. Rightmire, D. Zurakowski, M. Vrahas, Acute infections after fracture repair: management with hardware in place, Clin Orthop Relat Res, 466 (2008) 466-472.

[24] R.K. Hernandez, T.P. Do, C.W. Critchlow, R.E. Dent, S.S. Jick, Patient-related risk factors for fracture-healing complications in the United Kingdom General Practice Research Database, Acta Orthop, 83 (2012) 653-660.

[25] A.F. Mavrogenis, G.N. Panagopoulos, P.D. Megaloikonomos, V.G. Igoumenou, I. Galanopoulos, C.T. Vottis, P. Karabinas, P. Koulouvaris, V.A. Kontogeorgakos, J. Vlamis, P.J. Papagelopoulos, Complications After Hip Nailing for Fractures, Orthopedics, 39 (2016) e108-116.

[26] N.E. Epstein, Complications due to the use of BMP/INFUSE in spine surgery: The evidence continues to mount, Surg Neurol Int, 4 (2013) S343-352.

[27] T. Katagiri, K. Osawa, S. Tsukamoto, M. Fujimoto, A. Miyamoto, T. Mizuta, Bone morphogenetic protein-induced heterotopic formation: what have we learned from the history of a half century?, in, Japanese Dental Science Review, 2015, pp. 42-50.

[28] E.A. Bayer, R. Gottardi, M.V. Fedorchak, S.R. Little, The scope and sequence of growth factor delivery for vascularized bone tissue regeneration, J Control Release, 219 (2015) 129-140.

[29] M. Griffin, A. Bayat, Electrical stimulation in bone healing: critical analysis by evaluating levels of evidence, Eplasty, 11 (2011) e34.

[30] E. Dawson, H.W. Bae, J.K. Burkus, J.L. Stambough, S.D. Glassman, Recombinant human bone morphogenetic protein-2 on an absorbable collagen sponge with an osteoconductive bulking agent in posterolateral arthrodesis with instrumentation. A prospective randomized trial, J Bone Joint Surg Am, 91 (2009) 1604-1613.

[31] M. Beederman, J.D. Lamplot, G. Nan, J. Wang, X. Liu, L. Yin, R. Li, W. Shui, H. Zhang, S.H. Kim, W. Zhang, J. Zhang, Y. Kong, S. Denduluri, M.R. Rogers, A. Pratt, R.C. Haydon, H.H. Luu, J. Angeles, L.L. Shi, T.C. He, BMP signaling in mesenchymal stem cell differentiation and bone formation, J Biomed Sci Eng, 6 (2013) 32-52.

[32] H. Yu, P. VandeVord, W. Gong, B. Wu, Z. Song, H. Matthew, P. Wooley, S. Yang, Promotion of osteogenesis in tissue-engineered bone by pre-seeding endothelial progenitor cells-derived endothelial cells, in, Journal of Orhtopaedic Research, 2008, pp. 1147-1152.

[33] S. Endres, B. Hiebl, J. Hägele, C. Beltzer, R. Fuhrmann, V. Jäger, M. Almeida, E. Costa, C. Santos, H. Traupe, E.M. Jung, L. Prantl, F. Jung, A. Wilke, R.P. Franke, Angiogenesis and healing with non-shrinking, fast degradeable PLGA/CaP scaffolds in critical-sized defects in the rabbit femur with or without osteogenically induced mesenchymal stem cells, Clin Hemorheol Microcirc, 48 (2011) 29-40.

[34] I. Moreno-Miralles, J.C. Schisler, C. Patterson, New insights into bone morphogenetic protein signaling: focus on angiogenesis, Curr Opin Hematol, 16 (2009) 195-201.

[35] Y. Suzuki, N. Ohga, Y. Morishita, K. Hida, K. Miyazono, T. Watabe, BMP-9 induces proliferation of multiple types of endothelial cells in vitro and in vivo, J Cell Sci, 123 (2010) 1684-1692.

[36] M.M. Deckers, R.L. van Bezooijen, G. van der Horst, J. Hoogendam, C. van Der Bent, S.E. Papapoulos, C.W. Löwik, Bone morphogenetic proteins stimulate angiogenesis through osteoblast-derived vascular endothelial growth factor A, Endocrinology, 143 (2002) 1545-1553.

[37] P.J. Marie, Fibroblast growth factor signaling controlling bone formation: an update, Gene, 498 (2012) 1-4.

[38] J.E. Tengood, R. Ridenour, R. Brodsky, A.J. Russell, S.R. Little, Sequential delivery of basic fibroblast growth factor and platelet-derived growth factor for angiogenesis, Tissue Eng Part A, 17 (2011) 1181-1189.

[39] J. Borges, M.C. Müller, A. Momeni, G.B. Stark, N. Torio-Padron, In vitro analysis of the interactions between preadipocytes and endothelial cells in a 3D fibrin matrix, Minim Invasive Ther Allied Technol, 16 (2007) 141-148.

[40] Y.Q. Yang, Y.Y. Tan, R. Wong, A. Wenden, L.K. Zhang, A.B. Rabie, The role of vascular endothelial growth factor in ossification, Int J Oral Sci, 4 (2012) 64-68.

[41] N. Sato, J.G. Beitz, J. Kato, M. Yamamoto, J.W. Clark, P. Calabresi, A. Raymond, A.R. Frackelton, Platelet-derived growth factor indirectly stimulates angiogenesis in vitro, Am J Pathol, 142 (1993) 1119-1130.

[42] C. Rolny, I. Nilsson, P. Magnusson, A. Armulik, L. Jakobsson, P. Wentzel, P. Lindblom, J. Norlin, C. Betsholtz, R. Heuchel, M. Welsh, L. Claesson-Welsh, Platelet-derived growth factor receptor-beta promotes early endothelial cell differentiation, Blood, 108 (2006) 1877-1886.

[43] P.U. Magnusson, C. Looman, A. Ahgren, Y. Wu, L. Claesson-Welsh, R.L. Heuchel, Platelet-derived growth factor receptor-beta constitutive activity promotes angiogenesis in vivo and in vitro, Arterioscler Thromb Vasc Biol, 27 (2007) 2142-2149.

[44] J.O. Hollinger, C.E. Hart, S.N. Hirsch, S. Lynch, G.E. Friedlaender, Recombinant human platelet-derived growth factor: biology and clinical applications, J Bone Joint Surg Am, 90 Suppl 1 (2008) 48-54.

[45] E.A. Bayer, R. Gottardi, M.V. Fedorchak, S.R. Little, The scope and sequence of growth factor delivery for vascularized bone tissue regeneration, J Control Release, (2015).

[46] E.E. Johnson, M.R. Urist, G.A. Finerman, Resistant nonunions and partial or complete segmental defects of long bones. Treatment with implants of a composite of human bone morphogenetic protein (BMP) and autolyzed, antigen-extracted, allogeneic (AAA) bone, Clin Orthop Relat Res, (1992) 229-237.

[47] K. Elima, Osteoinductive proteins, Ann Med, 25 (1993) 395-402.

[48] T.K. Sampath, J.C. Maliakal, P.V. Hauschka, W.K. Jones, H. Sasak, R.F. Tucker, K.H. White, J.E. Coughlin, M.M. Tucker, R.H. Pang, Recombinant human osteogenic protein-1 (hOP-1) induces new bone formation in vivo with a specific activity comparable with natural bovine osteogenic protein and stimulates osteoblast proliferation and differentiation in vitro, J Biol Chem, 267 (1992) 20352-20362.

[49] H.S. Sandhu, L.E. Kanim, J.M. Kabo, J.M. Toth, E.N. Zeegen, D. Liu, R.B. Delamarter, E.G. Dawson, Effective doses of recombinant human bone morphogenetic protein-2 in experimental spinal fusion, Spine (Phila Pa 1976), 21 (1996) 2115-2122.

[50] S.D. Cook, S.L. Salkeld, D.C. Rueger, Evaluation of recombinant human osteogenic protein-1 (rhOP-1) placed with dental implants in fresh extraction sites, J Oral Implantol, 21 (1995) 281-289.

[51] E.H. Groeneveld, E.H. Burger, Bone morphogenetic proteins in human bone regeneration, Eur J Endocrinol, 142 (2000) 9-21.

[52] J.D. Boerckel, Y.M. Kolambkar, K.M. Dupont, B.A. Uhrig, E.A. Phelps, H.Y. Stevens, A.J. García, R.E. Guldberg, Effects of protein dose and delivery system on BMP-mediated bone regeneration, Biomaterials, 32 (2011) 5241-5251.

[53] L.H. Nguyen, N. Annabi, M. Nikkhah, H. Bae, L. Binan, S. Park, Y. Kang, Y. Yang, A. Khademhosseini, Vascularized bone tissue engineering: approaches for potential improvement, Tissue Eng Part B Rev, 18 (2012) 363-382.

[54] W. Kang, D.S. Lee, J.H. Jang, Evaluation of Sustained BMP-2 Release Profiles Using a Novel Fluorescence-Based Retention Assay, PLoS One, 10 (2015) e0123402.

[55] G.T.S. Kirby, L.J. White, C.V. Rahman, H.C. Cox, O. Qutachi, F.R.A.J. Rose, D.W. Hutmacher, K.M. Shakesheff, M.A. Woodruff, PLGA-Based Mircroparticles for the Sustained Release of BMP-2, in, Polymers, 2011, pp. 571-586.

[56] Y.-P. Yun, S.-Y. Lee, H.-J. Kim, J.-J. Song, S.E. Kim, Improvement of osteoblast functions by sustained release of bone morphogenetic protein-2 (BMP-2) from heparin-coated chitosan scaffold., in, Tissue Engineering and Regenerative Medicine, 2013, pp. 183-191.

[57] D.H. Kempen, L. Lu, A. Heijink, T.E. Hefferan, L.B. Creemers, A. Maran, M.J. Yaszemski, W.J. Dhert, Effect of local sequential VEGF and BMP-2 delivery on ectopic and orthotopic bone regeneration, Biomaterials, 30 (2009) 2816-2825.

[58] J.M. Kanczler, R.O. Oreffo, Osteogenesis and angiogenesis: the potential for engineering bone, Eur Cell Mater, 15 (2008) 100-114.

[59] T.P. Richardson, M.C. Peters, A.B. Ennett, D.J. Mooney, Polymeric system for dual growth factor delivery, Nat Biotechnol, 19 (2001) 1029-1034.

[60] Z.S. Patel, S. Young, Y. Tabata, J.A. Jansen, M.E. Wong, A.G. Mikos, Dual delivery of an angiogenic and an osteogenic growth factor for bone regeneration in a critical size defect model, Bone, 43 (2008) 931-940.

[61] Y.C. Huang, D. Kaigler, K.G. Rice, P.H. Krebsbach, D.J. Mooney, Combined angiogenic and osteogenic factor delivery enhances bone marrow stromal cell-driven bone regeneration, J Bone Miner Res, 20 (2005) 848-857.

[62] K. Lee, E.A. Silva, D.J. Mooney, Growth factor delivery-based tissue engineering: general approaches and a review of recent developments, J R Soc Interface, 8 (2011) 153-170.

[63] C.G. Wilson, F.M. Martín-Saavedra, N. Vilaboa, R.T. Franceschi, Advanced BMP gene therapies for temporal and spatial control of bone regeneration, J Dent Res, 92 (2013) 409-417.

[64] D.J. de Gorter, M. van Dinther, O. Korchynskyi, P. ten Dijke, Biphasic effects of transforming growth factor β on bone morphogenetic protein-induced osteoblast differentiation, J Bone Miner Res, 26 (2011) 1178-1187.

[65] D.H. Kempen, L.B. Creemers, J. Alblas, L. Lu, A.J. Verbout, M.J. Yaszemski, W.J. Dhert, Growth factor interactions in bone regeneration, Tissue Eng Part B Rev, 16 (2010) 551-566.

[66] M.C. Phipps, Y. Xu, S.L. Bellis, Delivery of platelet-derived growth factor as a chemotactic factor for mesenchymal stem cells by bone-mimetic electrospun scaffolds, PLoS One, 7 (2012) e40831.

[67] L.J. Marden, R.S. Fan, G.F. Pierce, A.H. Reddi, J.O. Hollinger, Platelet-derived growth factor inhibits bone regeneration induced by osteogenin, a bone morphogenetic protein, in rat craniotomy defects, J Clin Invest, 92 (1993) 2897-2905.

[68] A.K. Ekaputra, G.D. Prestwich, S.M. Cool, D.W. Hutmacher, The three-dimensional vascularization of growth factor-releasing hybrid scaffold of poly (epsilon-caprolactone)/collagen fibers and hyaluronic acid hydrogel, Biomaterials, 32 (2011) 8108-8117.

[69] M. Mehta, K. Schmidt-Bleek, G.N. Duda, D.J. Mooney, Biomaterial delivery of morphogens to mimic the natural healing cascade in bone, Adv Drug Deliv Rev, 64 (2012) 1257-1276.

[70] E.D. Rabinovsky, R. Draghia-Akli, Insulin-like growth factor I plasmid therapy promotes in vivo angiogenesis, Mol Ther, 9 (2004) 46-55.

[71] R. Subbiah, P. Du, M.P. Hwang, I.G. Kim, S.Y. Van, Y.K. Noh, H. Park, K. Park, Dual Growth Factor-Loaded Core-Shell Polymer Microcapsules Can Promote Osteogenesis and Angiogenesis, in, Macromolecular Research, 2014, pp. 1320-1329.

[72] J.M. Kanczler, P.J. Ginty, L. White, N.M. Clarke, S.M. Howdle, K.M. Shakesheff, R.O. Oreffo, The effect of the delivery of vascular endothelial growth factor and bone morphogenic protein-2 to osteoprogenitor cell populations on bone formation, Biomaterials, 31 (2010) 1242-1250.

[73] K. Fujimura, K. Bessho, Y. Okubo, K. Kusumoto, N. Segami, T. Iizuka, The effect of fibroblast growth factor-2 on the osteoinductive activity of recombinant human bone morphogenetic protein-2 in rat muscle, Arch Oral Biol, 47 (2002) 577-584.

[74] N. Kakudo, K. Kusumoto, A. Kuro, Y. Ogawa, Effect of recombinant human fibroblast growth factor-2 on intramuscular ectopic osteoinduction by recombinant human bone morphogenetic protein-2 in rats, Wound Repair Regen, 14 (2006) 336-342.

[75] Y. Nakamura, K. Tensho, H. Nakaya, M. Nawata, T. Okabe, S. Wakitani, Low dose fibroblast growth factor-2 (FGF-2) enhances bone morphogenetic protein-2 (BMP-2)-induced ectopic bone formation in mice, Bone, 36 (2005) 399-407.

[76] J. Ratanavaraporn, H. Furuya, H. Kohara, Y. Tabata, Synergistic effects of the dual release of stromal cell-derived factor-1 and bone morphogenetic protein-2 from hydrogels on bone regeneration, Biomaterials, 32 (2011) 2797-2811.

[77] J. Su, H. Xu, J. Sun, X. Gong, H. Zhao, Dual Delivery of BMP-2 and bFGF from a New Nano-Composite Scaffold, Loaded with Vascular Stents for Large-Size Mandibular Defect Regeneration, Int J Mol Sci, 14 (2013) 12714-12728.

[78] A. Hernández, R. Reyes, E. Sánchez, M. Rodríguez-Évora, A. Delgado, C. Evora, In vivo osteogenic response to different ratios of BMP-2 and VEGF released from a biodegradable porous system, J Biomed Mater Res A, 100 (2012) 2382-2391.

[79] G.F. Muschler, V.P. Raut, T.E. Patterson, J.C. Wenke, J.O. Hollinger, The design and use of animal models for translational research in bone tissue engineering and regenerative medicine, Tissue Eng Part B Rev, 16 (2010) 123-145.

[80] Y. Zhang, X. Li, T. Chihara, T. Mizoguchi, A. Hori, N. Udagawa, H. Nakamura, H. Hasegawa, A. Taguchi, A. Shinohara, H. Kagami, Comparing immunocompetent and immunodeficient mice as animal models for bone tissue engineering, Oral Dis, 21 (2015) 583-592.

[81] A.I. Pearce, R.G. Richards, S. Milz, E. Schneider, S.G. Pearce, Animal models for implant biomaterial research in bone: a review, Eur Cell Mater, 13 (2007) 1-10.

[82] T.N. Vo, F.K. Kasper, A.G. Mikos, Strategies for controlled delivery of growth factors and cells for bone regeneration, Adv Drug Deliv Rev, 64 (2012) 1292-1309.

[83] H. Seeherman, R. Li, M. Bouxsein, H. Kim, X.J. Li, E.A. Smith-Adaline, M. Aiolova, J.M. Wozney, rhBMP-2/calcium phosphate matrix accelerates osteotomy-site healing in a nonhuman primate model at multiple treatment times and concentrations, J Bone Joint Surg Am, 88 (2006) 144-160.

[84] T.M. McFadden, G.P. Duffy, A.B. Allen, H.Y. Stevens, S.M. Schwarzmaier, N. Plesnila, J.M. Murphy, F.P. Barry, R.E. Guldberg, F.J. O'Brien, The delayed addition of human mesenchymal stem cells to pre-formed endothelial cell networks results in functional vascularization of a collagen-glycosaminoglycan scaffold in vivo, Acta Biomater, 9 (2013) 9303-9316.

[85] J.E. Tengood, K.M. Kovach, P.E. Vescovi, A.J. Russell, S.R. Little, Sequential delivery of vascular endothelial growth factor and sphingosine 1-phosphate for angiogenesis, Biomaterials, 31 (2010) 7805-7812.

[86] R.R. Chen, E.A. Silva, W.W. Yuen, D.J. Mooney, Spatio-temporal VEGF and PDGF delivery patterns blood vessel formation and maturation, Pharm Res, 24 (2007) 258-264.

[87] A.I. Caplan, D. Correa, PDGF in bone formation and regeneration: new insights into a novel mechanism involving MSCs, J Orthop Res, 29 (2011) 1795-1803.

[88] G.E. Friedlaender, S. Lin, L.A. Solchaga, L.B. Snel, S.E. Lynch, The role of recombinant human platelet-derived growth factor-BB (rhPDGF-BB) in orthopaedic bone repair and regeneration, Curr Pharm Des, 19 (2013) 3384-3390.

[89] J.J. Delgado, E. Sánchez, M. Baro, R. Reyes, C. Evora, A. Delgado, A platelet derived growth factor delivery system for bone regeneration, J Mater Sci Mater Med, 23 (2012) 1903-1912.

[90] I.H. Kalfas, Principles of bone healing, Neurosurg Focus, 10 (2001) E1.

[91] J.I. Greenberg, D.J. Shields, S.G. Barillas, L.M. Acevedo, E. Murphy, J. Huang, L. Scheppke, C. Stockmann, R.S. Johnson, N. Angle, D.A. Cheresh, A role for VEGF as a negative regulator of pericyte function and vessel maturation, Nature, 456 (2008) 809-813.

[92] M. Simons, R.O. Bonow, N.A. Chronos, D.J. Cohen, F.J. Giordano, H.K. Hammond, R.J. Laham, W. Li, M. Pike, F.W. Sellke, T.J. Stegmann, J.E. Udelson, T.K. Rosengart, Clinical trials in coronary angiogenesis: issues, problems, consensus: An expert panel summary, Circulation, 102 (2000) E73-86.

[93] O.B. Betz, V.M. Betz, A. Nazarian, M. Egermann, L.C. Gerstenfeld, T.A. Einhorn, M.S. Vrahas, M.L. Bouxsein, C.H. Evans, Delayed administration of adenoviral BMP-2 vector improves the formation of bone in osseous defects, Gene Ther, 14 (2007) 1039-1044.

[94] S.T. Becker, H. Bolte, K. Schünemann, H. Seitz, J.J. Bara, B.E. Beck-Broichsitter, P.A. Russo, J. Wiltfang, P.H. Warnke, Endocultivation: the influence of delayed vs. simultaneous application of BMP-2 onto individually formed hydroxyapatite matrices for heterotopic bone induction, Int J Oral Maxillofac Surg, 41 (2012) 1153-1160.

[95] O. Jeon, S.J. Song, H.S. Yang, S.H. Bhang, S.W. Kang, M.A. Sung, J.H. Lee, B.S. Kim, Long-term delivery enhances in vivo osteogenic efficacy of bone morphogenetic protein-2 compared to short-term delivery, Biochem Biophys Res Commun, 369 (2008) 774-780.

[96] Y. Zou, J.L. Brooks, V. Talwalkar, T.A. Milbrandt, D.A. Puleo, Development of an injectable two-phase drug delivery system for sequential release of antiresorptive and osteogenic drugs, J Biomed Mater Res B Appl Biomater, 100 (2012) 155-162.

[97] G. Swennen, H. Schliephake, R. Dempf, H. Schierle, C. Malevez, Craniofacial distraction osteogenesis: a review of the literature: Part 1: clinical studies, Int J Oral Maxillofac Surg, 30 (2001) 89-103.

[98] A. Tocchio, M. Tamplenizza, F. Martello, I. Gerges, E. Rossi, S. Argentiere, S. Rodighiero, W. Zhao, P. Milani, C. Lenardi, Versatile fabrication of vascularizable scaffolds for large tissue engineering in bioreactor, Biomaterials, 45 (2015) 124-131.

[99] B. Dhandayuthapani, Y. Yoshida, T. Maekawa, D.S. Kumar, Polymeric Scaffolds in Tissue Engineering Application: A Review, in, Hindawi Publishing Corporation, International Journal of Polymer Science, 2011.

[100] M.J. Whitaker, R.A. Quirk, S.M. Howdle, K.M. Shakesheff, Growth factor release from tissue engineering scaffolds, J Pharm Pharmacol, 53 (2001) 1427-1437.

[101] F.B. Basmanav, G.T. Kose, V. Hasirci, Sequential growth factor delivery from complexed microspheres for bone tissue engineering, Biomaterials, 29 (2008) 4195-4204.

[102] S. Kim, Y. Kang, C.A. Krueger, M. Sen, J.B. Holcomb, D. Chen, J.C. Wenke, Y. Yang, Sequential delivery of BMP-2 and IGF-1 using a chitosan gel with gelatin microspheres enhances early osteoblastic differentiation, Acta Biomater, 8 (2012) 1768-1777.

[103] S.N. Rothstein, C. Donahue, L.D. Falo Jr., S.R. Little, In silico programming of degradable microparticles to hide and then reveal immunogenic payloads in vivo, in, J. Mater. Chem. B., 2014, pp. 6183-6187.

[104] D.P. Link, J. van den Dolder, W.J. Jurgens, J.G. Wolke, J.A. Jansen, Mechanical evaluation of implanted calcium phosphate cement incorporated with PLGA microparticles, Biomaterials, 27 (2006) 4941-4947.

[105] R.P. Félix Lanao, S.C. Leeuwenburgh, J.G. Wolke, J.A. Jansen, Bone response to fast-degrading, injectable calcium phosphate cements containing PLGA microparticles, Biomaterials, 32 (2011) 8839-8847.

[106] H. Liao, X.F. Walboomers, W.J. Habraken, Z. Zhang, Y. Li, D.W. Grijpma, A.G. Mikos, J.G. Wolke, J.A. Jansen, Injectable calcium phosphate cement with PLGA, gelatin and PTMC microspheres in a rabbit femoral defect, Acta Biomater, 7 (2011) 1752-1759.

[107] D.P. Link, J. van den Dolder, J.J. van den Beucken, W. Habraken, A. Soede, O.C. Boerman, A.G. Mikos, J.A. Jansen, Evaluation of an orthotopically implanted calcium phosphate cement containing gelatin microparticles, J Biomed Mater Res A, 90 (2009) 372-379.

[108] D.P. Link, J. van den Dolder, J.J.J.P. van den Beucken, W. Habraken, A. Soede, O.C. Boerman, A.G. Mikos, J.A. Jansen, Evaluation of an orthotopically implanted calcium phosphate cement containing gelatin microparticles, in, Journal of Biomedical Materials Research Part A, 2008, pp. 372-379.

[109] S. Girod Fullana, H. Ternet, M. Freche, J.L. Lacout, F. Rodriguez, Controlled release properties and final macroporosity of a pectin microspheres-calcium phosphate composite bone cement, Acta Biomater, 6 (2010) 2294-2300.

[110] P.Q. Ruhe, E.L. Hedberg, N.T. Padron, P.H. Spauwen, J.A. Jansen, A.G. Mikos, rhBMP-2 release from injectable poly(DL-lactic-co-glycolic acid)/calcium-phosphate cement composites, J Bone Joint Surg Am, 85-A Suppl 3 (2003) 75-81.

[111] E.J. Blom, J. Klein-Nulend, J.G. Wolke, M.A. van Waas, F.C. Driessens, E.H. Burger, Transforming growth factor-beta1 incorporation in a calcium phosphate bone cement: material properties and release characteristics, J Biomed Mater Res, 59 (2002) 265-272.

[112] Microparticulate Systems for the Delivery of Proteins and Vaccines, 1st ed., CRC Press, 1996.

[113] G. Zhu, S.R. Mallery, S.P. Schwendeman, Stabilization of proteins encapsulated in injectable poly (lactide- co-glycolide), Nat Biotechnol, 18 (2000) 52-57.

[114] W. Yuan, Z. Liu, Controlled-release and preserved bioactivity of proteins from (self-assembled) core-shell double-walled microspheres, Int J Nanomedicine, 7 (2012) 257-270.

[115] E.J. Pollauf, C. Berkland, K.K. Kim, D.W. Pack, In vitro degradation of polyanhydride/polyester core-shell double-wall microspheres, Int J Pharm, 301 (2005) 294-303.

[116] R.A. Perez, H.W. Kim, Core-shell designed scaffolds for drug delivery and tissue engineering, Acta Biomater, (2015).

[117] R.A. Perez, H.W. Kim, Core-shell designed scaffolds of alginate/alpha-tricalcium phosphate for the loading and delivery of biological proteins, J Biomed Mater Res A, 101 (2013) 1103-1112.

[118] C. Wu, W. Fan, M. Gelinsky, Y. Xiao, J. Chang, T. Friis, G. Cuniberti, In situ preparation and protein delivery of silicate-alginate composite microspheres with core-shell structure, J R Soc Interface, 8 (2011) 1804-1814.

[119] S. Wang, W. Ju, P. Shang, L. Lei, H. Nie, Core-shell miscropheres delivering FGF-2 and BMP-2 in different release patterns for bone regeneration., in, Journal of Materials Chemistry B, 2015, pp. 1907-1920.

[120] E. Boanini, A. Bigi, Biomimetic gelatin-octacalcium phosphate core-shell microspheres, J Colloid Interface Sci, 362 (2011) 594-599.

[121] A.T. Raiche, D.A. Puleo, In vitro effects of combined and sequential delivery of two bone growth factors, Biomaterials, 25 (2004) 677-685.

[122] K. Kim, J. Lam, S. Lu, P.P. Spicer, A. Lueckgen, Y. Tabata, M.E. Wong, J.A. Jansen, A.G. Mikos, F.K. Kasper, Osteochondral tissue regeneration using a bilayered composite hydrogel with modulating dual growth factor release kinetics in a rabbit model, J Control Release, 168 (2013) 166-178.

[123] N.J. Shah, M.N. Hyder, M.A. Quadir, N.M. Dorval Courchesne, H.J. Seeherman, M. Nevins, M. Spector, P.T. Hammond, Adaptive growth factor delivery from a polyelectrolyte coating promotes synergistic bone tissue repair and reconstruction, Proc Natl Acad Sci U S A, (2014).

[124] N.J. Shah, M.L. Macdonald, Y.M. Beben, R.F. Padera, R.E. Samuel, P.T. Hammond, Tunable dual growth factor delivery from polyelectrolyte multilayer films, Biomaterials, 32 (2011) 6183-6193.

[125] S. Lu, J. Lam, J.E. Trachtenberg, E.J. Lee, H. Seyednejad, J.J. van den Beucken, Y. Tabata, M.E. Wong, J.A. Jansen, A.G. Mikos, F.K. Kasper, Dual growth factor delivery from bilayered, biodegradable hydrogel composites for spatially-guided osteochondral tissue repair, Biomaterials, 35 (2014) 8829-8839.

[126] P.T. Hammond, Building biomedical materials layer-by-layer, in, Materials Today, 2012, pp. 196-206.

[127] J. Min, R.D. Braatz, P.T. Hammond, Tunable staged release of therapeutics from layer-by-layer coatings with clay interlayer barrier, Biomaterials, 35 (2014) 2507-2517.

[128] C. Picart, F. Caruso, J.-C. Voegel, Layer-by-layer Films for Biomedical Applications, Wiley-VCH, 2015.

[129] N.S. Arora, T. Ramanayake, Y.F. Ren, G.E. Romanos, Platelet-rich plasma: a literature review, Implant Dent, 18 (2009) 303-310.

[130] P. Borrione, A.D. Gianfrancesco, M.T. Pereira, F. Pigozzi, Platelet-rich plasma in muscle healing, Am J Phys Med Rehabil, 89 (2010) 854-861.

[131] H.S. Cho, I.H. Song, S.Y. Park, M.C. Sung, M.W. Ahn, K.E. Song, Individual variation in growth factor concentrations in platelet-rich plasma and its influence on human mesenchymal stem cells, Korean J Lab Med, 31 (2011) 212-218.

[132] H.-T. Liao, J.-P. Chen, M.-Y. Lee, Bone Tissue Engineering with Adipose-Derived Stem Cells in Bioactive Composites of Laser-Sintered Porous Polycaprolactone Scaffolds and Platelet-Rich Plasma, in, Materials, 2013, pp. 4911-4929.

[133] I.A. Rodriguez, S.A. Sell, J.M. McCool, G. Saxena, A.J. Spence, G.L. Bowlin, A preliminary evaluation of lyophilized gelatin sponges, enhanced with platelet-rich plasma, hydroxyapatite and chitin whiskers for bone regeneration, Cells, 2 (2013) 244-265.

[134] X. Xie, C. Zhang, R.S. Tuan, Biology of platelet-rich plasma and its clinical application in cartilage repair, Arthritis Res Ther, 16 (2014) 204.

[135] R.M. El Backly, S.H. Zaky, A. Muraglia, L. Tonachini, F. Brun, B. Canciani, D. Chiapale, F. Santolini, R. Cancedda, M. Mastrogiacomo, A platelet-rich plasma-based membrane as a periosteal substitute with enhanced osteogenic and angiogenic properties: a new concept for bone repair, Tissue Eng Part A, 19 (2013) 152-165.

[136] H.H. Lu, J.M. Vo, H.S. Chin, J. Lin, M. Cozin, R. Tsay, S. Eisig, R. Landesberg, Controlled delivery of platelet-rich plasma-derived growth factors for bone formation, J Biomed Mater Res A, 86 (2008) 1128-1136.

[137] I.A. Rodriguez, E.A. Growney Kalaf, G.L. Bowlin, S.A. Sell, Platelet-rich plasma in bone regeneration: engineering the delivery for improved clinical efficacy, Biomed Res Int, 2014 (2014) 392398.

[138] J. Fang, Y.Y. Zhu, E. Smiley, J. Bonadio, J.P. Rouleau, S.A. Goldstein, L.K. McCauley, B.L. Davidson, B.J. Roessler, Stimulation of new bone formation by direct transfer of osteogenic plasmid genes, Proc Natl Acad Sci U S A, 93 (1996) 5753-5758.

[139] J. Bonadio, E. Smiley, P. Patil, S. Goldstein, Localized, direct plasmid gene delivery in vivo: prolonged therapy results in reproducible tissue regeneration, Nat Med, 5 (1999) 753-759.

[140] J.H. Jang, C.B. Rives, L.D. Shea, Plasmid delivery in vivo from porous tissue-engineering scaffolds: transgene expression and cellular transfection, Mol Ther, 12 (2005) 475-483.

[141] T. Luo, W. Zhang, B. Shi, X. Cheng, Y. Zhang, Enhanced bone regeneration around dental implant with bone morphogenetic protein 2 gene and vascular endothelial growth factor protein delivery, Clin Oral Implants Res, 23 (2012) 467-473.

[142] R.T. Franceschi, Biological approaches to bone regeneration by gene therapy, J Dent Res, 84 (2005) 1093-1103.

[143] K. Osawa, Y. Okubo, K. Nakao, N. Koyama, K. Bessho, Osteoinduction by repeat plasmid injection of human bone morphogenetic protein-2, J Gene Med, 12 (2010) 937-944.

[144] C.T. Laurencin, K.M. Ashe, N. Henry, H.M. Kan, K.W. Lo, Delivery of small molecules for bone regenerative engineering: preclinical studies and potential clinical applications, Drug Discov Today, 19 (2014) 794-800.

[145] K.W. Lo, T. Jiang, K.A. Gagnon, C. Nelson, C.T. Laurencin, Small-molecule based musculoskeletal regenerative engineering, Trends Biotechnol, 32 (2014) 74-81.

[146] I.C. Tai, Y.C. Fu, C.K. Wang, J.K. Chang, M.L. Ho, Local delivery of controlled-release simvastatin/PLGA/HAp microspheres enhances bone repair, Int J Nanomedicine, 8 (2013) 3895-3904.

[147] M. Monjo, M. Rubert, J.C. Wohlfahrt, H.J. Rønold, J.E. Ellingsen, S.P. Lyngstadaas, In vivo performance of absorbable collagen sponges with rosuvastatin in critical-size cortical bone defects, Acta Biomater, 6 (2010) 1405-1412.

[148] P. Megas, M. Panagiotis, Classification of non-union, Injury, 36 Suppl 4 (2005) S30-37.

[149] K.D. Hankenson, M. Dishowitz, C. Gray, M. Schenker, Angiogenesis in bone regeneration, Injury, 42 (2011) 556-561.

[150] M.A. Flierl, W.R. Smith, C. Mauffrey, K. Irgit, A.E. Williams, E. Ross, G. Peacher, D.J. Hak, P.F. Stahel, Outcomes and complication rates of different bone grafting modalities in long bone fracture nonunions: a retrospective cohort study in 182 patients, J Orthop Surg Res, 8 (2013) 33.

[151] W.F. McKay, S.M. Peckham, J.M. Badura, A comprehensive clinical review of recombinant human bone morphogenetic protein-2 (INFUSE Bone Graft), Int Orthop, 31 (2007) 729-734.

[152] L.L. Southwood, D.D. Frisbie, C.E. Kawcak, C.W. McIlwraith, Delivery of growth factors using gene therapy to enhance bone healing, Vet Surg, 33 (2004) 565-578.

[153] M.C. Chan, A.C. Hilyard, C. Wu, B.N. Davis, N.S. Hill, A. Lal, J. Lieberman, G. Lagna, A. Hata, Molecular basis for antagonism between PDGF and the TGFbeta family of signalling pathways by control of miR-24 expression, EMBO J, 29 (2010) 559-573.

[154] F.M. Chen, M. Zhang, Z.F. Wu, Toward delivery of multiple growth factors in tissue engineering, Biomaterials, 31 (2010) 6279-6308.

[155] A.R. Amini, C.T. Laurencin, S.P. Nukavarapu, Bone tissue engineering: recent advances and challenges, Crit Rev Biomed Eng, 40 (2012) 363-408.

[156] S. Vukicevic, H. Kleinman, F. Luyten, A. Roberts, N. Roche, A. Reddi, Identification of multiple active growth factors in basement membrane Matrigel suggests caution in interpretation of cellular activity related to extracellular matrix components, in, Experimental Cell Research, 1992, pp. 1-8.

[157] I. Arnaoutova, H.K. Kleinman, In vitro angiogenesis: endothelial cell tube formation on gelled basement membrane extract, Nat Protoc, 5 (2010) 628-635.

[158] R. Benelli, A. Albini, In vitro models of angiogenesis: the use of Matrigel, Int J Biol Markers, 14 (1999) 243-246.

[159] T. Adair, J. Montani, Angiogenesis, Morgan & Claypool Lifesciences, 2010.

[160] E.T. Bishop, G.T. Bell, S. Bloor, I.J. Broom, N.F. Hendry, D.N. Wheatley, An in vitro model of angiogenesis: basic features, Angiogenesis, 3 (1999) 335-344.

[161] C.A. Staton, M.W. Reed, N.J. Brown, A critical analysis of current in vitro and in vivo angiogenesis assays, Int J Exp Pathol, 90 (2009) 195-221.

[162] I. Lang, M.A. Pabst, U. Hiden, A. Blaschitz, G. Dohr, T. Hahn, G. Desoye, Heterogeneity of microvascular endothelial cells isolated from human term placenta and macrovascular umbilical vein endothelial cells, Eur J Cell Biol, 82 (2003) 163-173.

[163] C.J. Jackson, M. Nguyen, Human microvascular endothelial cells differ from macrovascular endothelial cells in their expression of matrix metalloproteinases, Int J Biochem Cell Biol, 29 (1997) 1167-1177.

[164] S.J. Mills, A.J. Cowin, P. Kaur, Pericytes, mesenchymal stem cells and the wound healing process, Cells, 2 (2013) 621-634.

[165] J.C. Park, J.C. Kim, B.K. Kim, K.S. Cho, G.I. Im, B.S. Kim, C.S. Kim, Dose- and time-dependent effects of recombinant human bone morphogenetic protein-2 on the osteogenic and adipogenic potentials of alveolar bone-derived stromal cells, J Periodontal Res, 47 (2012) 645-654.

[166] N. Matsuda, W.L. Lin, N.M. Kumar, M.I. Cho, R.J. Genco, Mitogenic, chemotactic, and synthetic responses of rat periodontal ligament fibroblastic cells to polypeptide growth factors in vitro, J Periodontol, 63 (1992) 515-525.

[167] S.J. Grainger, A.J. Putnam, Assessing the permeability of engineered capillary networks in a 3D culture, PLoS One, 6 (2011) e22086.

[168] A.C. Hielscher, C. Qiu, S. Gerecht, Breast cancer cell-derived matrix supports vascular morphogenesis, Am J Physiol Cell Physiol, 302 (2012) C1243-1256.

[169] E.J. Battegay, J. Rupp, L. Iruela-Arispe, E.H. Sage, M. Pech, PDGF-BB modulates endothelial proliferation and angiogenesis in vitro via PDGF beta-receptors, J Cell Biol, 125 (1994) 917-928.

[170] P.J. Bouletreau, S.M. Warren, J.A. Spector, D.S. Steinbrech, B.J. Mehrara, M.T. Longaker, Factors in the fracture microenvironment induce primary osteoblast angiogenic cytokine production, Plast Reconstr Surg, 110 (2002) 139-148.

[171] C. Baudelet, G.O. Cron, R. Ansiaux, N. Crokart, J. DeWever, O. Feron, B. Gallez, The role of vessel maturation and vessel functionality in spontaneous fluctuations of T2*-weighted GRE signal within tumors, NMR Biomed, 19 (2006) 69-76.

[172] D. Bonkowski, V. Katyshev, R.D. Balabanov, A. Borisov, P. Dore-Duffy, The CNS microvascular pericyte: pericyte-astrocyte crosstalk in the regulation of tissue survival, Fluids Barriers CNS, 8 (2011) 8.

[173] A. Birbrair, T. Zhang, Z.M. Wang, M.L. Messi, A. Mintz, O. Delbono, Pericytes at the intersection between tissue regeneration and pathology, Clin Sci (Lond), 128 (2015) 81-93.

[174] E.A. Winkler, R.D. Bell, B.V. Zlokovic, Central nervous system pericytes in health and disease, Nat Neurosci, 14 (2011) 1398-1405.

[175] A.W. James, Review of Signaling Pathways Governing MSC Osteogenic and Adipogenic Differentiation, Scientifica (Cairo), 2013 (2013) 684736.

[176] D. Barati, S.R. Shariati, S. Moeinzadeh, J.M. Melero-Martin, A. Khademhosseini, E. Jabbari, Spatiotemporal release of BMP-2 and VEGF enhances osteogenic and vasculogenic differentiation of human mesenchymal stem cells and endothelial colony-forming cells co-encapsulated in a patterned hydrogel, J Control Release, 223 (2016) 126-136.

[177] S. Enoch, D.J. Leaper, Basic science of wound healing., in, Surgery(Oxford), 2008, pp. 31-37.

[178] H. Sinno, S. Prakash, Complements and the wound healing cascade: an updated review, Plast Surg Int, 2013 (2013) 146764.

[179] C. Sfeir, L. Ho, B.A. Doll, K. Azari, J.O. Hollinger, Fracture Repair, in: J.R. Lieberman, G.E. Friedlaender (Eds.) Bone Regeneration and Repair: Biology and Clinical Applications, Humana Press, Inc., Totowa, NJ, 2005, pp. 21-46.

[180] X. Yu, S.C. Hsieh, W. Bao, D.T. Graves, Temporal expression of PDGF receptors and PDGF regulatory effects on osteoblastic cells in mineralizing cultures, Am J Physiol, 272 (1997) C1709-1716.

[181] W.V. Giannobile, C.S. Lee, M.P. Tomala, K.M. Tejeda, Z. Zhu, Platelet-derived growth factor (PDGF) gene delivery for application in periodontal tissue engineering, J Periodontol, 72 (2001) 815-823.

[182] C.S. Hughes, L.M. Postovit, G.A. Lajoie, Matrigel: a complex protein mixture required for optimal growth of cell culture, Proteomics, 10 (2010) 1886-1890.

[183] Y.K. Zhu, T. Umino, X.D. Liu, H.J. Wang, D.J. Romberger, J.R. Spurzem, S.I. Rennard, Contraction of fibroblast-containing collagen gels: initial collagen concentration regulates the degree of contraction and cell survival, In Vitro Cell Dev Biol Anim, 37 (2001) 10-16.

[184] D.R. Eyre, J.J. Wu, Collagen of fibrocartilage: a distinctive molecular phenotype in bovine meniscus, FEBS Lett, 158 (1983) 265-270.

[185] V.C. Duance, D.J. Restall, H. Beard, F.J. Bourne, A.J. Bailey, The location of three collagen types in skeletal muscle, FEBS Lett, 79 (1977) 248-252.

[186] U. Klinge, Z.Y. Si, H. Zheng, V. Schumpelick, R.S. Bhardwaj, B. Klosterhalfen, Collagen I/III and matrix metalloproteinases (MMP) 1 and 13 in the fascia of patients with incisional hernias, J Invest Surg, 14 (2001) 47-54.

[187] S.H. Liu, R.S. Yang, R. al-Shaikh, J.M. Lane, Collagen in tendon, ligament, and bone healing. A current review, Clin Orthop Relat Res, (1995) 265-278.

[188] C. Stecco, R. Stern, A. Porzionato, V. Macchi, S. Masiero, A. Stecco, R. De Caro, Hyaluronan within fascia in the etiology of myofascial pain, Surg Radiol Anat, 33 (2011) 891-896.

[189] D. Uebelhart, J.M. Williams, Effects of hyaluronic acid on cartilage degradation, Curr Opin Rheumatol, 11 (1999) 427-435.

[190] J. Necas, L. Bartosikova, P. Brauner, J. Kolar, Hyaluronic acid (hyaluronan): a review, in, Veterinarni Medicina, 2008, pp. 397-411.

[191] T. Hoshiba, G. Chen, C. Endo, H. Maruyama, M. Wakui, E. Nemoto, N. Kawazoe, M. Tanaka, Decellularized Extracellular Matrix as an In Vitro Model to Study the Comprehensive Roles of the ECM in Stem Cell Differentiation, Stem Cells Int, 2016 (2016) 6397820.

[192] Y. Kam, C. Guess, L. Estrada, B. Weidow, V. Quaranta, A novel circular invasion assay mimics in vivo invasive behavior of cancer cell lines and distinguishes single-cell motility in vitro, BMC Cancer, 8 (2008) 198.

[193] M.M. Stevens, Biomaterials for bone tissue engineering, in, Materials Today, 2008.

[194] S. Stevenson, Enhancement of fracture healing with autogenous and allogeneic bone grafts, Clin Orthop Relat Res, (1998) S239-246.

[195] J.C. Reichert, S. Saifzadeh, M.E. Wullschleger, D.R. Epari, M.A. Schütz, G.N. Duda, H. Schell, M. van Griensven, H. Redl, D.W. Hutmacher, The challenge of establishing preclinical models for segmental bone defect research, Biomaterials, 30 (2009) 2149-2163.

[196] H.G. Moghadam, G.K. Sándor, H.H. Holmes, C.M. Clokie, Histomorphometric evaluation of bone regeneration using allogeneic and alloplastic bone substitutes, J Oral Maxillofac Surg, 62 (2004) 202-213.

[197] K.W. Lo, B.D. Ulery, K.M. Ashe, C.T. Laurencin, Studies of bone morphogenetic protein-based surgical repair, Adv Drug Deliv Rev, 64 (2012) 1277-1291.

[198] S.N. Lissenberg-Thunnissen, D.J. de Gorter, C.F. Sier, I.B. Schipper, Use and efficacy of bone morphogenetic proteins in fracture healing, Int Orthop, 35 (2011) 1271-1280.

[199] J. Shepherd, S. Best, Calcium phosphate scaffolds for bone repair, in, JOM, 2011.

[200] P. Lichte, H.C. Pape, T. Pufe, P. Kobbe, H. Fischer, Scaffolds for bone healing: concepts, materials and evidence, Injury, 42 (2011) 569-573.

[201] P. Kumta, C. Sfeir, A. Roy, Bone Substitute Compositions, Methods of Preparation and Clinical Applications., in, University of Pittsburgh, United States, 2013.

[202] S. Bose, S. Tarafder, Calcium phosphate ceramic systems in growth factor and drug delivery for bone tissue engineering: a review, Acta Biomater, 8 (2012) 1401-1421.

[203] H.R. Ramay, M. Zhang, Biphasic calcium phosphate nanocomposite porous scaffolds for load-bearing bone tissue engineering, Biomaterials, 25 (2004) 5171-5180.

[204] A.J. Ambard, L. Mueninghoff, Calcium phosphate cement: review of mechanical and biological properties, J Prosthodont, 15 (2006) 321-328.

[205] D.W. Hutmacher, J.T. Schantz, C.X. Lam, K.C. Tan, T.C. Lim, State of the art and future directions of scaffold-based bone engineering from a biomaterials perspective, J Tissue Eng Regen Med, 1 (2007) 245-260.

[206] A. Roy, S. Jhunjhunwala, E. Bayer, M. Fedorchak, S.R. Little, P.N. Kumta, Porous calcium phosphate-poly (lactic-co-glycolic) acid composite bone cement: A viable tunable drug delivery system, Mater Sci Eng C Mater Biol Appl, 59 (2016) 92-101.

[207] V. Karageorgiou, D. Kaplan, Porosity of 3D biomaterial scaffolds and osteogenesis, Biomaterials, 26 (2005) 5474-5491.

[208] S.C. Balmert, A.C. Zmolek, A.J. Glowacki, T.D. Knab, S.N. Rothstein, J.M. Wokpetah, M.V. Fedorchak, S.R. Little, Positive Charge of "Sticky" Peptides and Proteins Impedes Release From Negatively Charged PLGA Matrices, J Mater Chem B Mater Biol Med, 3 (2015) 4723-4734.

[209] K.Y. Lee, M.C. Peters, D.J. Mooney, Comparison of vascular endothelial growth factor and basic fibroblast growth factor on angiogenesis in SCID mice, J Control Release, 87 (2003) 49-56.

[210] K.Y. Lee, D.J. Mooney, Alginate: properties and biomedical applications, Prog Polym Sci, 37 (2012) 106-126.

[211] E.A. Silva, D.J. Mooney, Effects of VEGF temporal and spatial presentation on angiogenesis, Biomaterials, 31 (2010) 1235-1241.

[212] B. Bellich, M. Borgogna, M. Cok, A. Cersaro, Release Properties of Hydrogels: Water Evaporation from Alginate Gel Beads, in, Food Biophysics, 2011, pp. 259-266.

[213] Z.S. Ai-Aql, A.S. Alagl, D.T. Graves, L.C. Gerstenfeld, T.A. Einhorn, Molecular mechanisms controlling bone formation during fracture healing and distraction osteogenesis, J Dent Res, 87 (2008) 107-118.

[214] P. Wang, L. Zhao, J. Liu, M.D. Weir, X. Zhou, H.H. Xu, Bone tissue engineering via nanostructured calcium phosphate biomaterials and stem cells, Bone Res, 2 (2014) 14017.

[215] N.K. Lee, H. Sowa, E. Hinoi, M. Ferron, J.D. Ahn, C. Confavreux, R. Dacquin, P.J. Mee, M.D. McKee, D.Y. Jung, Z. Zhang, J.K. Kim, F. Mauvais-Jarvis, P. Ducy, G. Karsenty, Endocrine regulation of energy metabolism by the skeleton, Cell, 130 (2007) 456-469.

[216] M. Sila-Asna, A. Bunyaratvej, S. Maeda, H. Kitaguchi, N. Bunyaratavej, Osteoblast differentiation and bone formation gene expression in strontium-inducing bone marrow mesenchymal stem cell, Kobe J Med Sci, 53 (2007) 25-35.

[217] P.D. Delmas, R. Eastell, P. Garnero, M.J. Seibel, J. Stepan, C.o.S.A.o.t.I.O. Foundation], The use of biochemical markers of bone turnover in osteoporosis. Committee of Scientific Advisors of the International Osteoporosis Foundation, Osteoporos Int, 11 Suppl 6 (2000) S2-17.

[218] M.J. Cuddihy, N.A. Kotov, Poly(lactic-co-glycolic acid) bone scaffolds with inverted colloidal crystal geometry, Tissue Eng Part A, 14 (2008) 1639-1649.

[219] C.F. João, J.M. Vasconcelos, J.C. Silva, J.P. Borges, An overview of inverted colloidal crystal systems for tissue engineering, Tissue Eng Part B Rev, 20 (2014) 437-454.

[220] K. Takagi, T. Takahashi, K. Kikuchi, A. Kawasaki, Fabrication of bioceramic scaffolds with ordered pore structure by inverse replication of assembled particles, in, Journal of the European Ceramic Society, 2010, pp. 2049-2055.

[221] Y. Zhang, C. Sung-Wook, Y. Xia, Inverse opal scaffolds for applications in regenerative medicine, in, Soft Matter, 2013, pp. 9747-9754.

[222] S.W. Choi, J. Xie, Y. Xia, Chitosan-Based Inverse Opals: Three-Dimensional Scaffolds with Uniform Pore Structures for Cell Culture, Adv Mater, 21 (2009) 2997-3001.

[223] N.A. Kotov, Y. Liu, S. Wang, C. Cumming, M. Eghtedari, G. Vargas, M. Motamedi, J. Nichols, J. Cortiella, Inverted colloidal crystals as three-dimensional cell scaffolds, Langmuir, 20 (2004) 7887-7892.

[224] S.C. Balmert, S.R. Little, Biomimetic delivery with micro- and nanoparticles, Adv Mater, 24 (2012) 3757-3778.

[225] A. Matsumoto, Y. Matsukawa, Y. Horikiri, T. Suzuki, Rupture and drug release characteristics of multi-reservoir type microspheres with poly(dl-lactide-co-glycolide) and poly(dl-lactide), Int J Pharm, 327 (2006) 110-116.

[226] J. Ong, M. Appleford, G. Mani, Introduction to Biomaterials: Basic Theory with Engineering Applications, in: Particulate Systems: Polymeric microparticles, Cambridge University Press, 2013, pp. 335-340.

[227] H.K. Makadia, S.J. Siegel, Poly Lactic-co-Glycolic Acid (PLGA) as Biodegradable Controlled Drug Delivery Carrier, Polymers (Basel), 3 (2011) 1377-1397.

[228] K. Avgoustakis, Poly-lactic-co-glycolic acid (PLGA), in, Taylor and Francis, Encyclopedia of Biomaterials and Biomedical Engineering, 2005.

[229] F. De Marchis, D. Ribatti, C. Giampietri, A. Lentini, D. Faraone, M. Scoccianti, M.C. Capogrossi, A. Facchiano, Platelet-derived growth factor inhibits basic fibroblast growth factor angiogenic properties in vitro and in vivo through its alpha receptor, Blood, 99 (2002) 2045-2053.

[230] M.H. Lash, M.V. Fedorchak, J.J. McCarthy, S.R. Little, Scaling up self-assembly: bottom-up approaches to macroscopic particle organization, Soft Matter, 11 (2015) 5597-5609.

[231] F.M. Klenke, Y. Liu, H. Yuan, E.B. Hunziker, K.A. Siebenrock, W. Hofstetter, Impact of pore size on the vascularization and osseointegration of ceramic bone substitutes in vivo, J Biomed Mater Res A, 85 (2008) 777-786.

[232] S.W. Choi, Y. Zhang, M.R. Macewan, Y. Xia, Neovascularization in biodegradable inverse opal scaffolds with uniform and precisely controlled pore sizes, Adv Healthc Mater, 2 (2013) 145-154.

[233] J.T. Lee, K.L. Chow, SEM sample preparation for cells on 3D scaffolds by freeze-drying and HMDS, Scanning, 34 (2012) 12-25.

[234] S. An, Y. Gao, J. Ling, Characterization of human periodontal ligament cells cultured on three-dimensional biphasic calcium phosphate scaffolds in the presence and absence of L-

ascorbic acid, dexamethasone and β-glycerophosphate in vitro, Exp Ther Med, 10 (2015) 1387-1393.

[235] X. Xiao, W. Wang, D. Liu, H. Zhang, P. Gao, L. Geng, Y. Yuan, J. Lu, Z. Wang, The promotion of angiogenesis induced by three-dimensional porous beta-tricalcium phosphate scaffold with different interconnection sizes via activation of PI3K/Akt pathways, Sci Rep, 5 (2015) 9409.

[236] X. Ye, S. Cai, G. Xu, Y. Dou, H. Hu, Preparation and in vitro evaluation of mesoporous hydroxyapatite coated β-TCP porous scaffolds, Mater Sci Eng C Mater Biol Appl, 33 (2013) 5001-5007.